

1 **Supplementary Figure 1: *E. coli* BW25113 fluorescence signals for 143 fluorophores.**  
2 The signals for the non-dye control (Autofluorescence) and all fluorophores ( $\log_{10}$  values, Y-  
3 axis) are compiled for each of the 13 channels of the Intellicyt® flow cytometer (X-axis). The  
4 median for autofluorescence (orange bars) is drawn for every channel. Colour coded  
5 distribution of data by concentration of fluorophore (micromolar) are shown. The subtitles  
6 contain our internal code (Fxxx). The number of biological replicates ( $n$ ) for each fluorophore  
7 at a given concentration represent data from different experiments carried out over a period  
8 of five months.

9 **Supplementary Figure 2. Compilation of the fluorescence detected for 143 fluorescent**  
10 **molecules by the Intellicyt® in *E. coli* BW25113.** **A:** Density distribution of the  
11 fluorescence of the full set of fluorophores (blue dash line) using their individual optimal  
12 excitation-emission channels at their optimal concentrations (as in Supplementary Table 1).  
13 **B:** The signals for all fluorophores are compiled against autofluorescence for each channel.  
14 Colour-coded distribution of data by concentration of fluorophore (micromolar) are shown.  
15 Orange bar: median value of autofluorescence (note that some dyes can quench  
16 autofluorescence). **C:** Density distribution after autofluorescence data were subtracted. The  
17 median fluorescence was reduced (blue dash line moved to the left) as a consequence of  
18 the subtraction of the autofluorescence. **D:** New spread of the signals distribution for all  
19 fluorophores for the 13 channels after subtracting autofluorescence. Colour-coded  
20 distribution of data by concentration of fluorophore (micromolar).

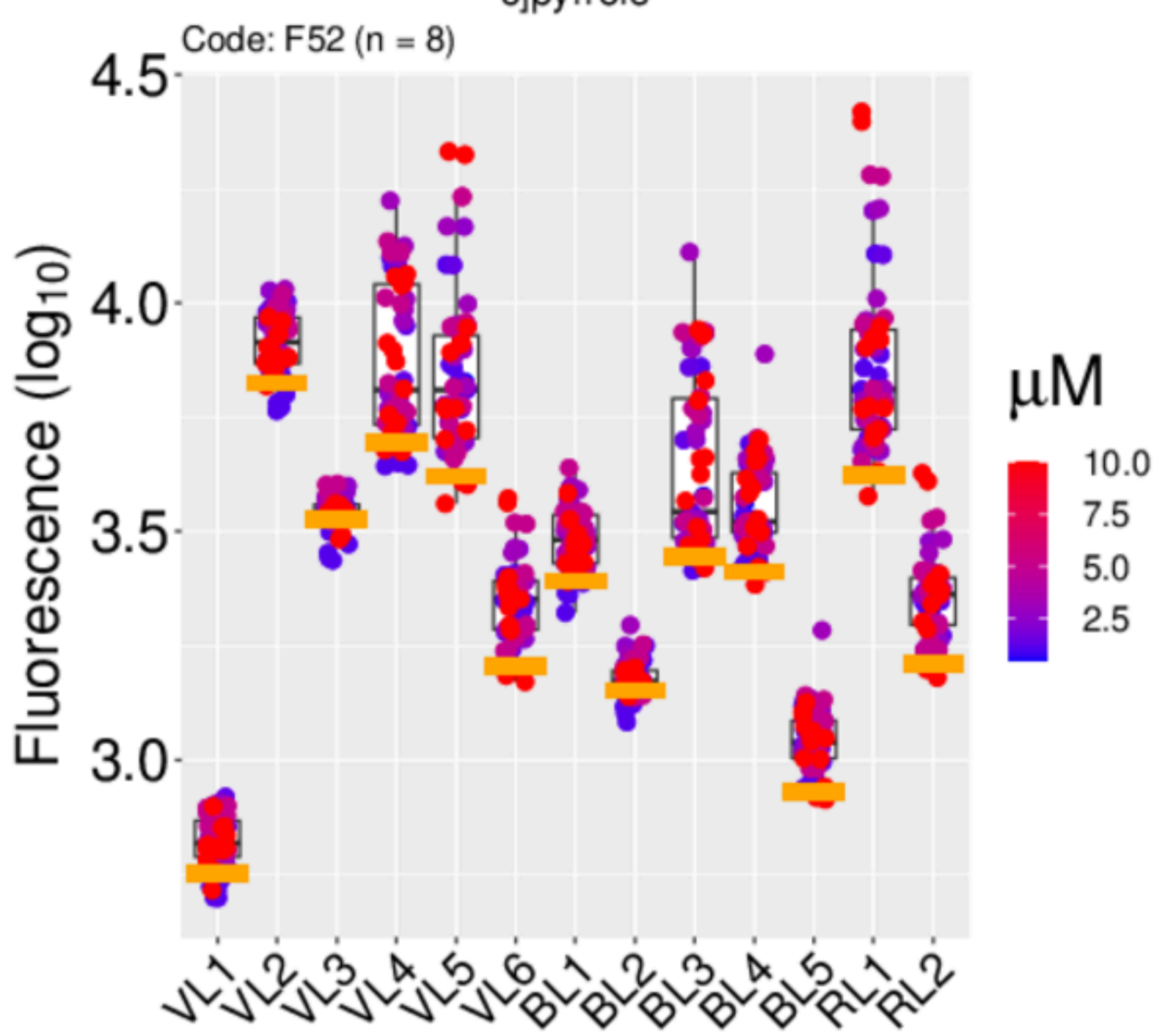
21 **Supplementary Figure 3: Dose-response fluorophore uptake.** Regression analysis for  
22 each of the initial 47 fluorophores that had a two-fold or higher activity (in terms of median  
23 values of uptake) in *E. coli* BW25113. Locally weighted scatterplot smoothing was applied to  
24 fluorescence signal versus fluorophore concentration data. X-axis: the  $\log_{10}$  of the  
25 concentrations in micromolar. Y-axis: the  $\log_{10}$  of fluorescence signals. The subtitles contain  
26 the relevant channel for each fluorophore and our internal code (Fxxx).

27 **Supplementary Figure 4: Effect of pH and CPZ on the uptake of 40 fluorophores.** *E.*  
28 *coli* BW25113 ( $10^6$  cells.mL<sup>-1</sup>) were incubated with 3  $\mu$ M fluorophores for 15 minutes at 37°C  
29 (red lines). Similar samples were incubated with both 3  $\mu$ M fluorophores and 10 $\mu$ M CPZ  
30 under the same experimental conditions (blue lines). The incubations were carried out at  
31 different pH values: 6.0, 6.5, 7.0, 7.5, 8.0, and 8.5. X-axis: pH values. Y-axis:  $\log_{10}$  of  
32 fluorescence signals after locally weighted scatterplot smoothing.

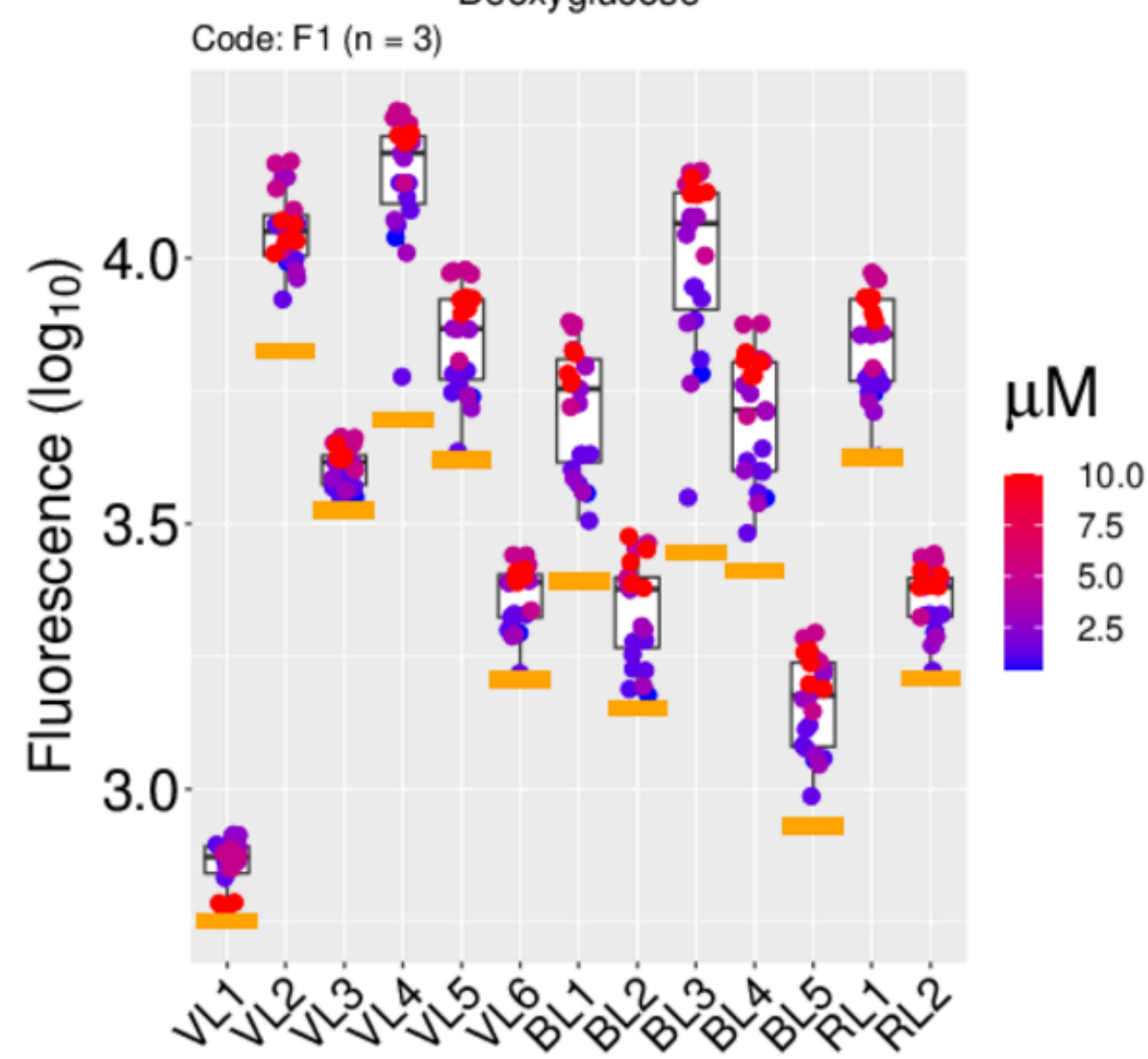
33 **Supplementary Figure 5: Effect of *yhjV* deletion on fluorophore uptake in *E. coli***  
34 **BW25113.** Fluorescence signals are presented as the  $\log_{10}$  of ratios of the fluorescence from  
35 the *yhjV* knock out cells ( $\Delta yhjV$ ) over the fluorescence signals from the reference cells  
36 (BW25113). X-axis:  $\log_{10}$  of the ratios ( $\log_{10} = 0$ ). No difference between the two strain  
37 would have a ratio of 1 ( $\log_{10} = 0$ ). Boxplots are ordered by median (highest on top of the  
38 plot). The legend lists the concentrations used for each fluorophore. The legend lists the  
39 concentrations used for each fluorophore. The clearly related structures of the two most  
40 differentiating dyes from the palette of 39 are shown.

41 **Supplementary Figure 6: Differential uptake of 39 dyes between three different**  
42 **knockout strain of *E. coli*.** Experiments were performed as described in the legends to  
43 Supplementary Figure 5 and 11 Figure 9, and in Table 2. Several dyes showing the largest  
44 effect in  $\Delta yihN$  are marked.

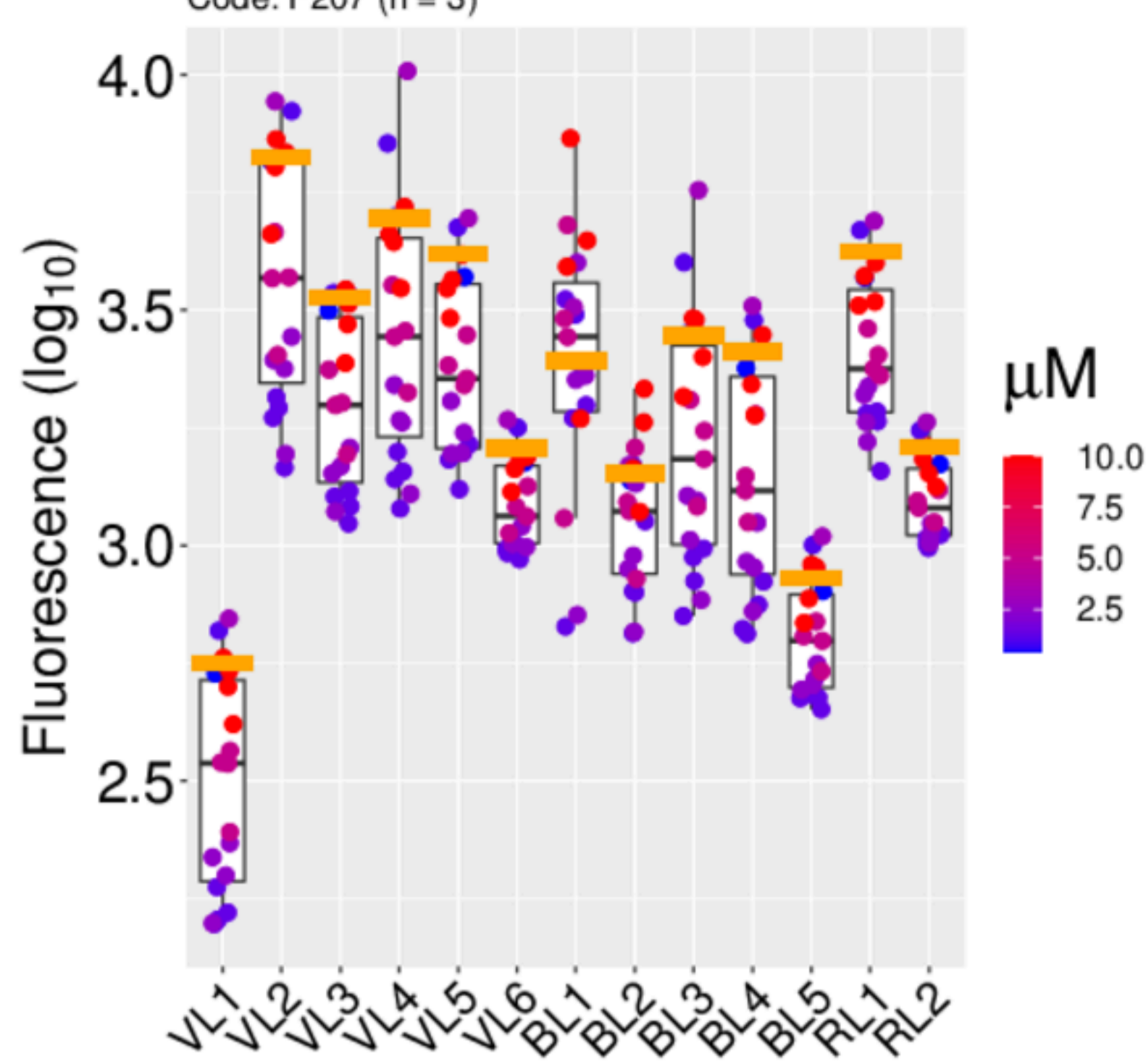
1,4-Diketo-3-((4-[N-(3,5-dichloro-4-hydroxyphenyl)amino]sulfonyl)phenyl)-6-phenylpyrrolo[3,4-c]pyrrole



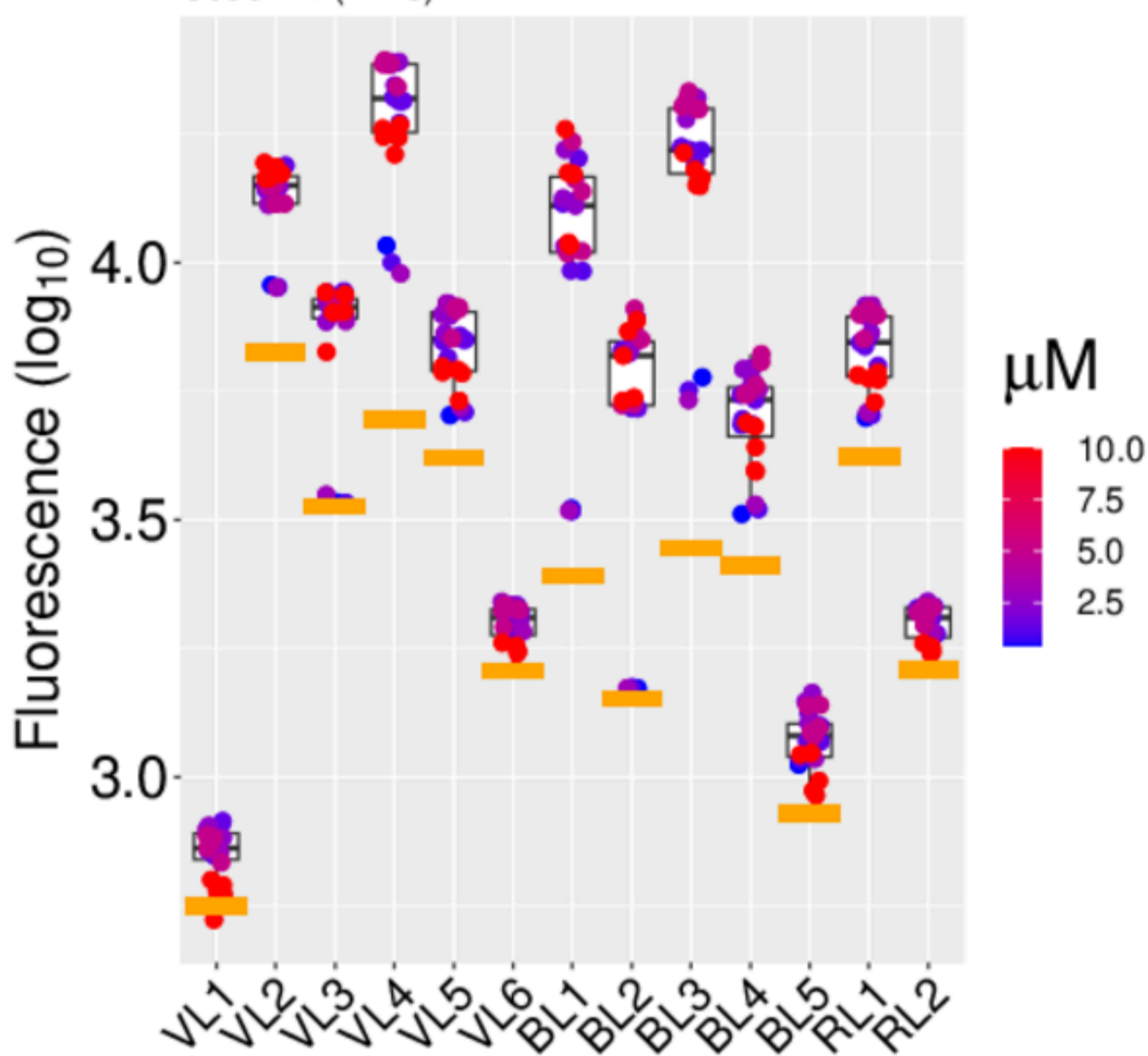
2-(N-(7-Nitrobenz-2-oxa-1,3-diazol-4-yl)Amino)-2-Deoxyglucose



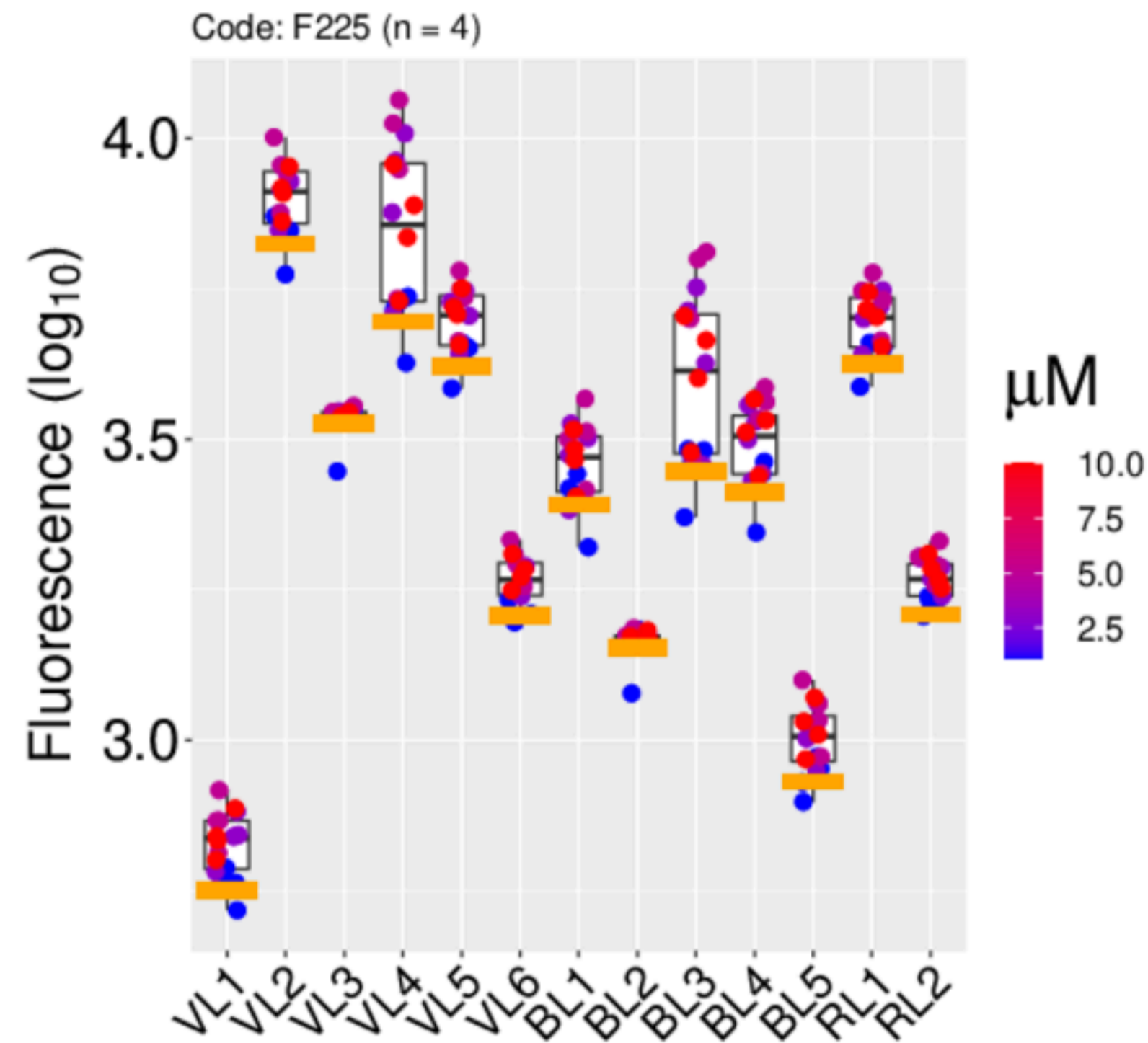
2,5-Dihydro-3,6-di-2-thienyl-pyrrolo[3,4-c]pyrrole-1,4-dione



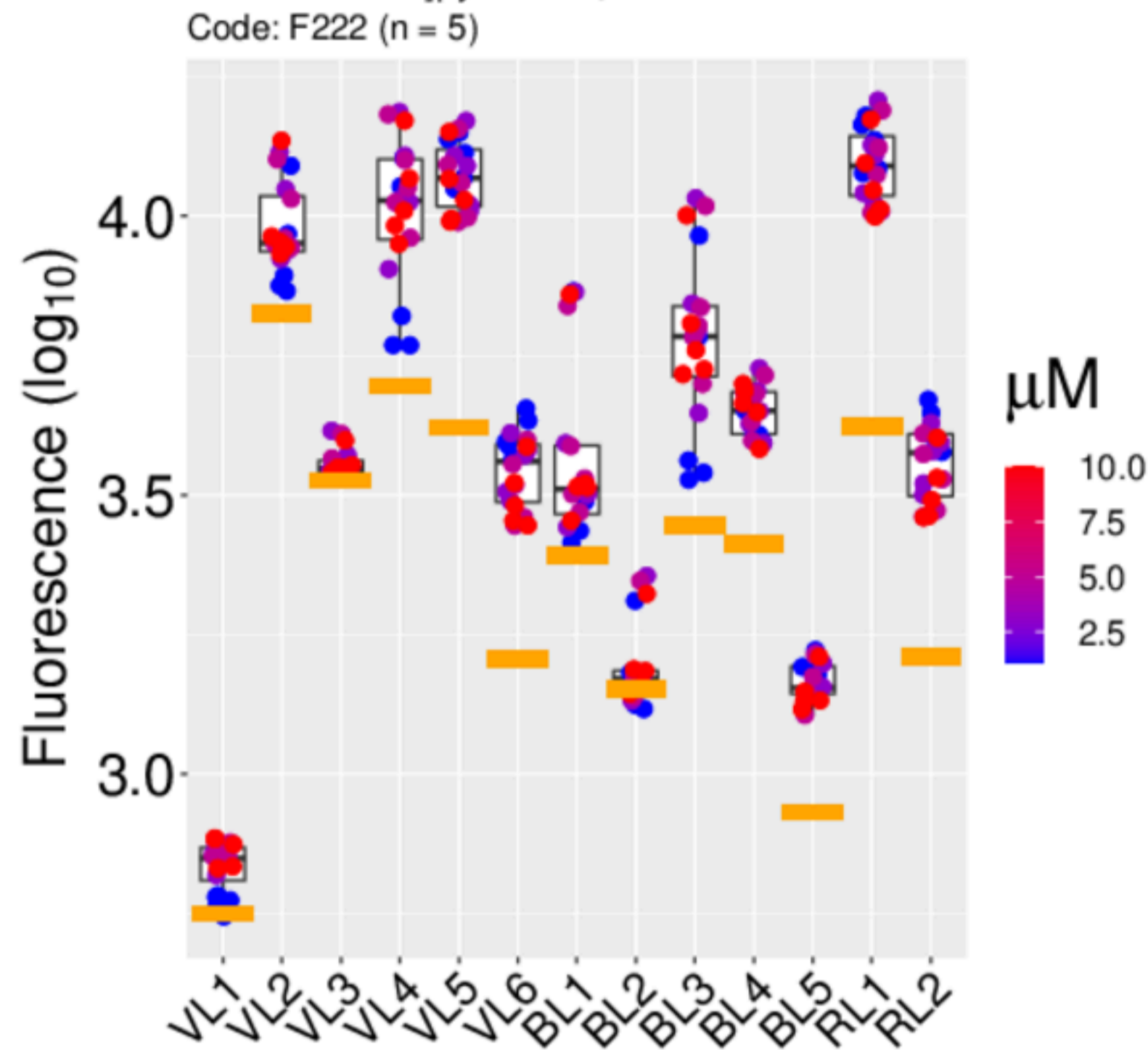
2',7'-Dichlorofluorescein



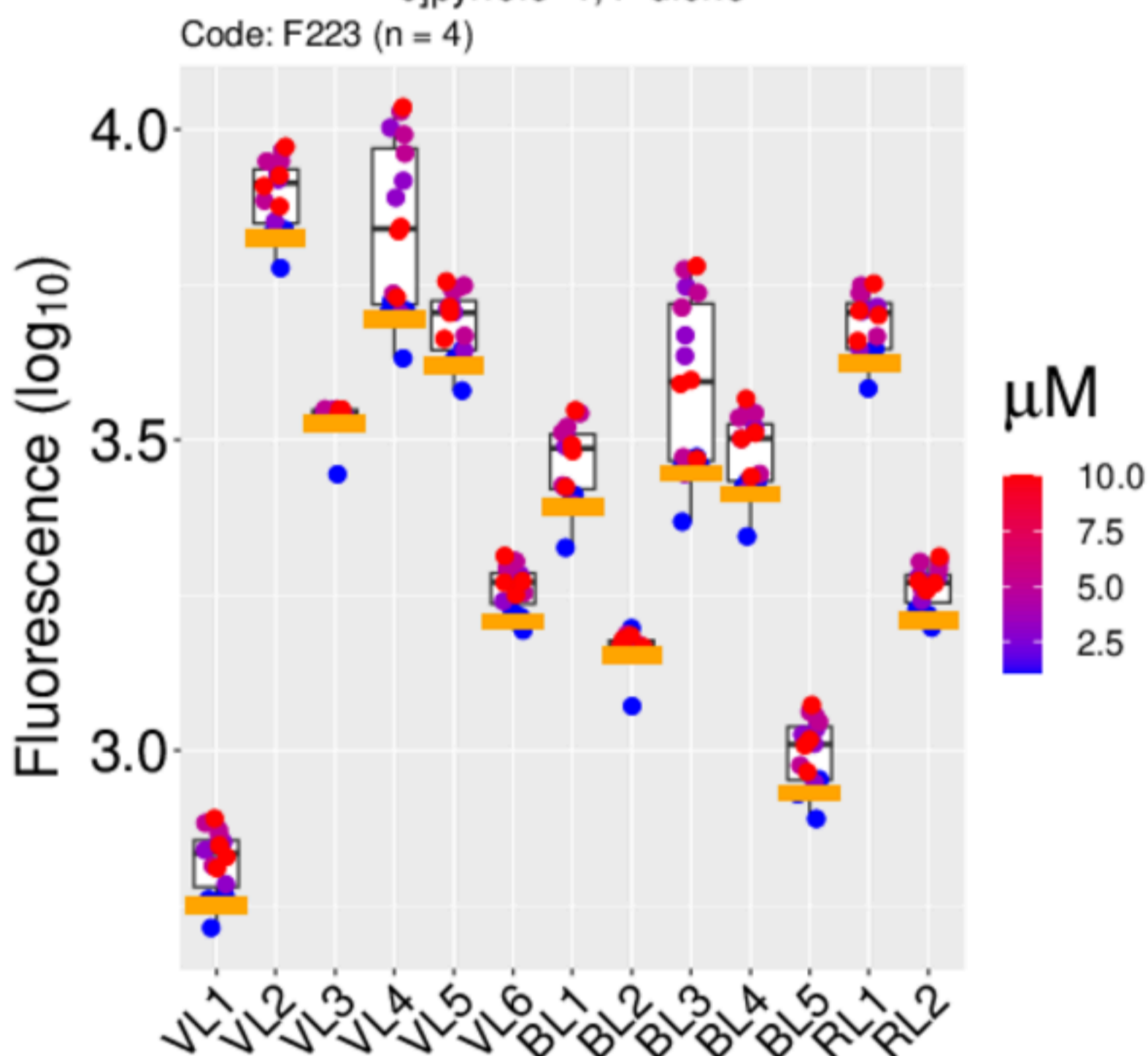
3,6-Bis(4-biphenyl)-2,5-dihydropyrrolo[3,4-c]pyrrole-1,4-dione



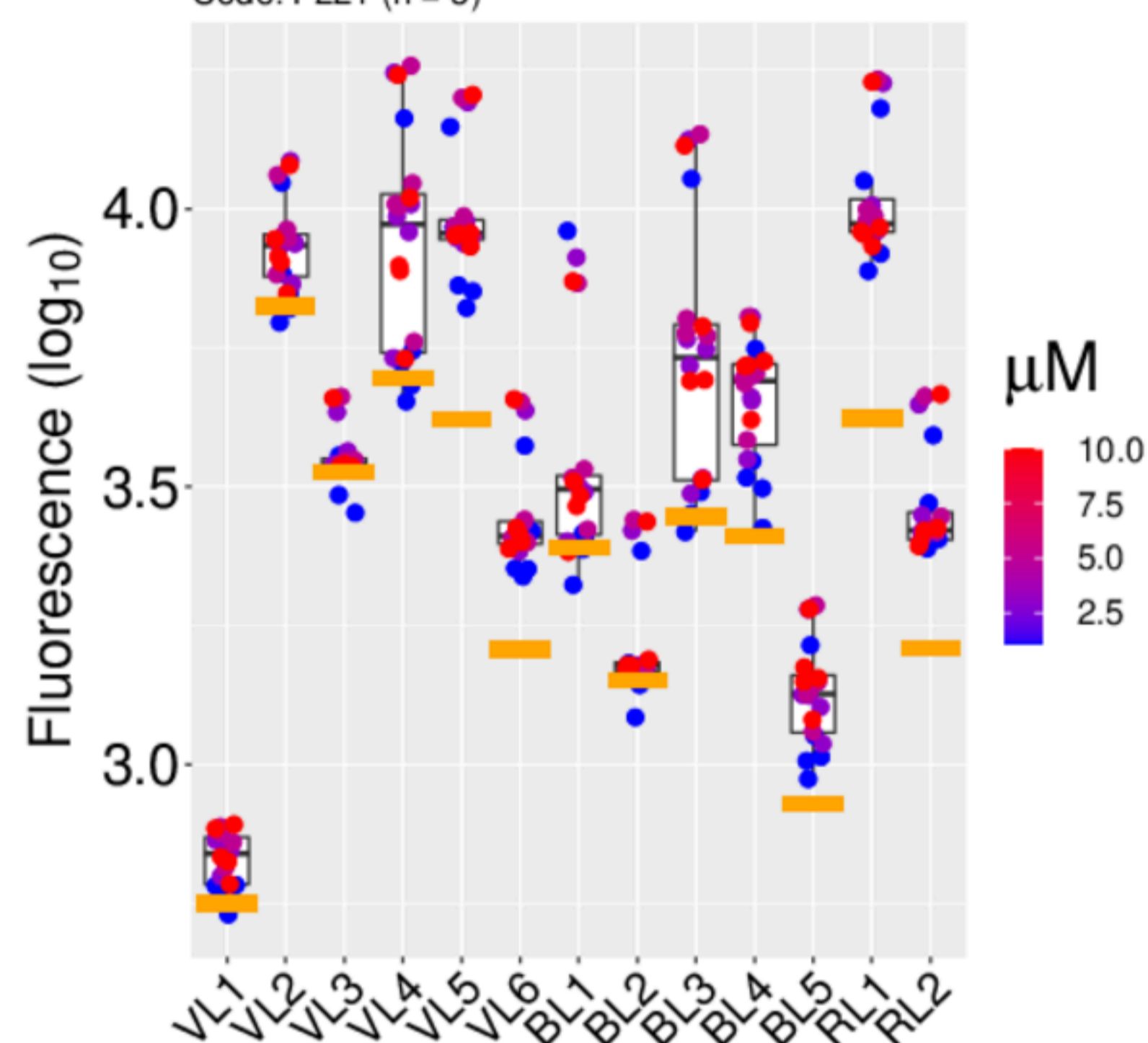
3,6-Bis(4-chlorophenyl)-2,5-dihydropyrrolo[3,4-c]pyrrole-1,4-dione



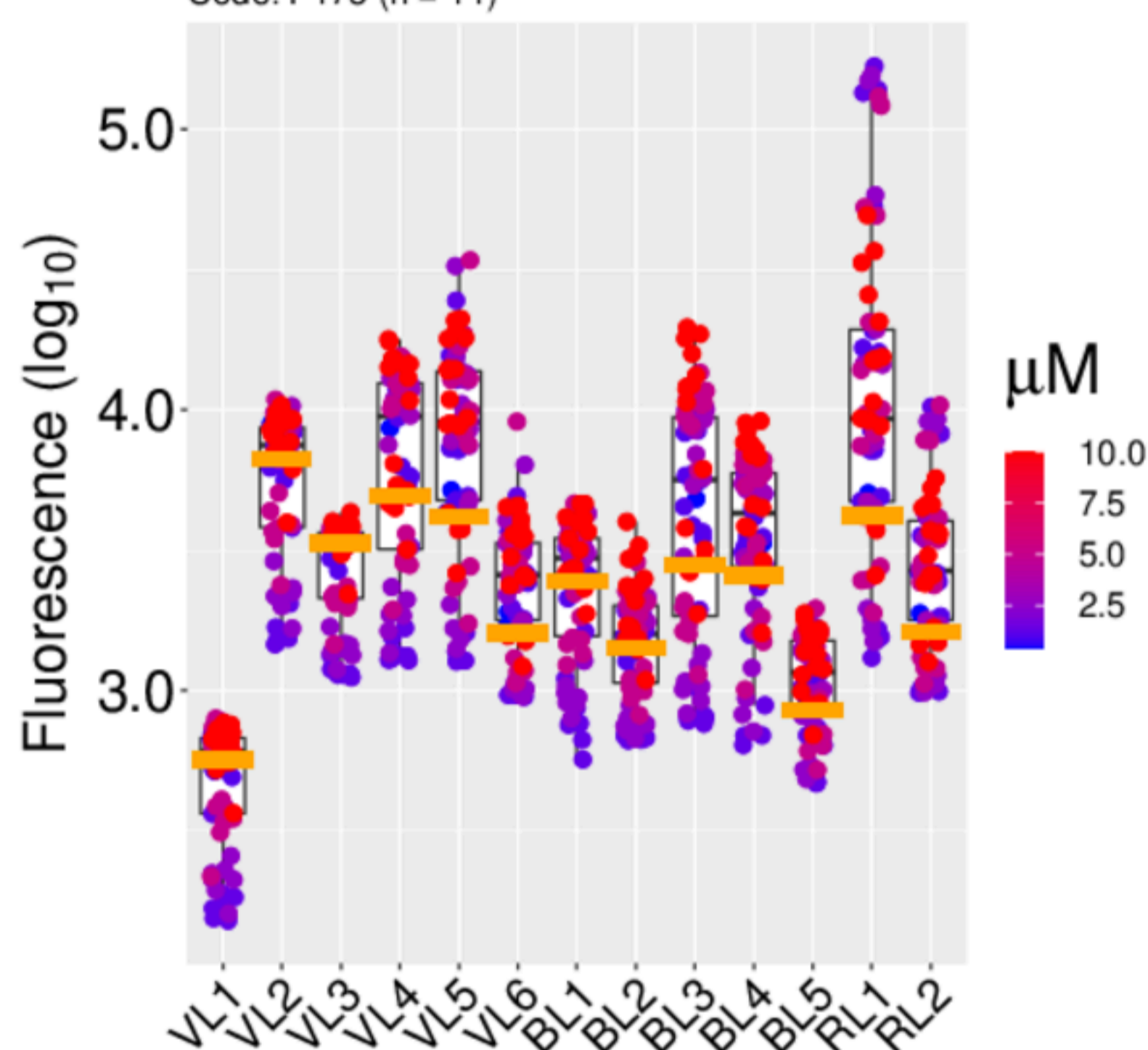
3,6-Bis(4-tert-butylphenyl)-2,5-dihydropyrrolo[3,4-c]pyrrole-1,4-dione



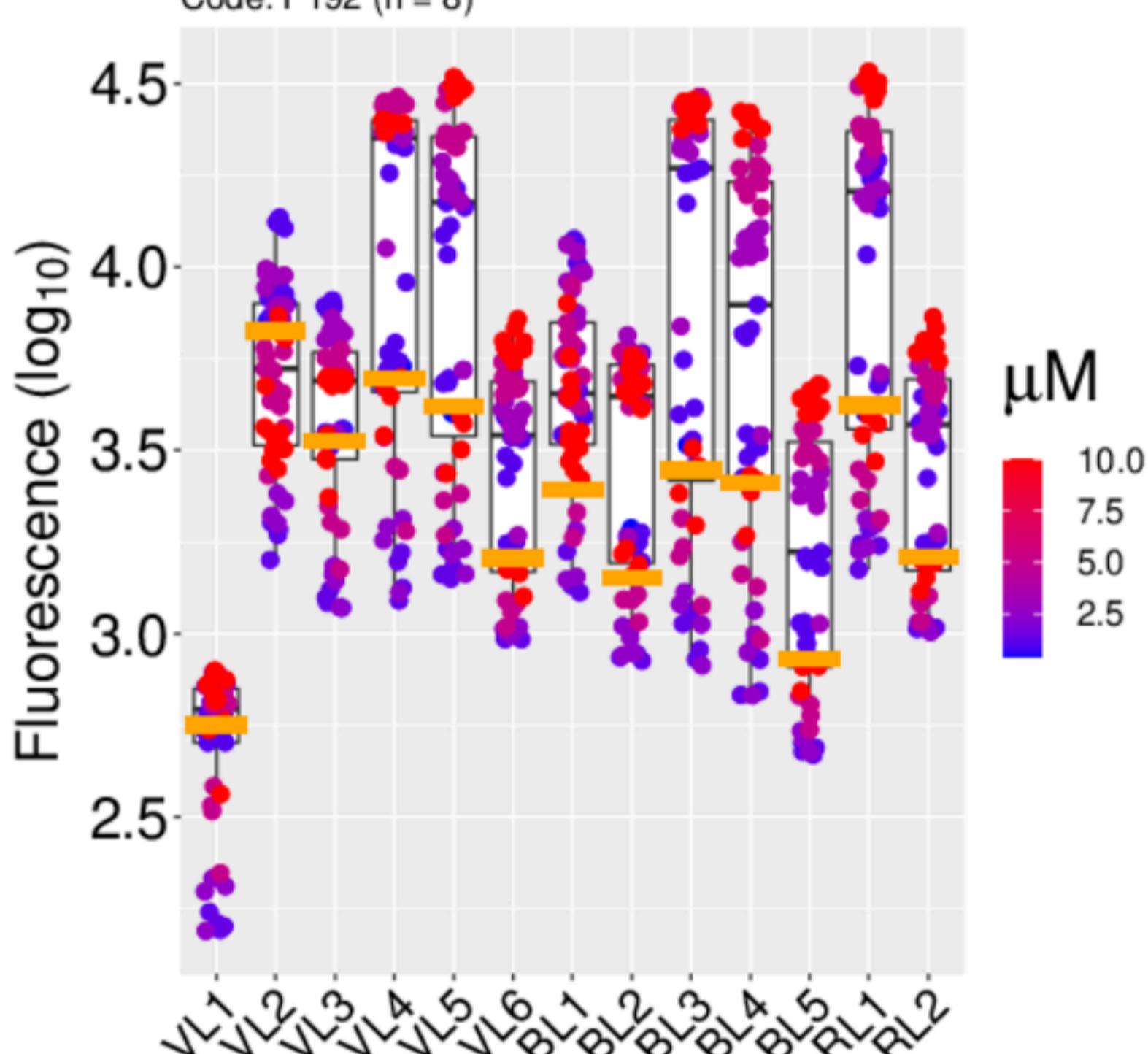
3,6-Diphenyl-2,5-dihydropyrrolo[3,4-c]pyrrole-1,4-dione



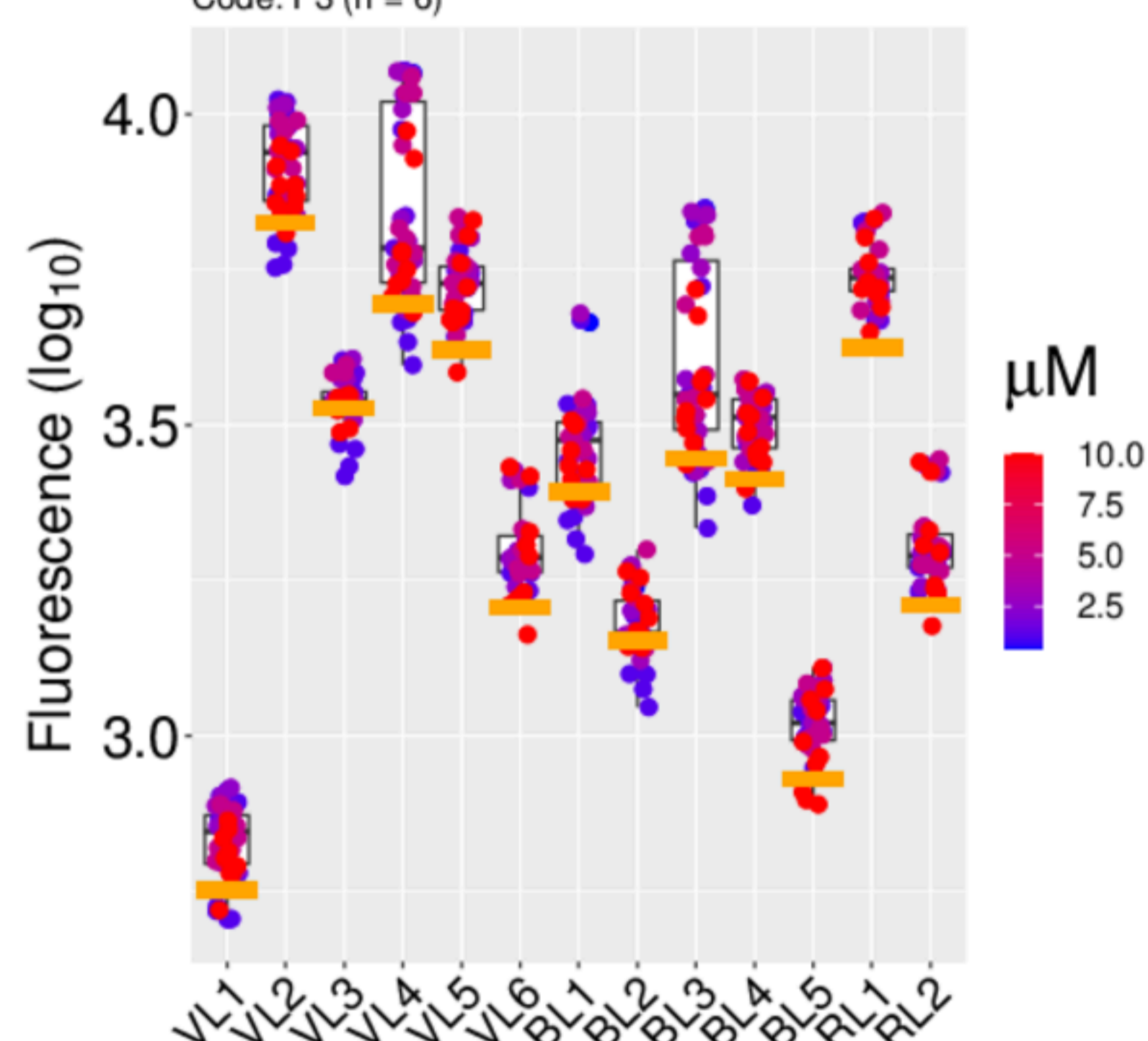
4-(4-(Dimethylamino)styryl)-N-methylpyridinium (ASP+)



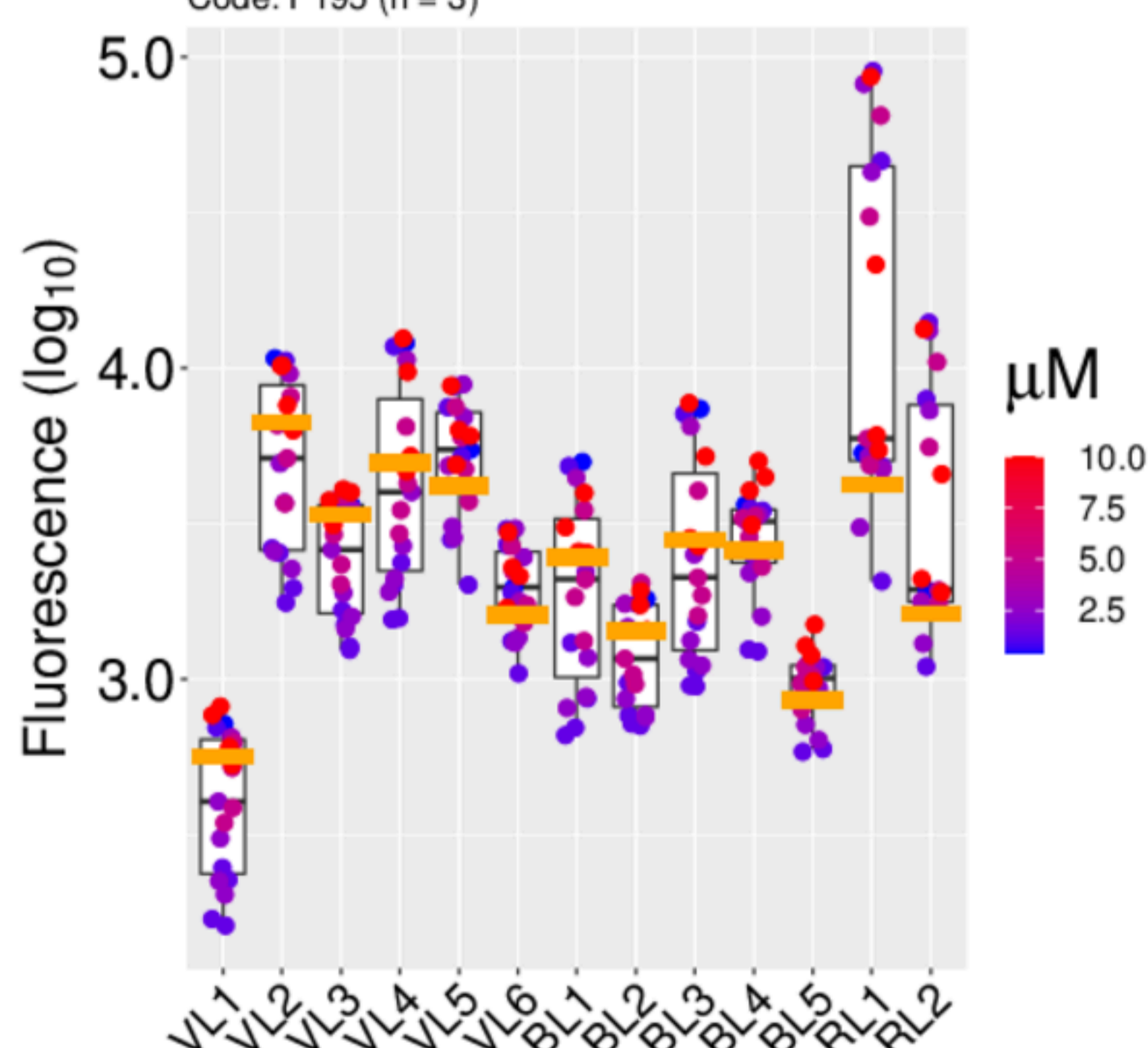
5-Carboxyfluorescein



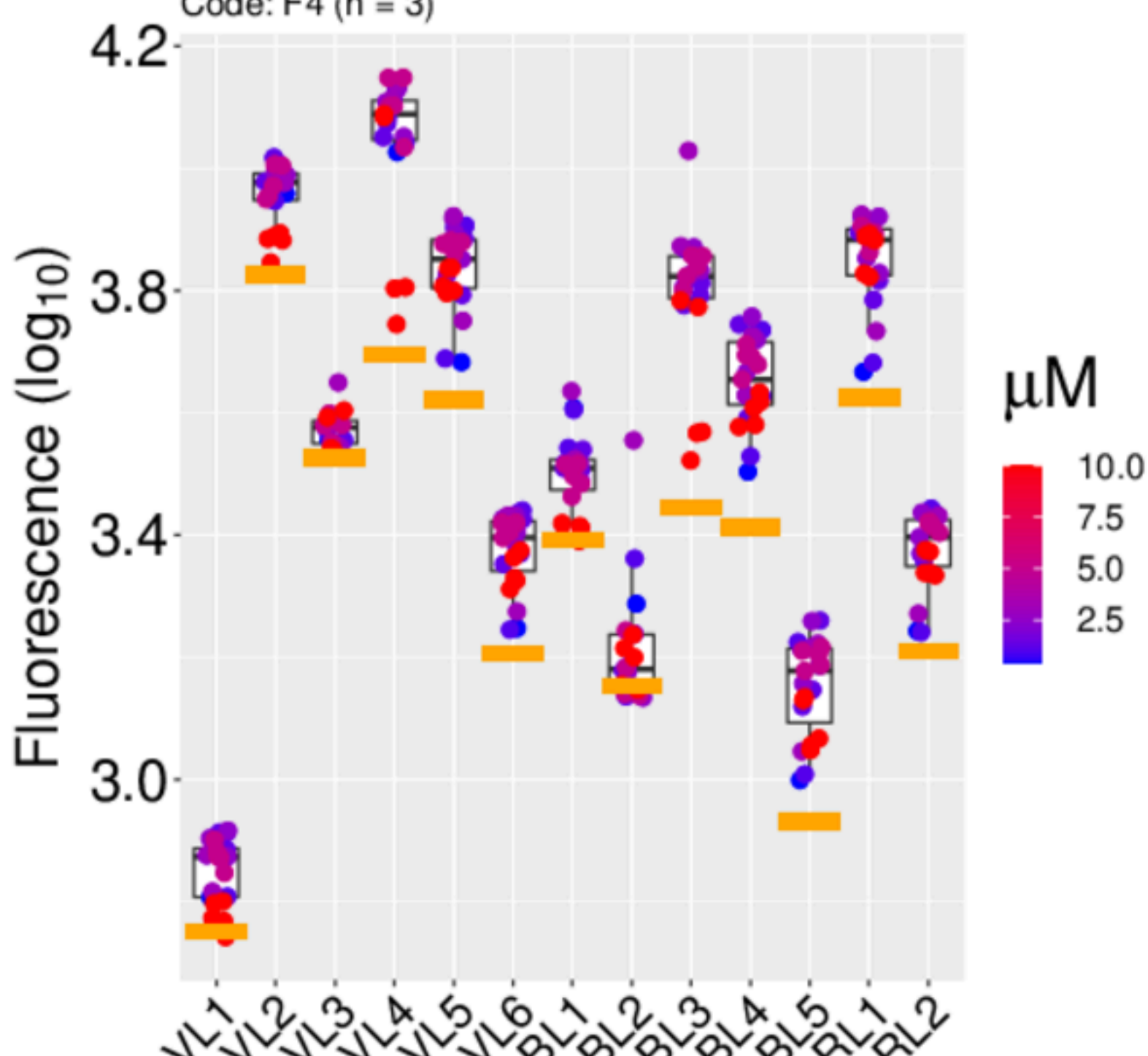
5-hydroxytryptamine (serotonin)



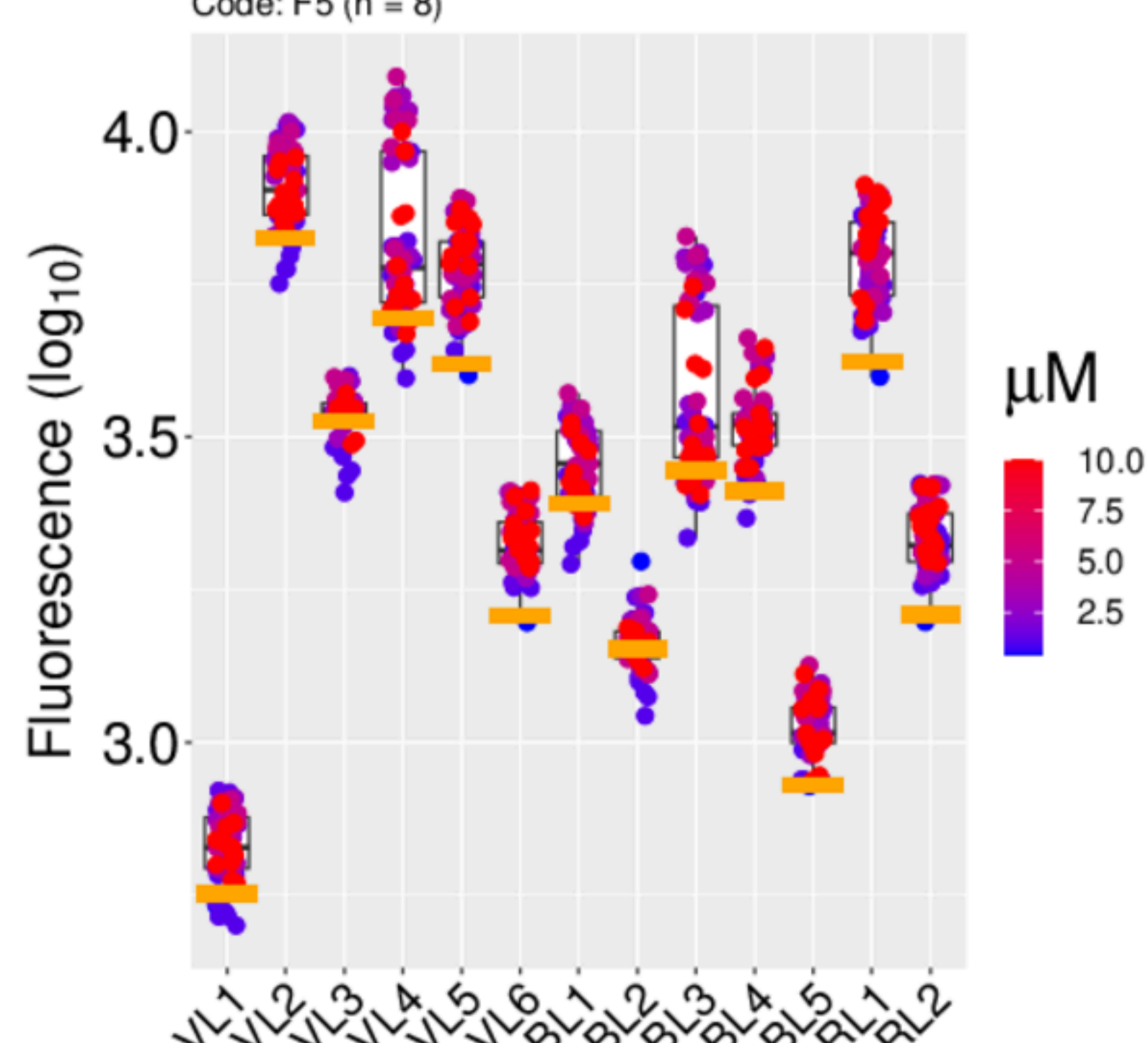
6-Carboxyfluorescein



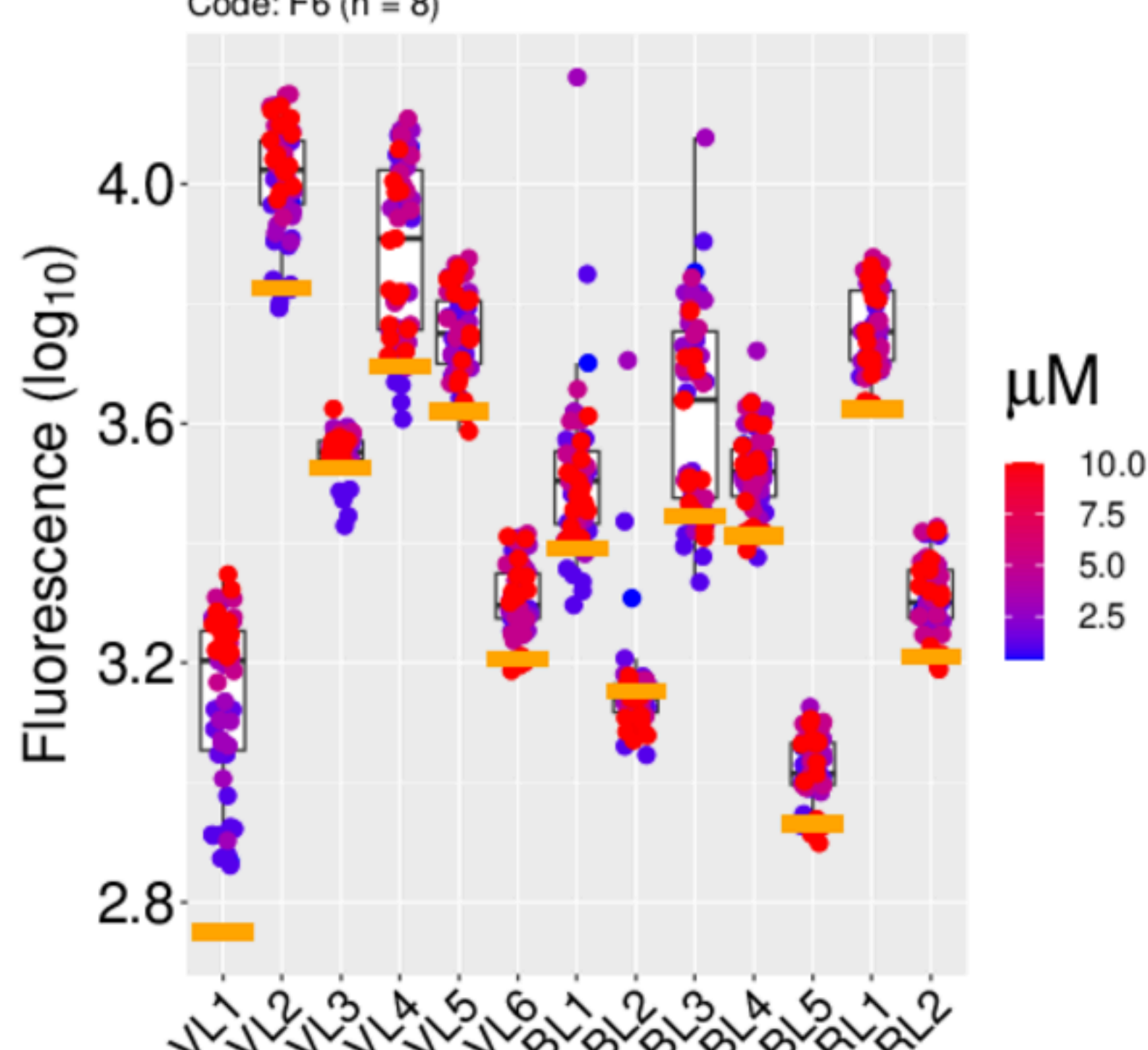
7-Aminoactinomycin D



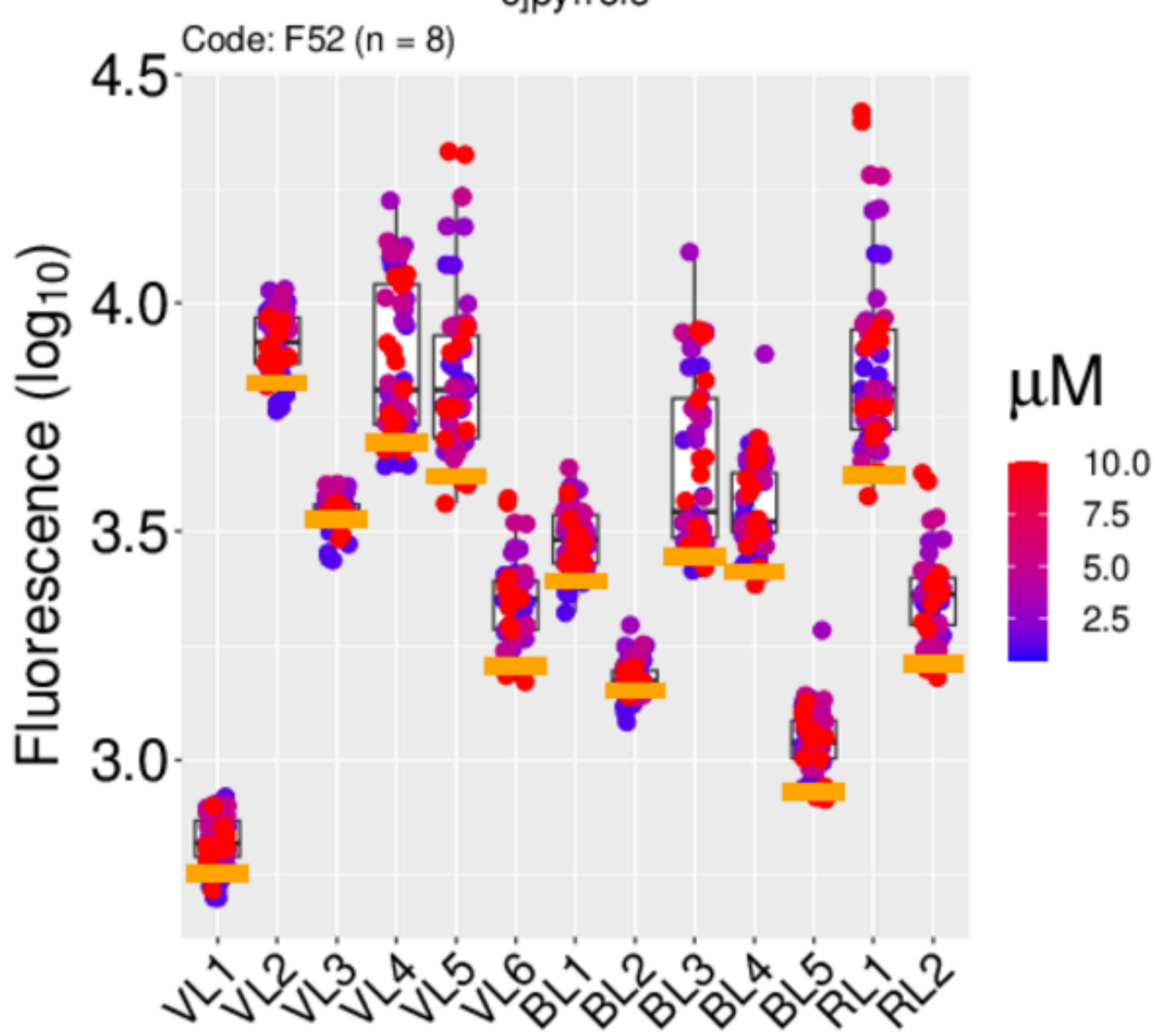
8-Anilinoanthracene-1-sulfonic acid



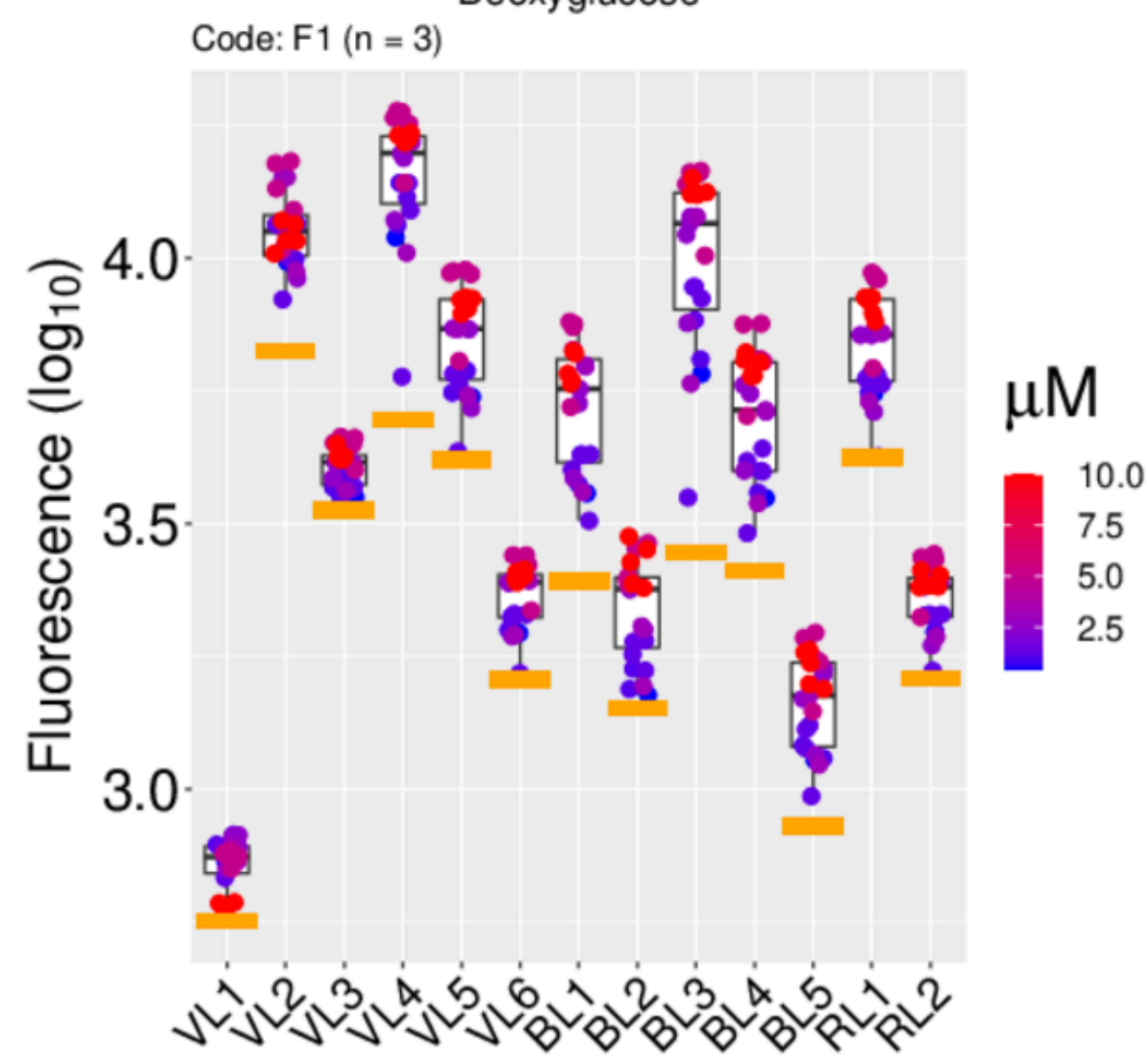
9-aminoacridine



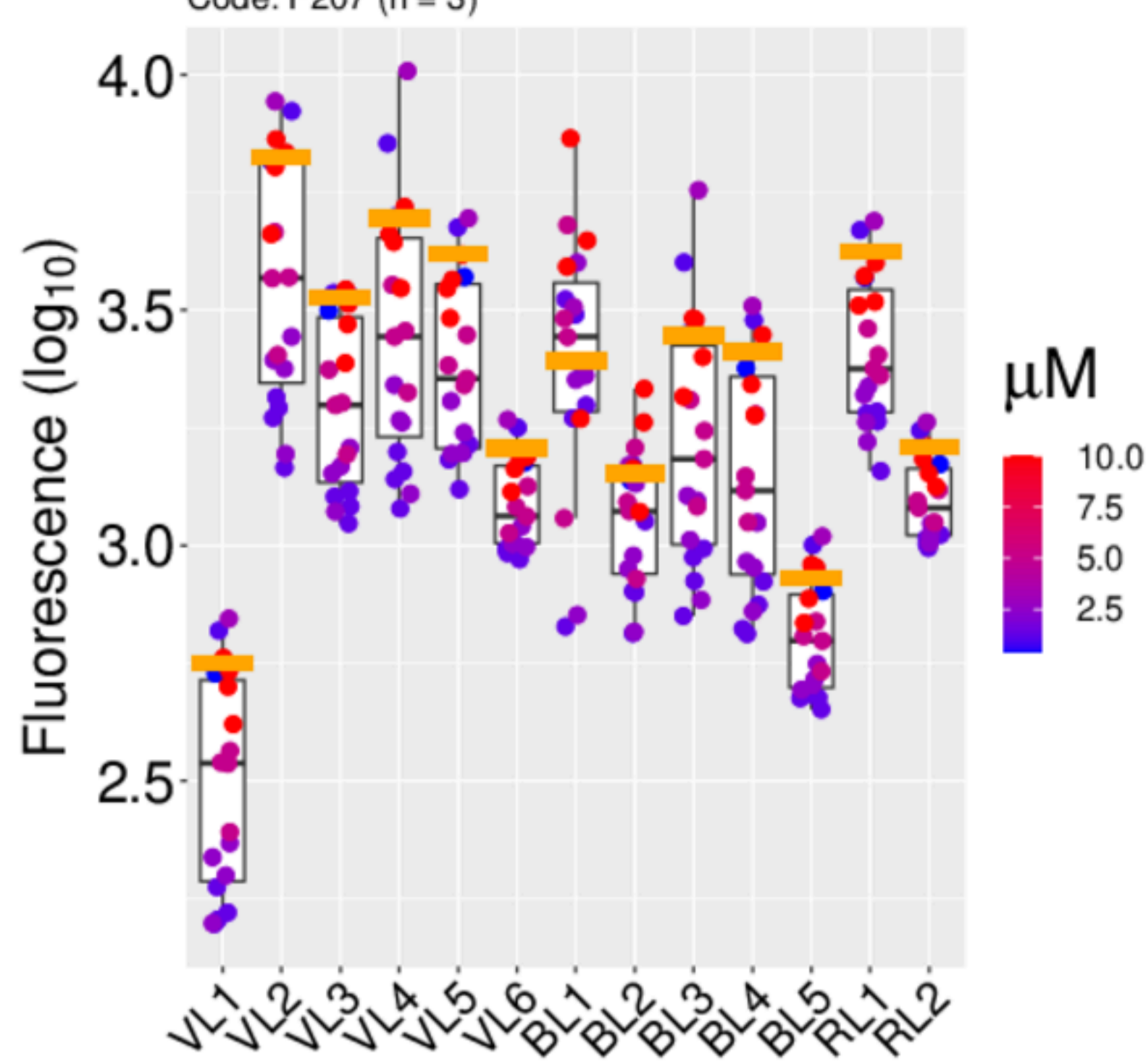
1,4-Diketo-3-((4-[N-(3,5-dichloro-4-hydroxyphenyl)amino)sulfonyl]phenyl)-6-phenylpyrrolo[3,4-c]pyrrole



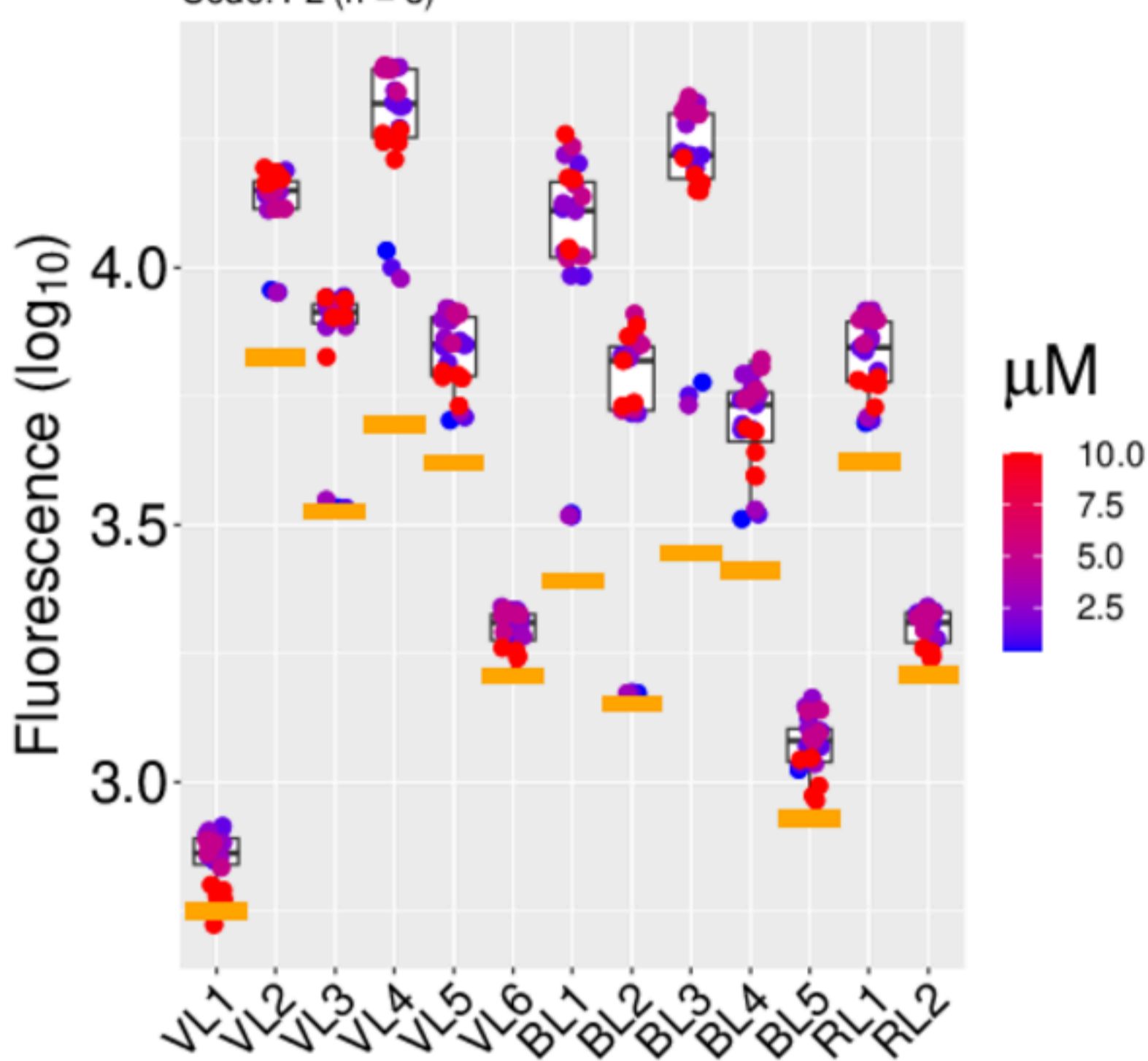
2-(N-(7-Nitrobenz-2-oxa-1,3-diazol-4-yl)Amino)-2-Deoxyglucose



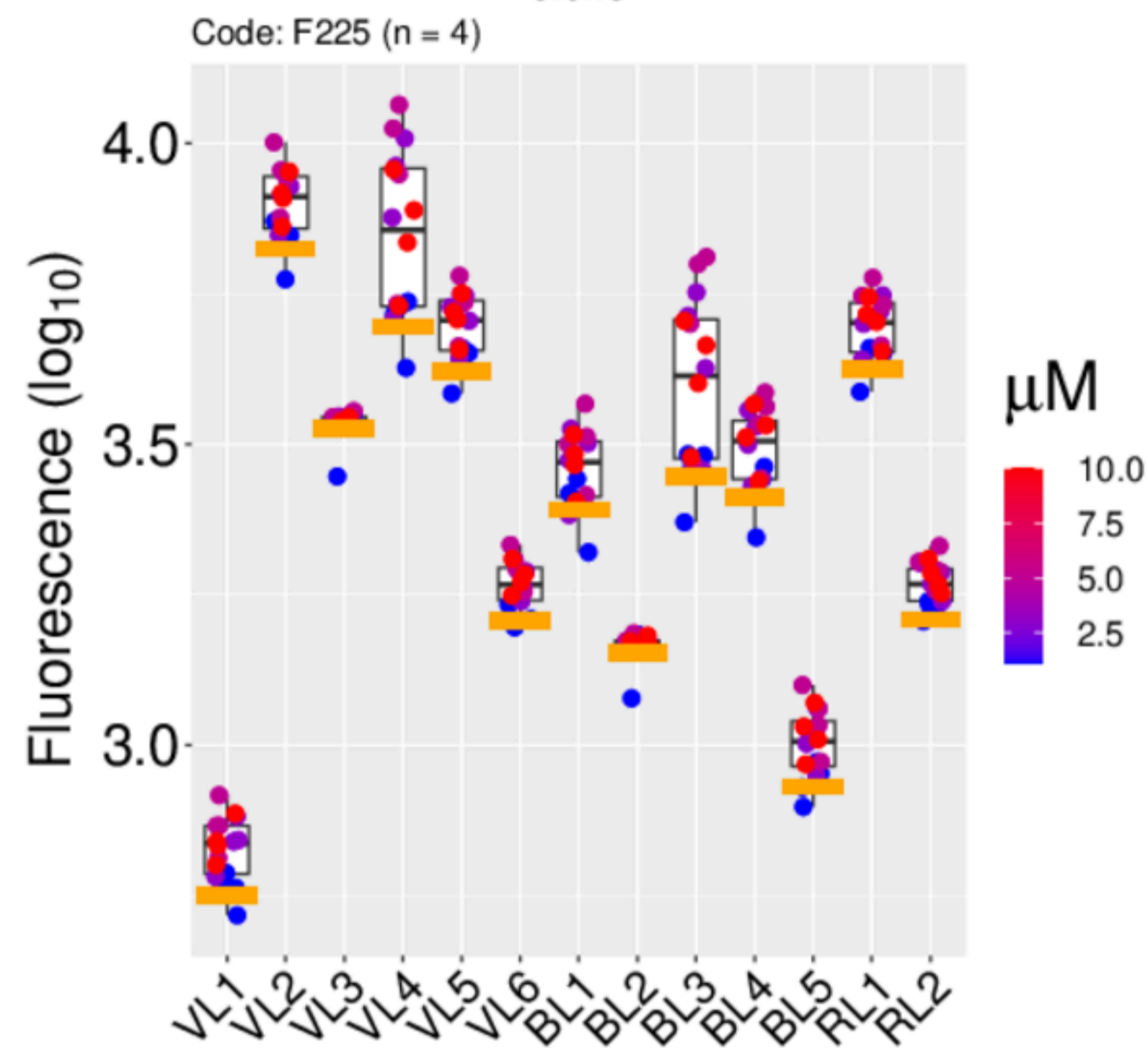
2,5-Dihydro-3,6-di-2-thienyl-pyrrolo[3,4-c]pyrrole-1,4-dione



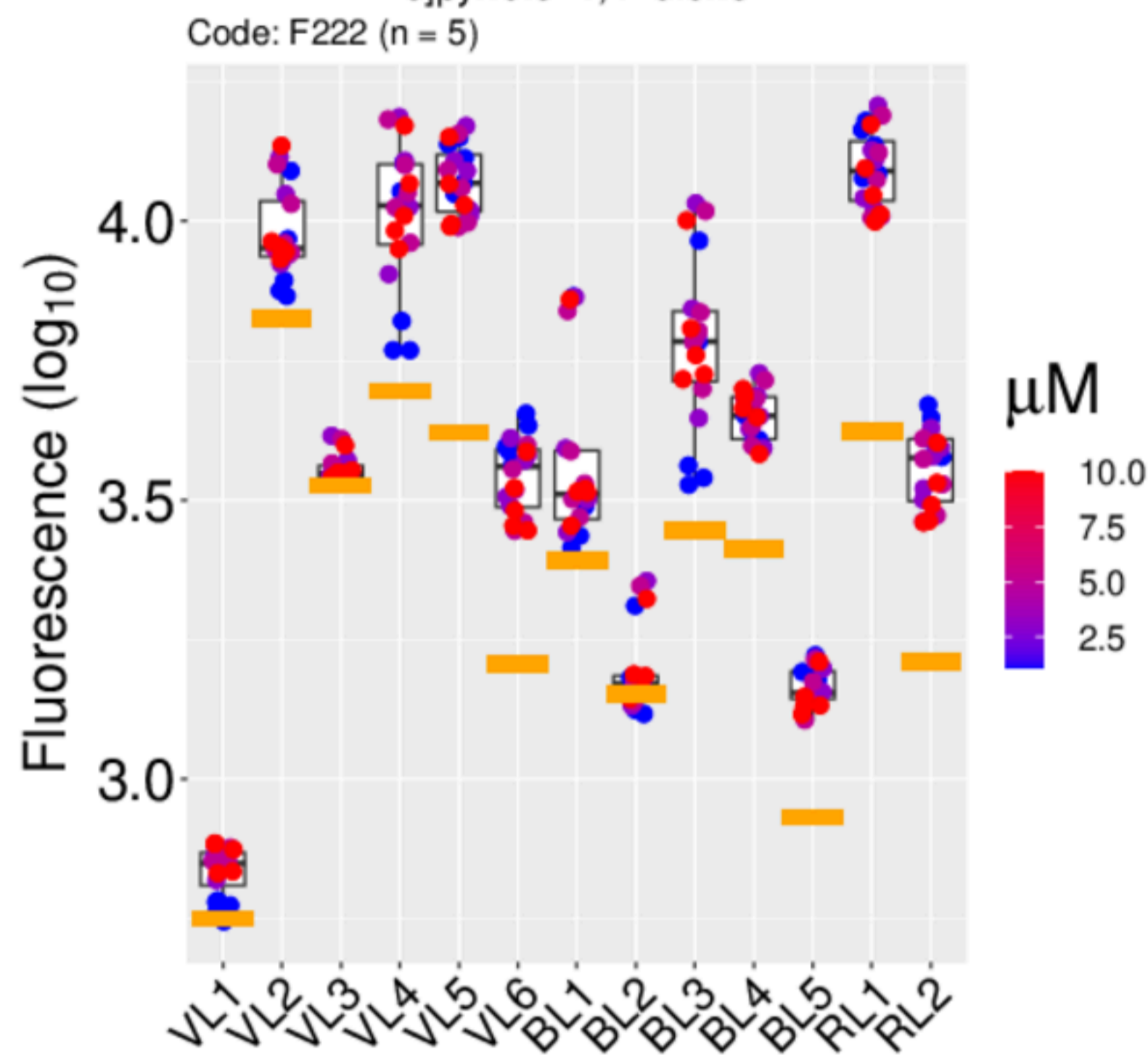
2',7'-Dichlorofluorescein



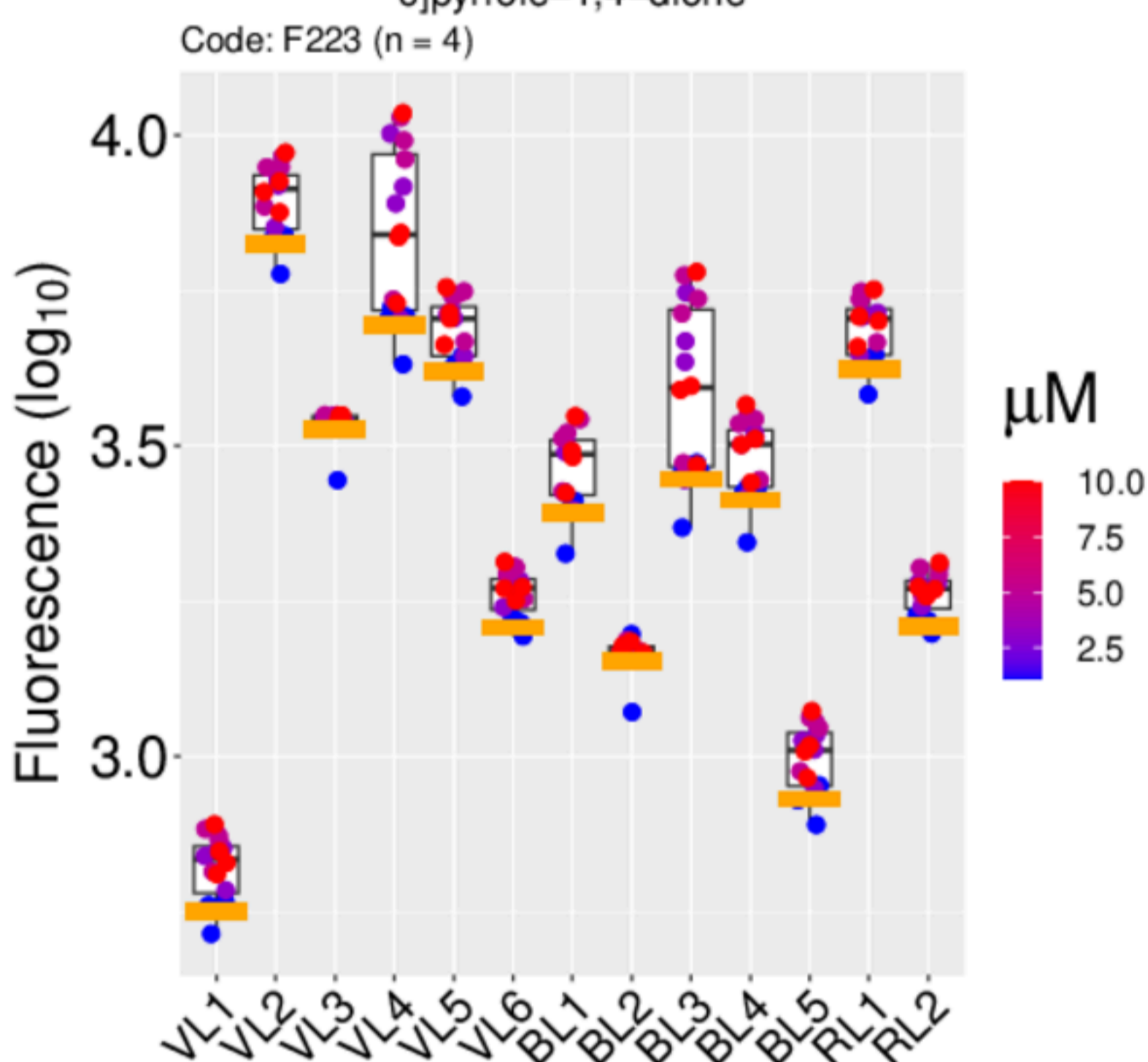
3,6-Bis(4-biphenyl)-2,5-dihydropyrrolo[3,4-c]pyrrole-1,4-dione



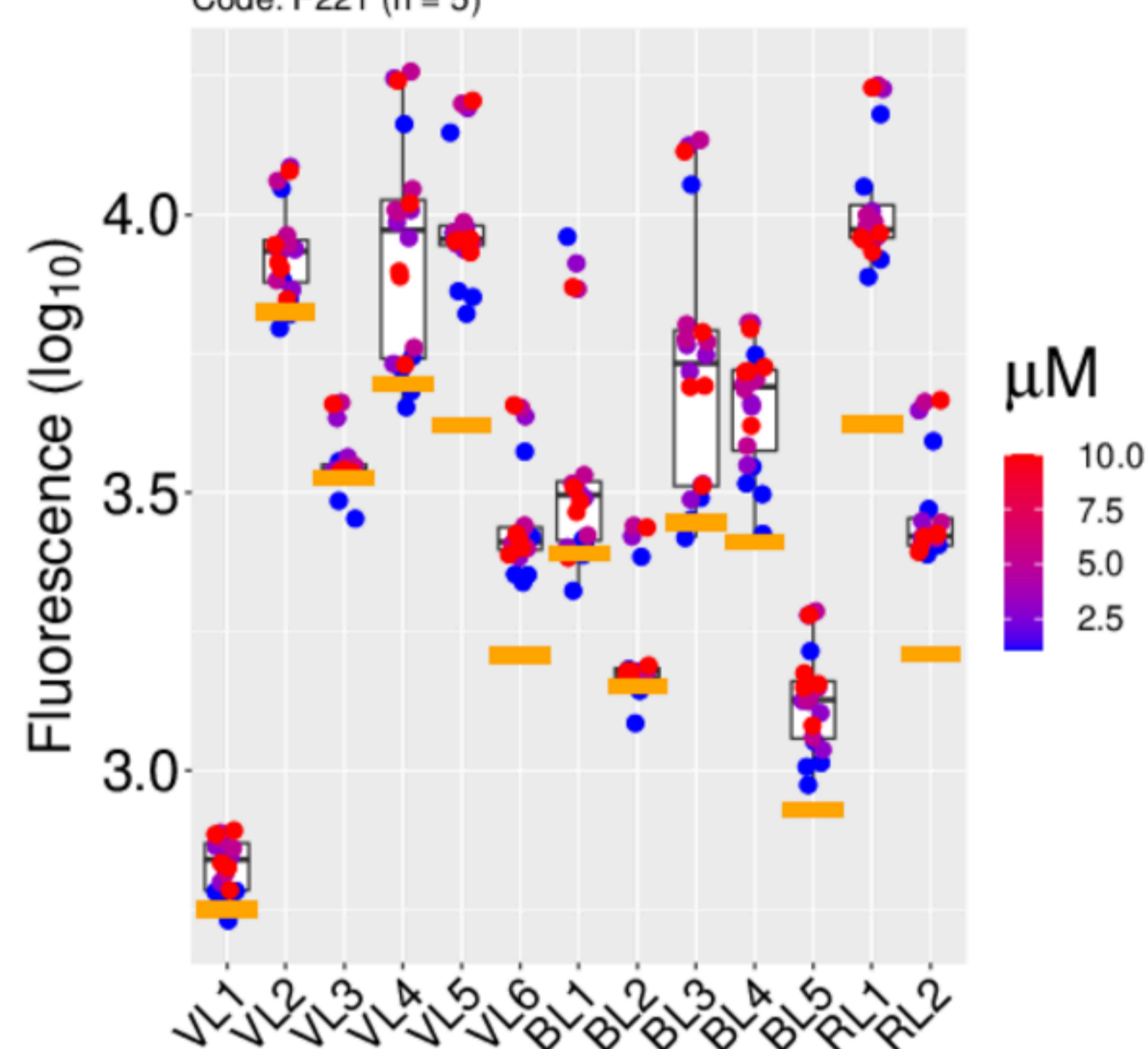
3,6-Bis(4-chlorophenyl)-2,5-dihydropyrrolo[3,4-c]pyrrole-1,4-dione



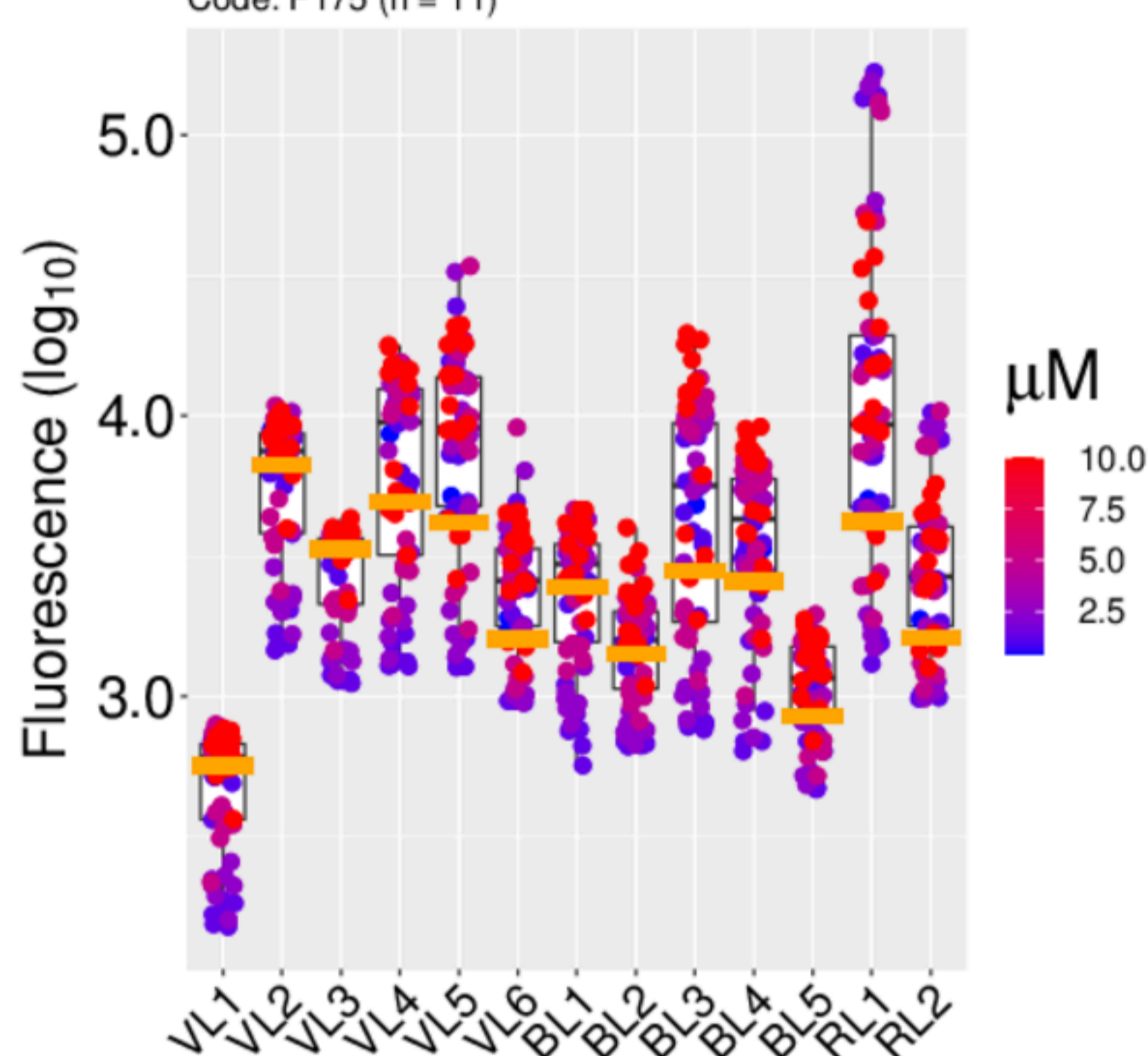
3,6-Bis(4-tert-butylphenyl)-2,5-dihydropyrrolo[3,4-c]pyrrole-1,4-dione



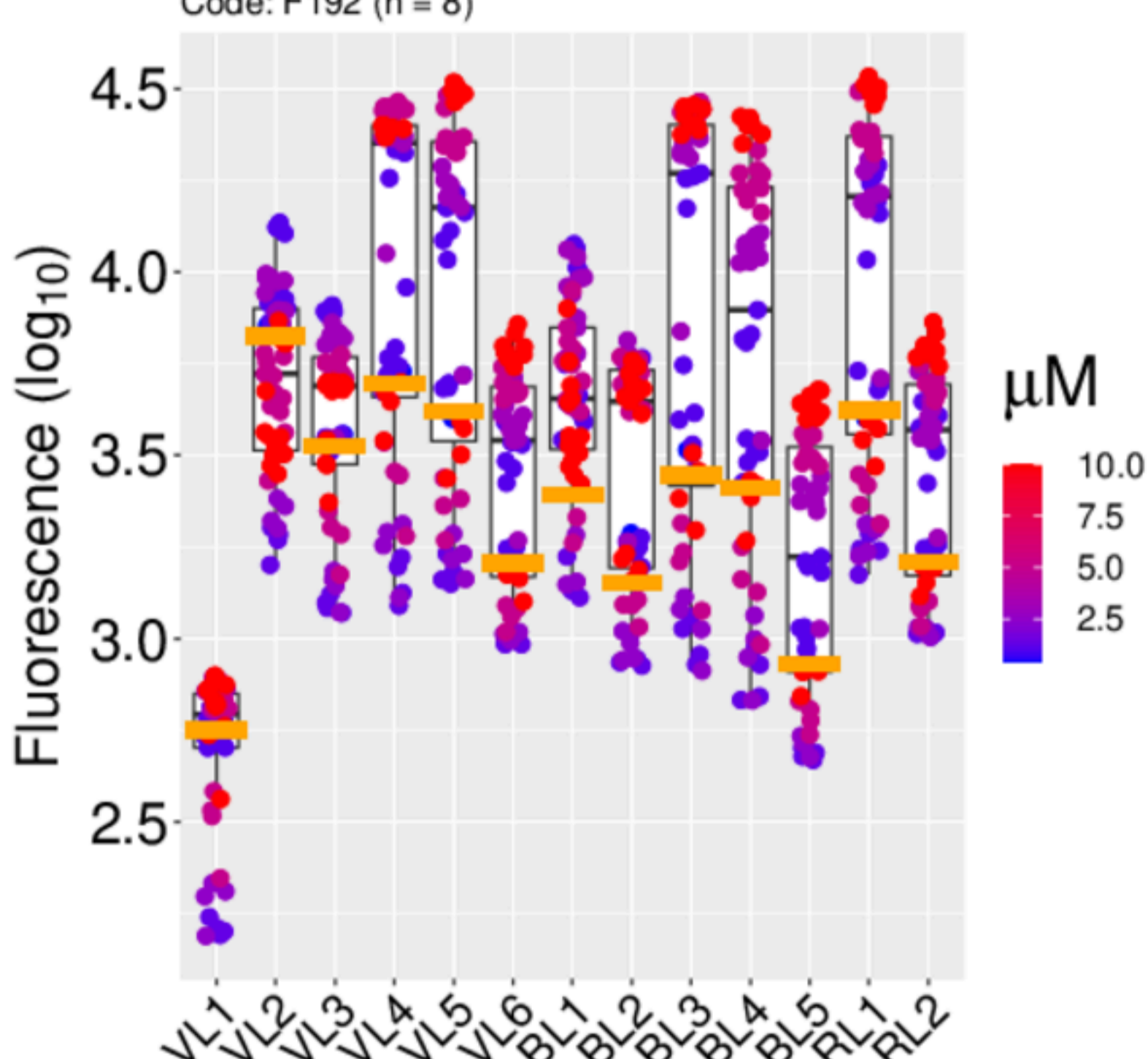
3,6-Diphenyl-2,5-dihydropyrrolo[3,4-c]pyrrole-1,4-dione



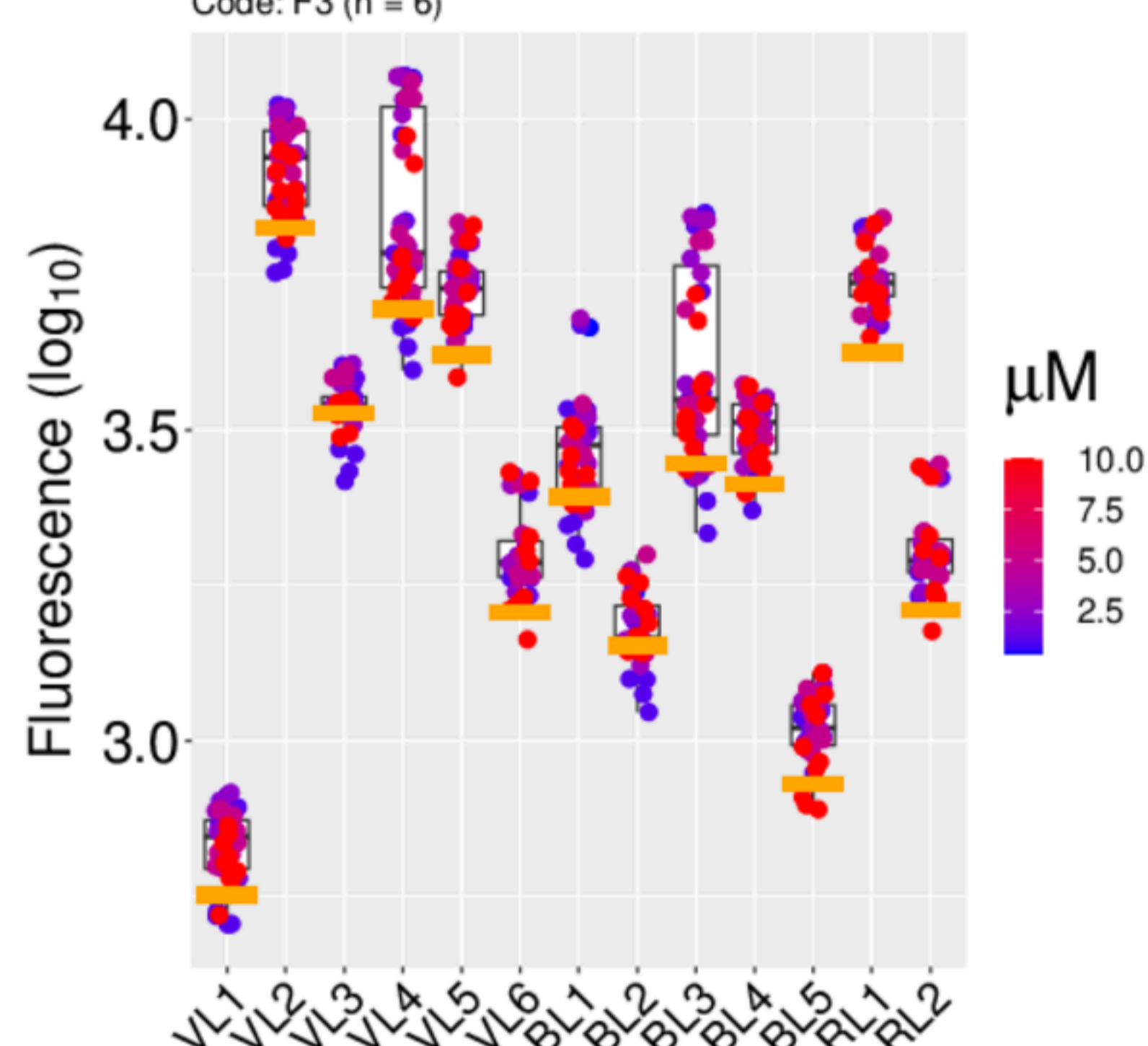
4-(4-(Dimethylamino)styryl)-N-methylpyridinium (ASP+)



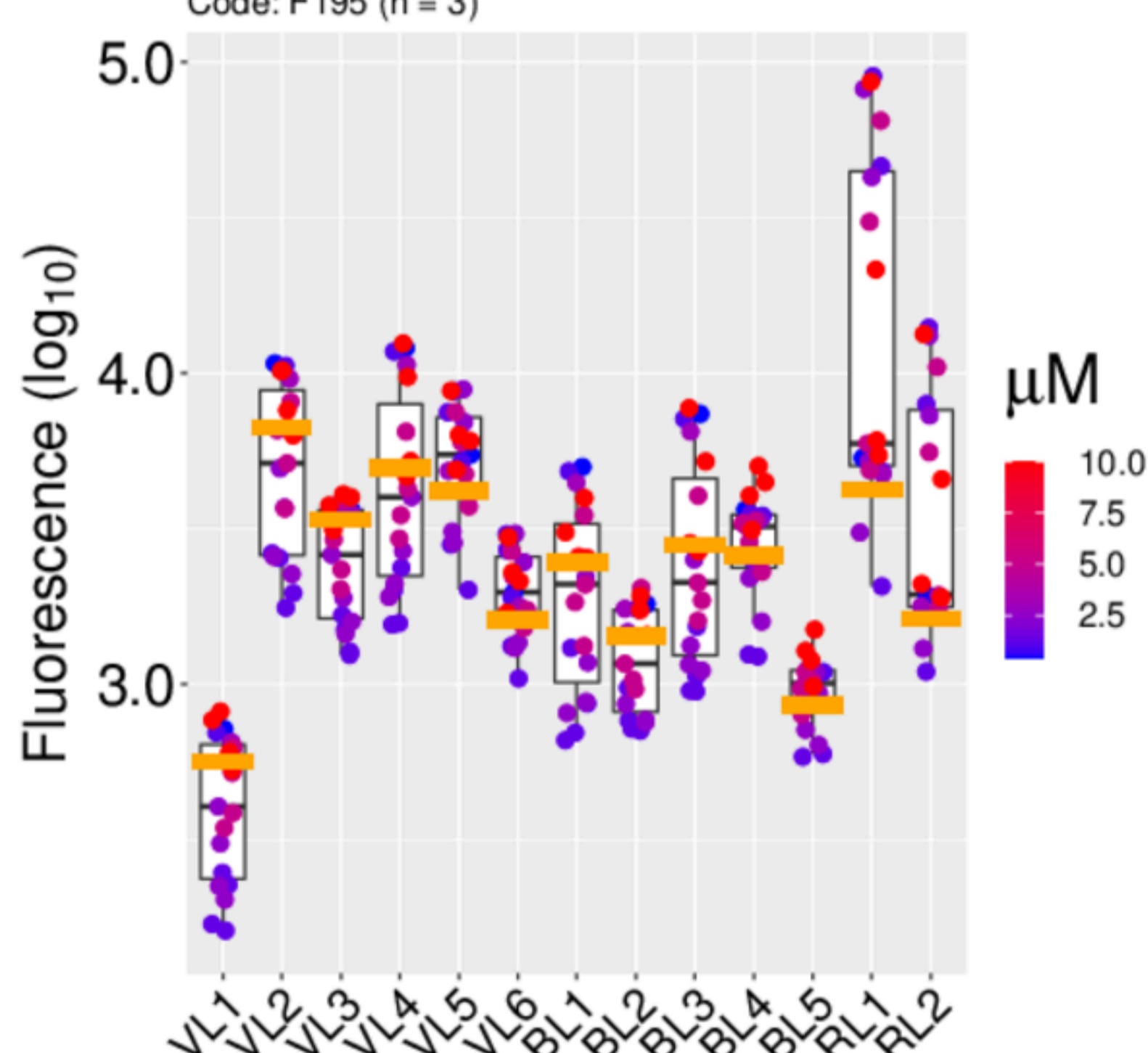
5-Carboxyfluorescein



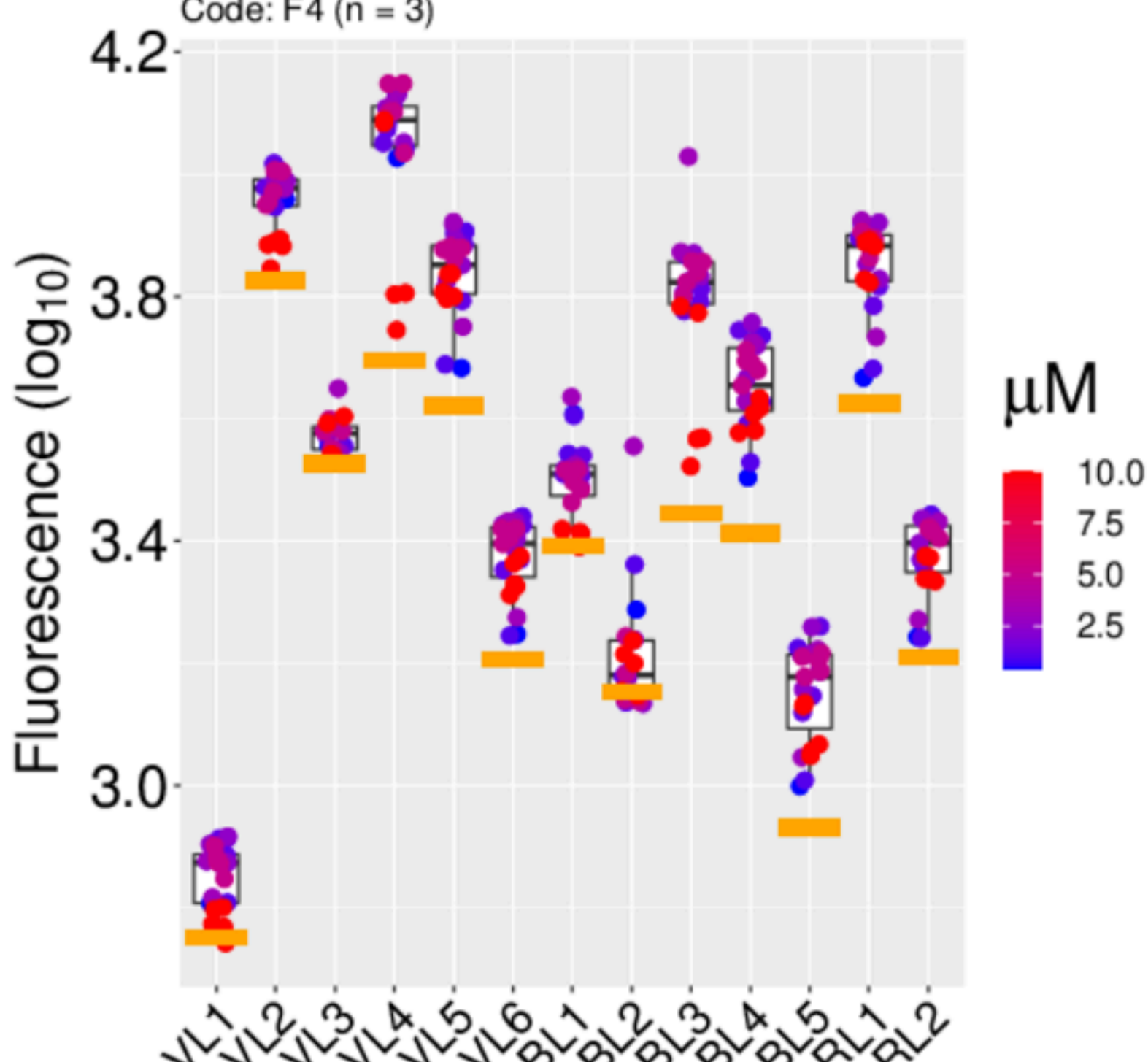
5-hydroxytryptamine (serotonin)



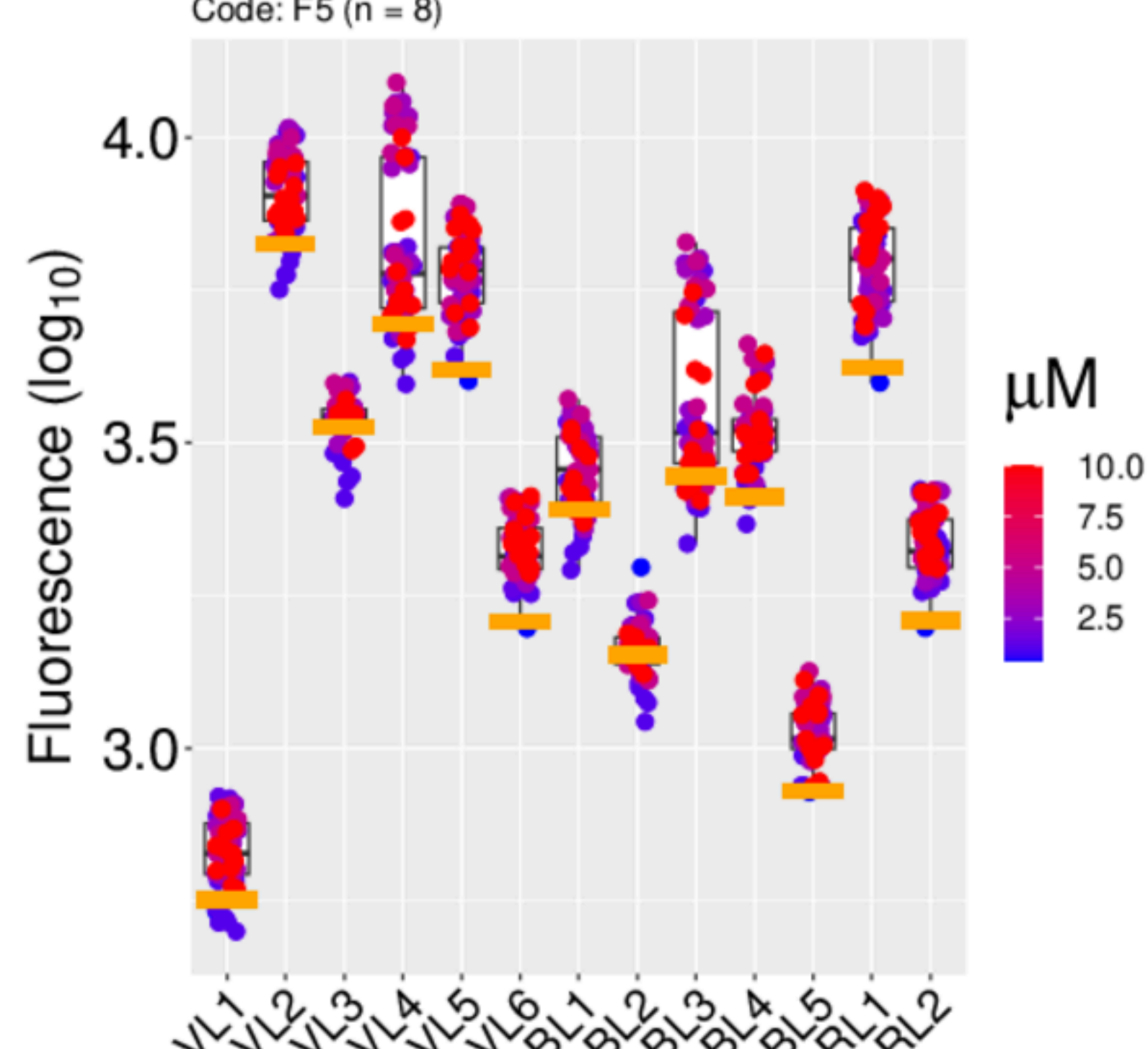
6-Carboxyfluorescein



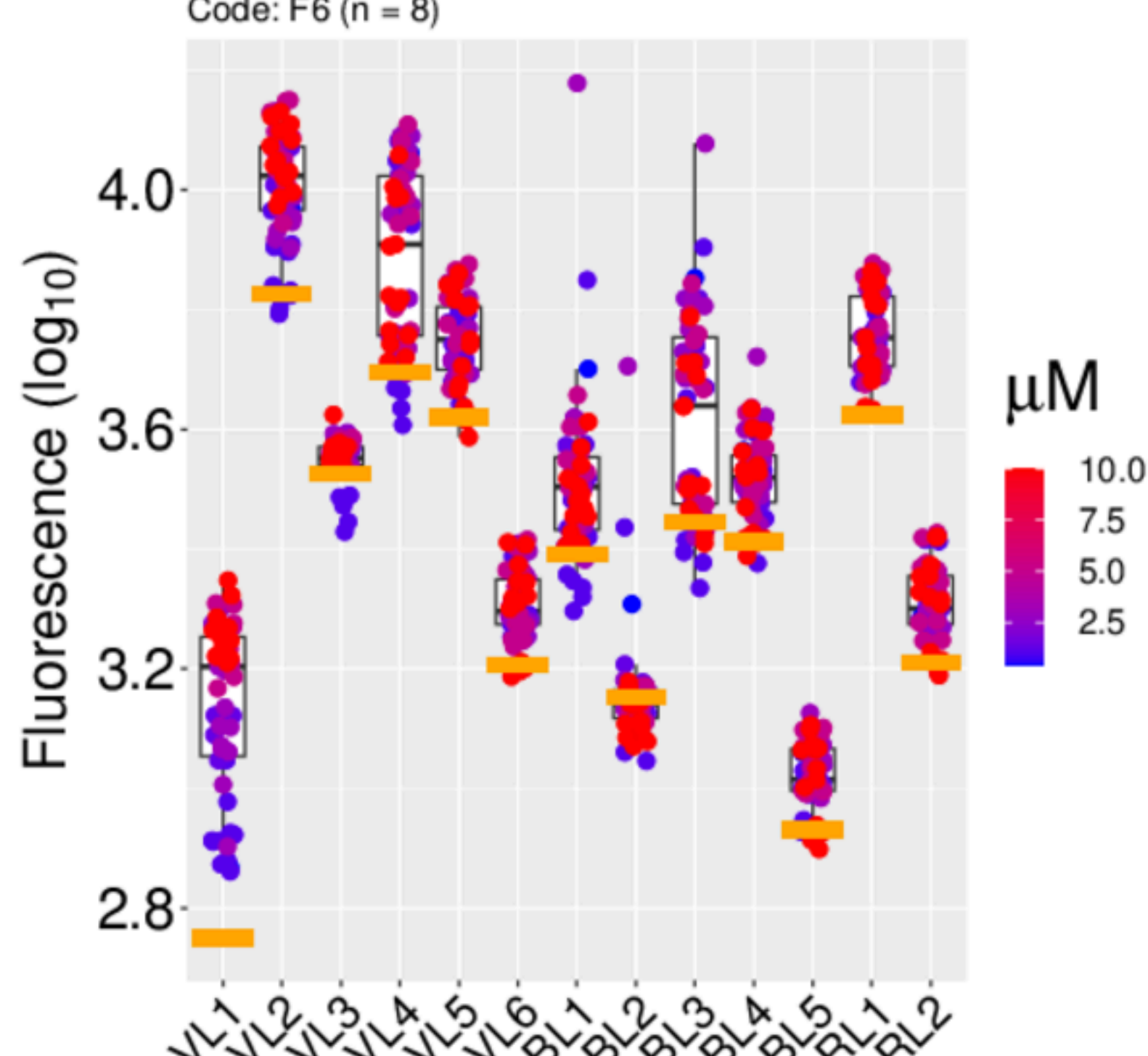
7-Aminoactinomycin D

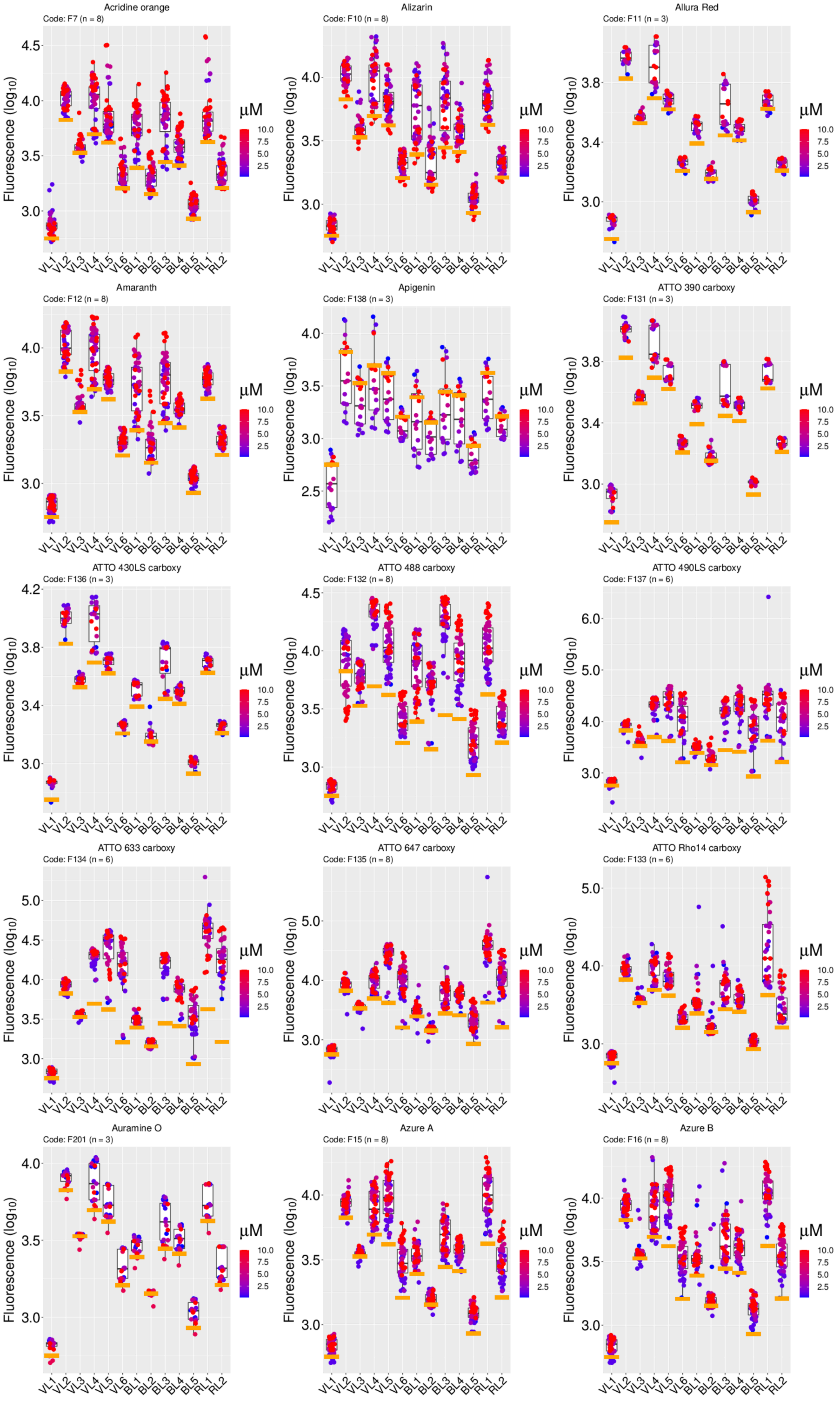


8-Anilinoanthracene-1-sulfonic acid

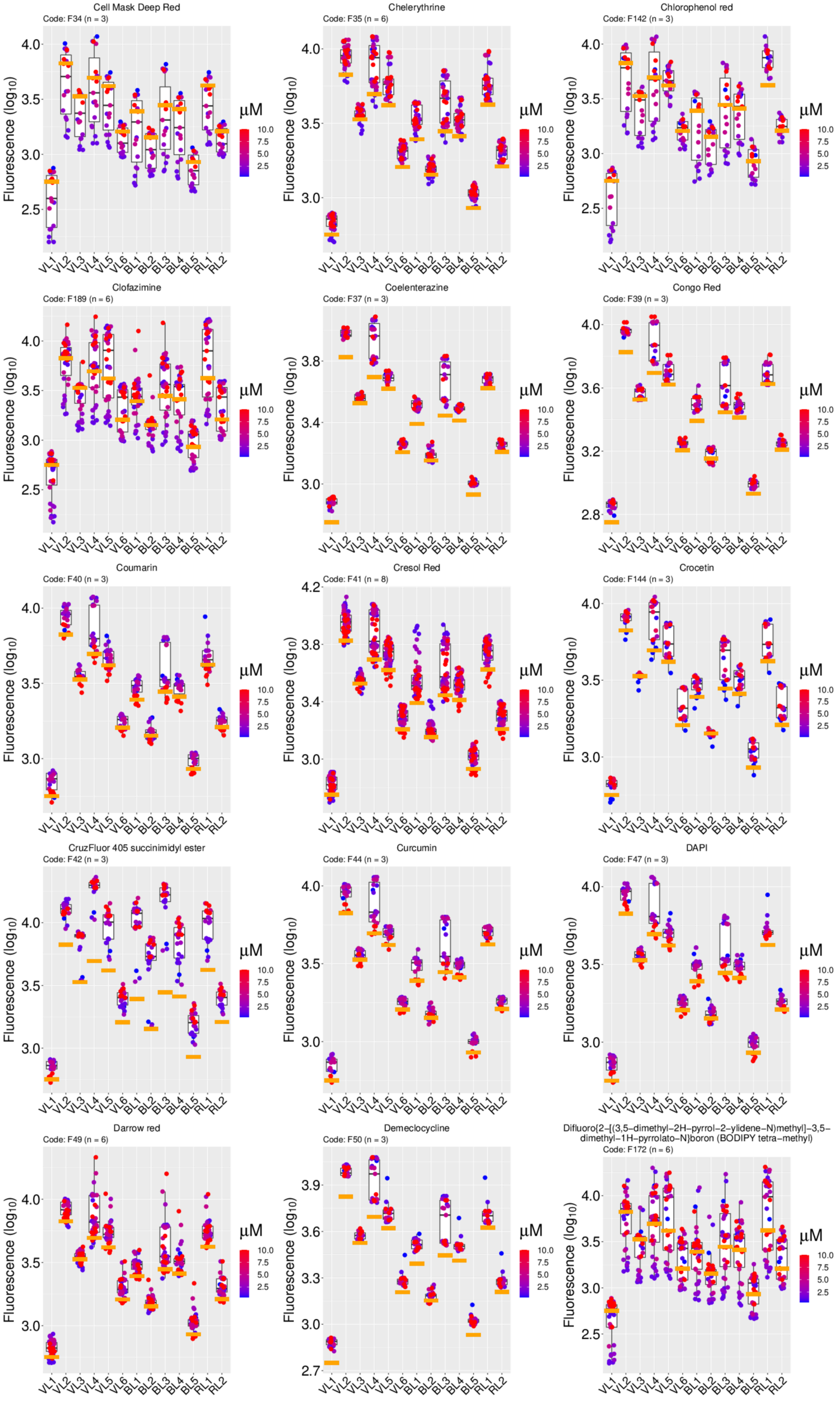


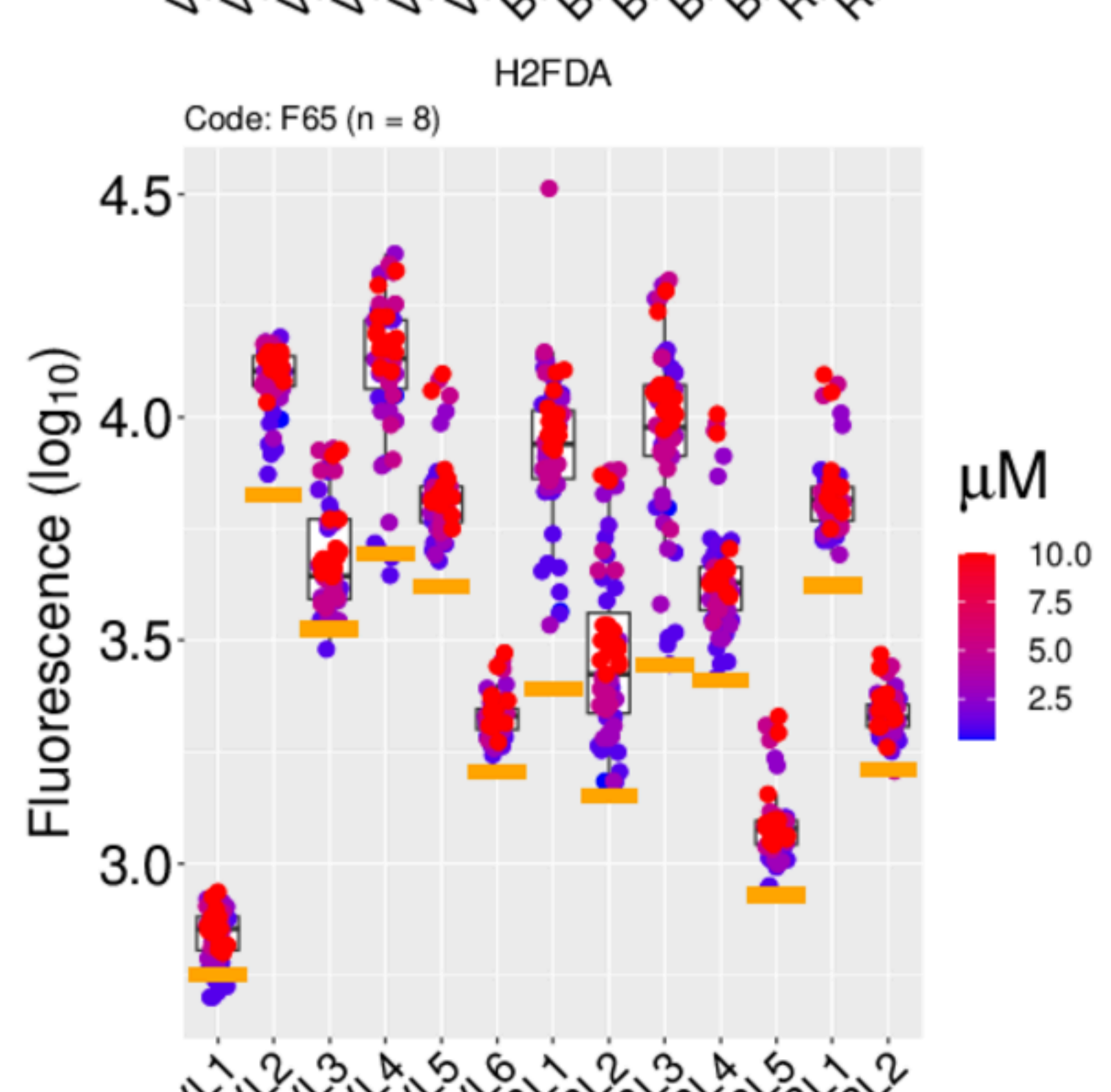
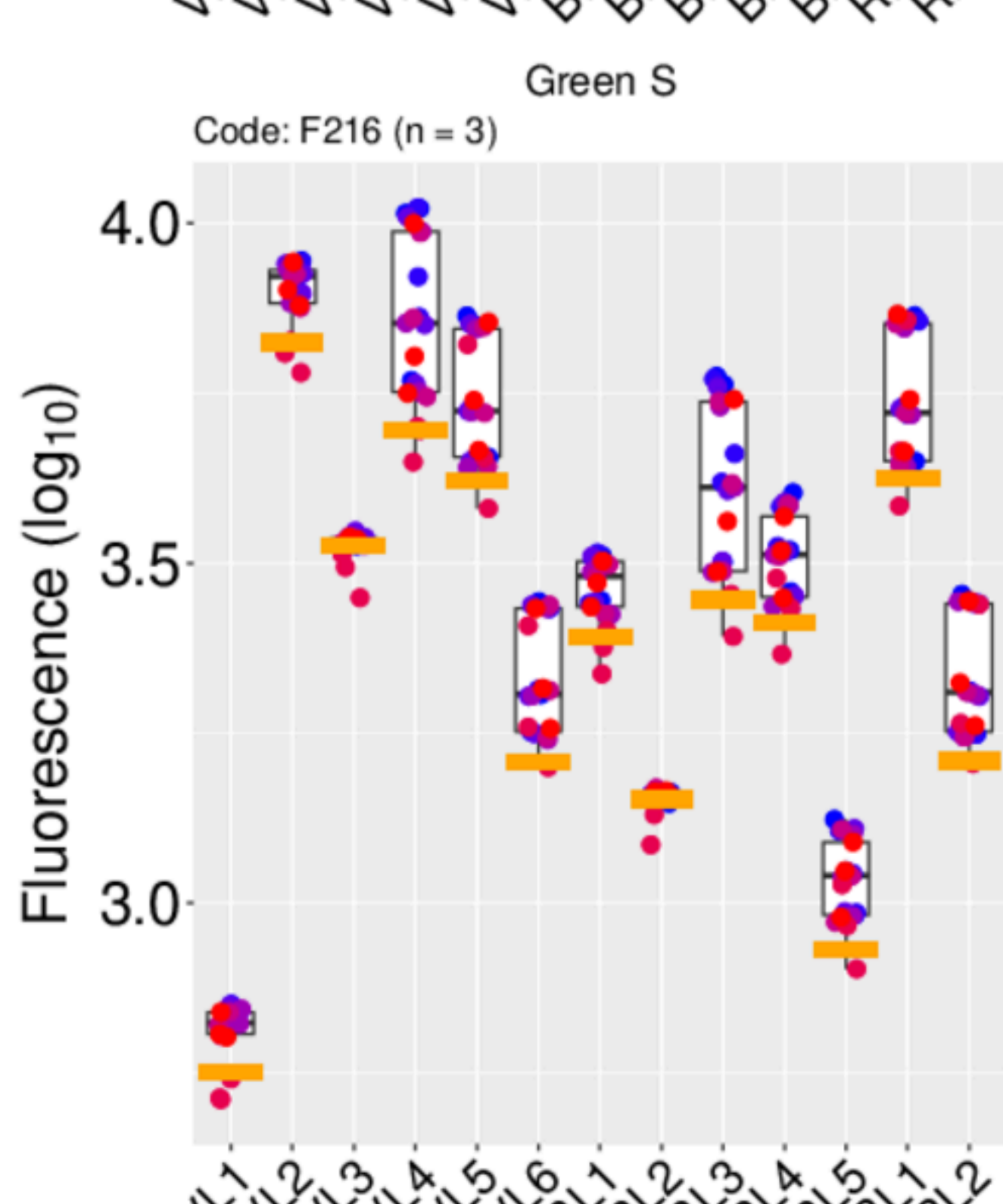
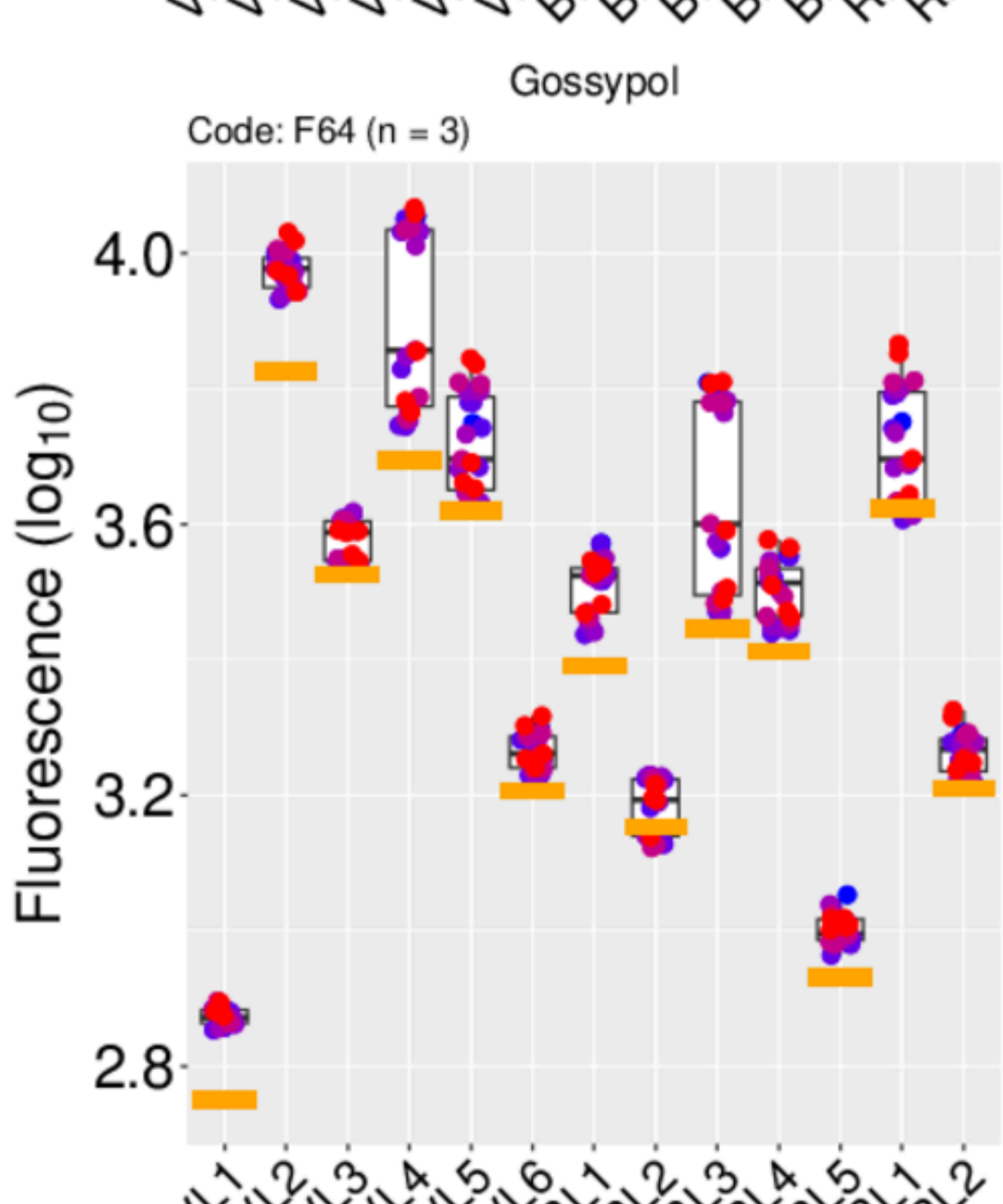
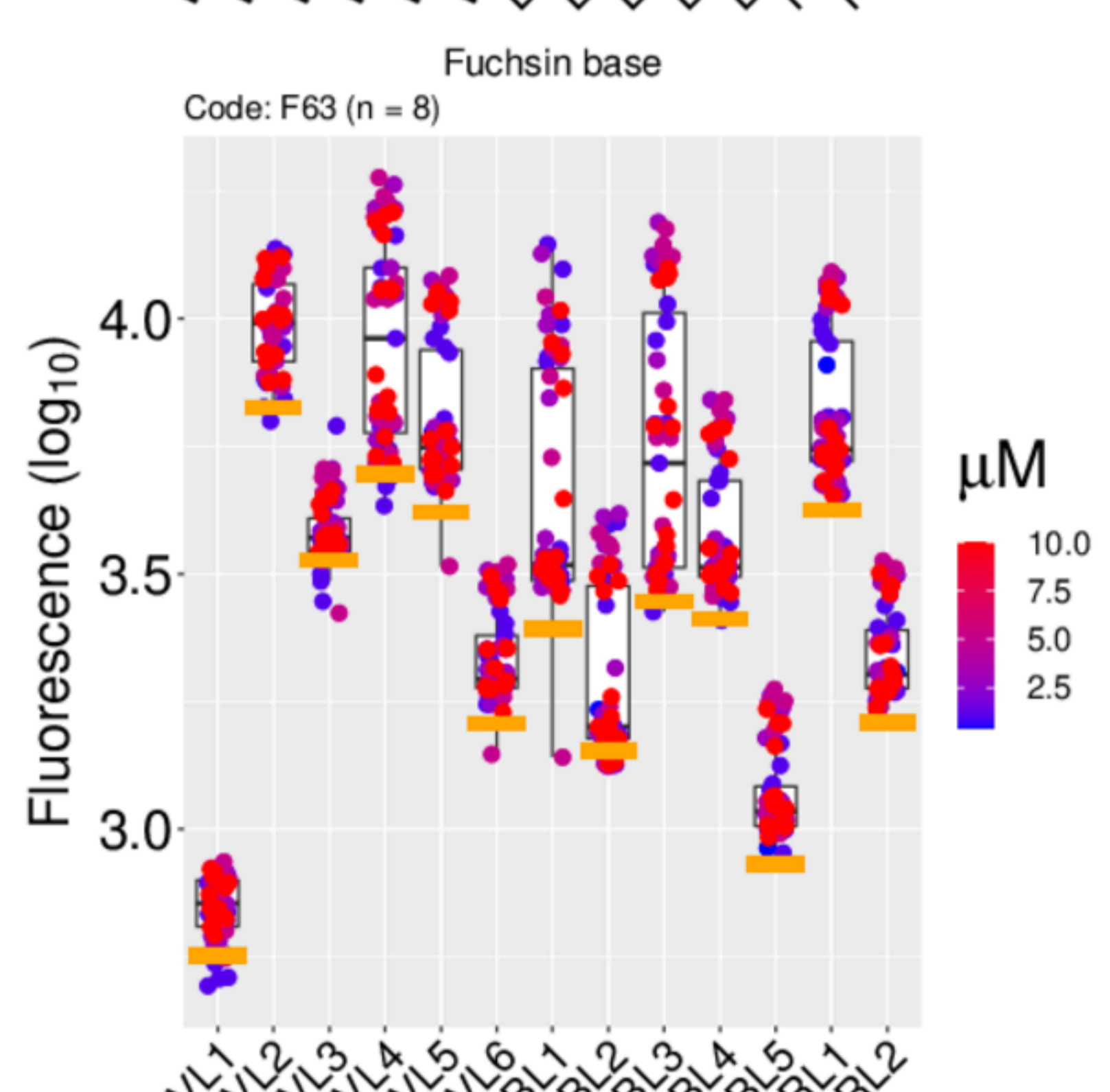
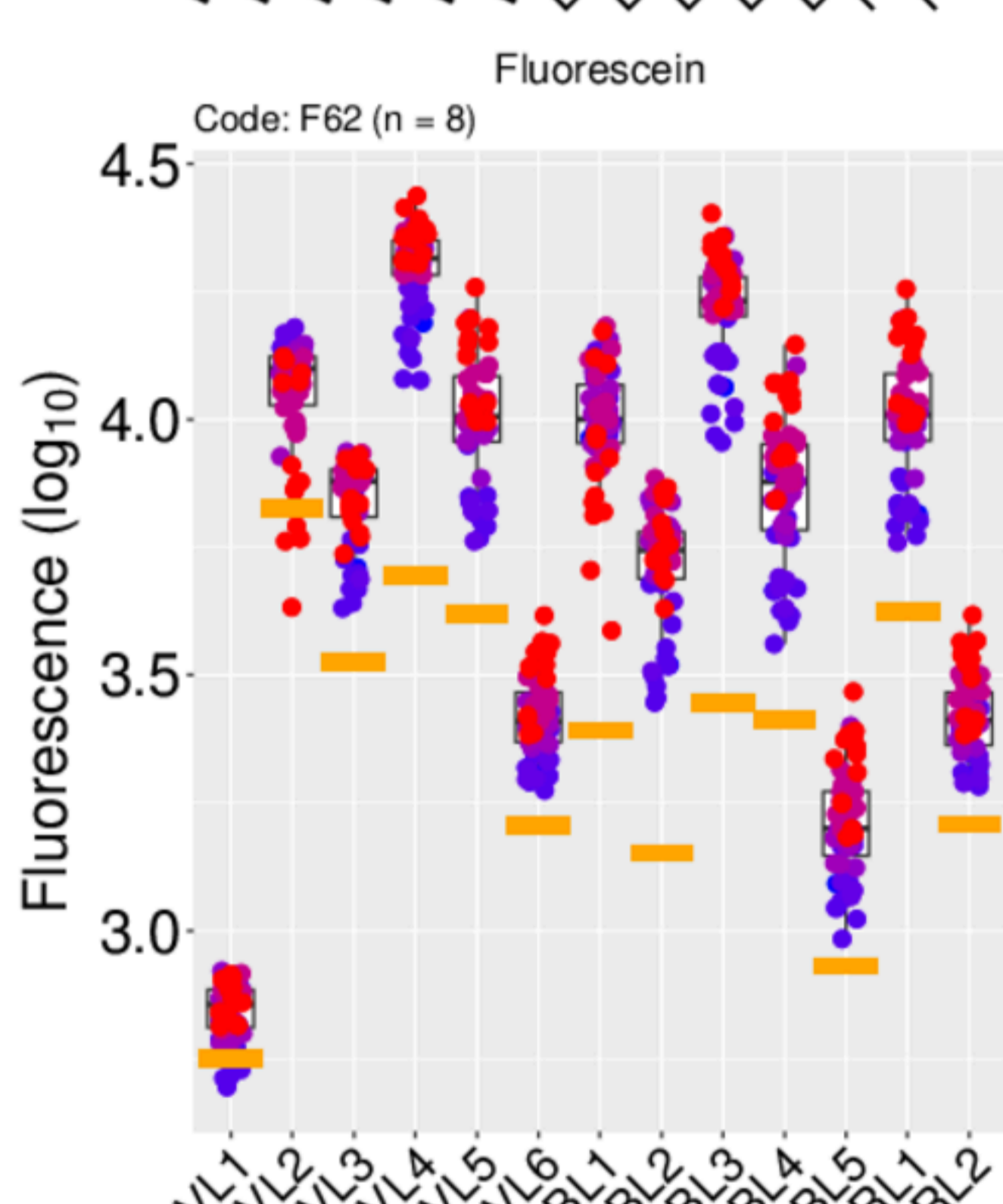
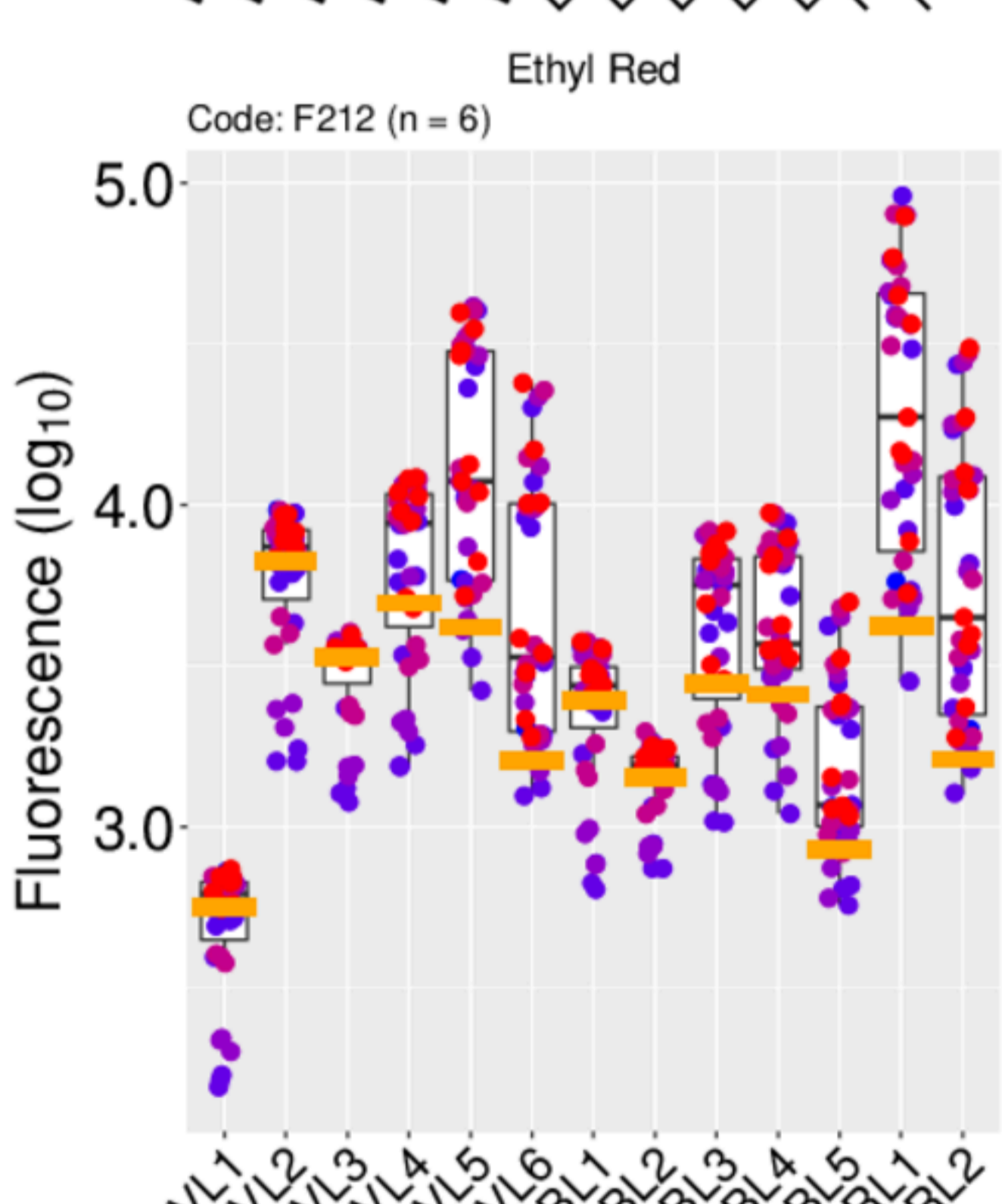
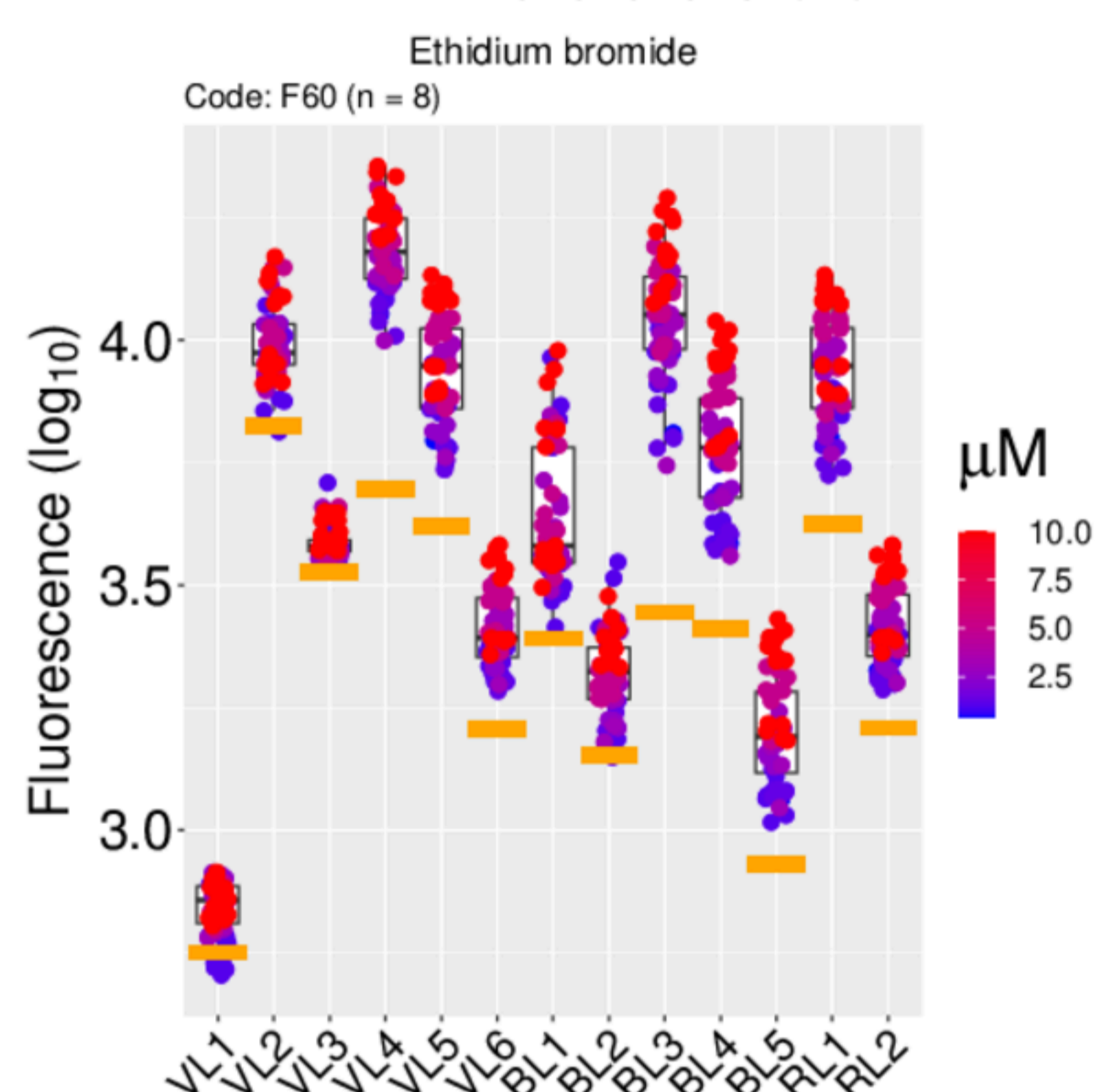
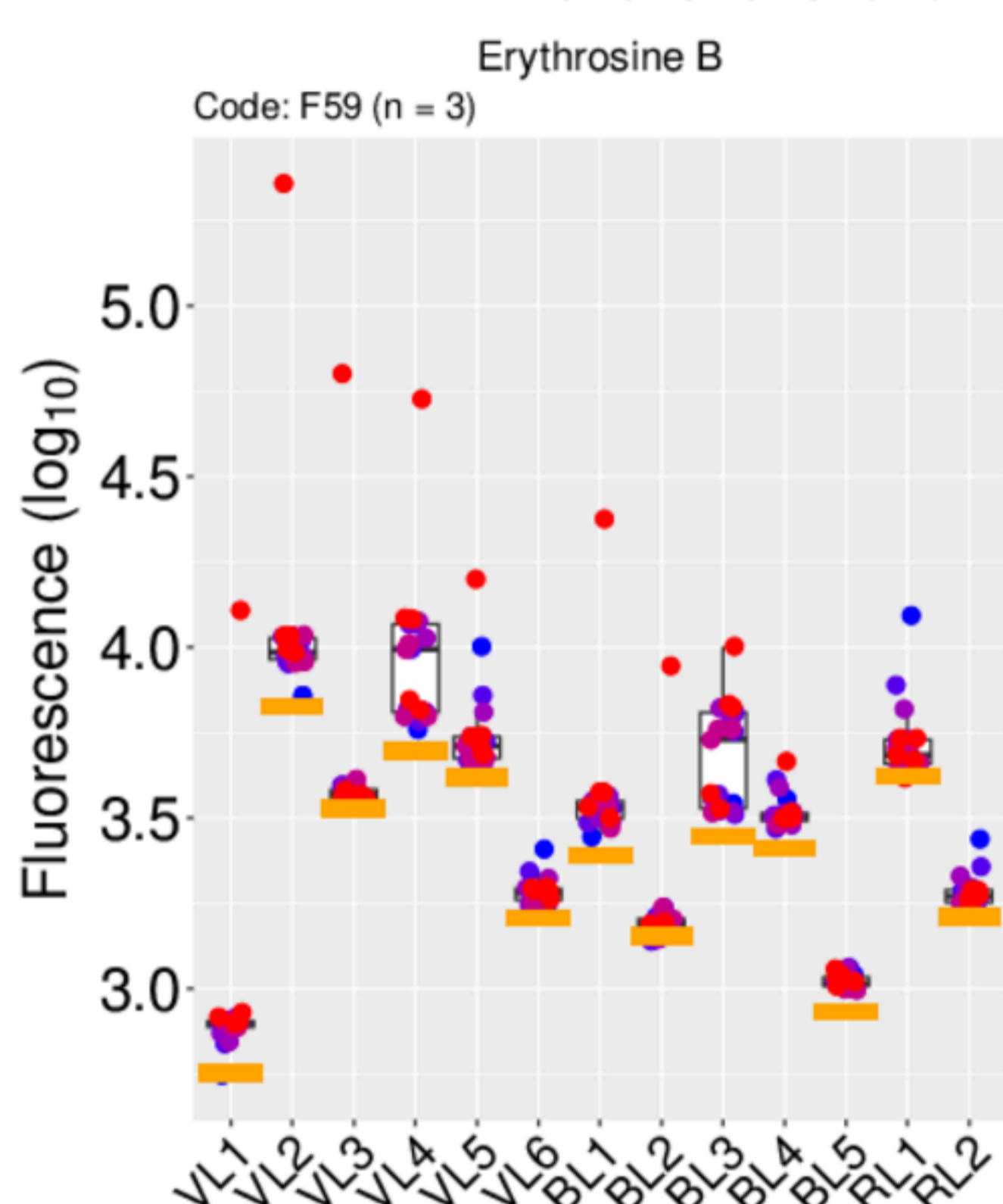
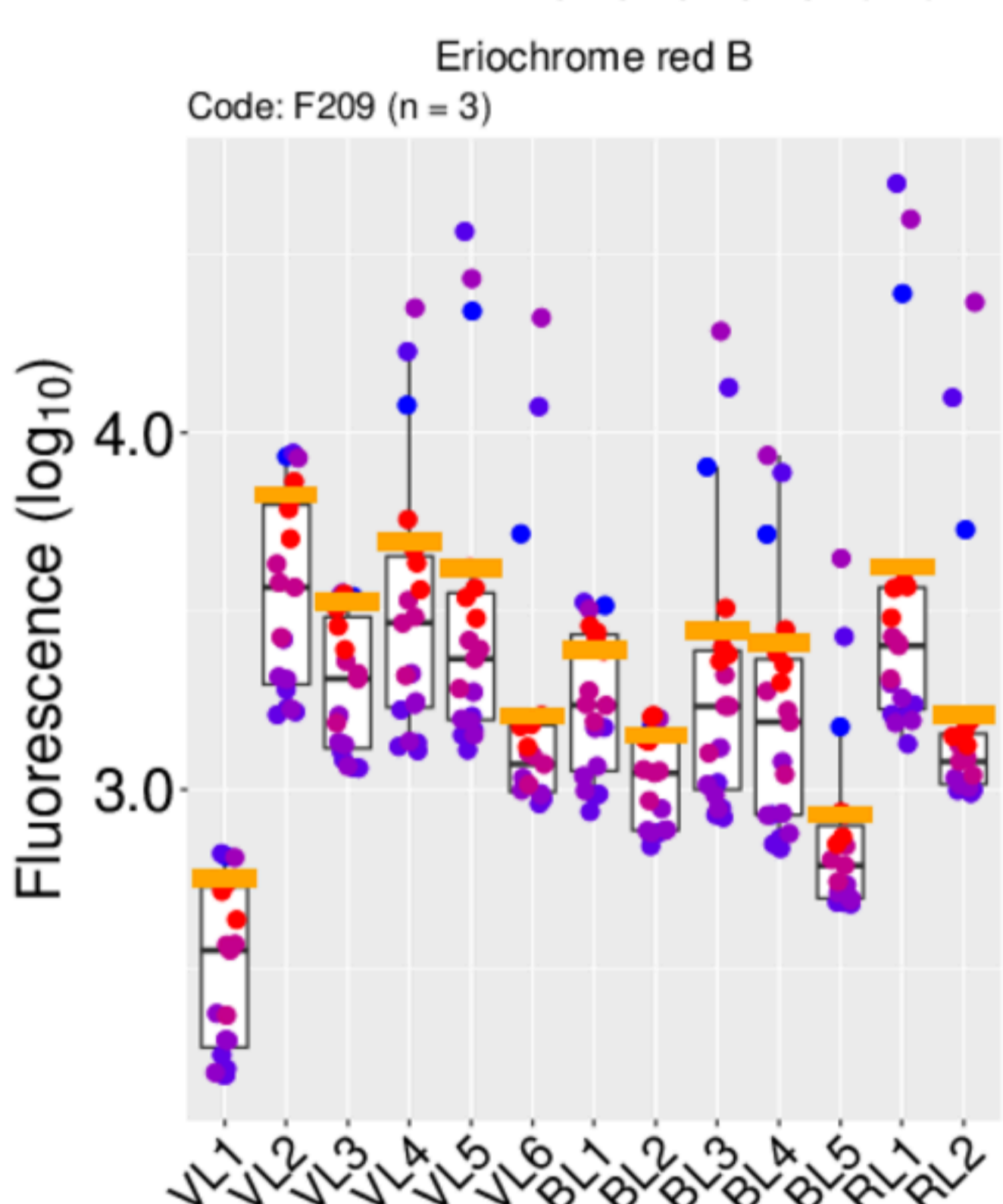
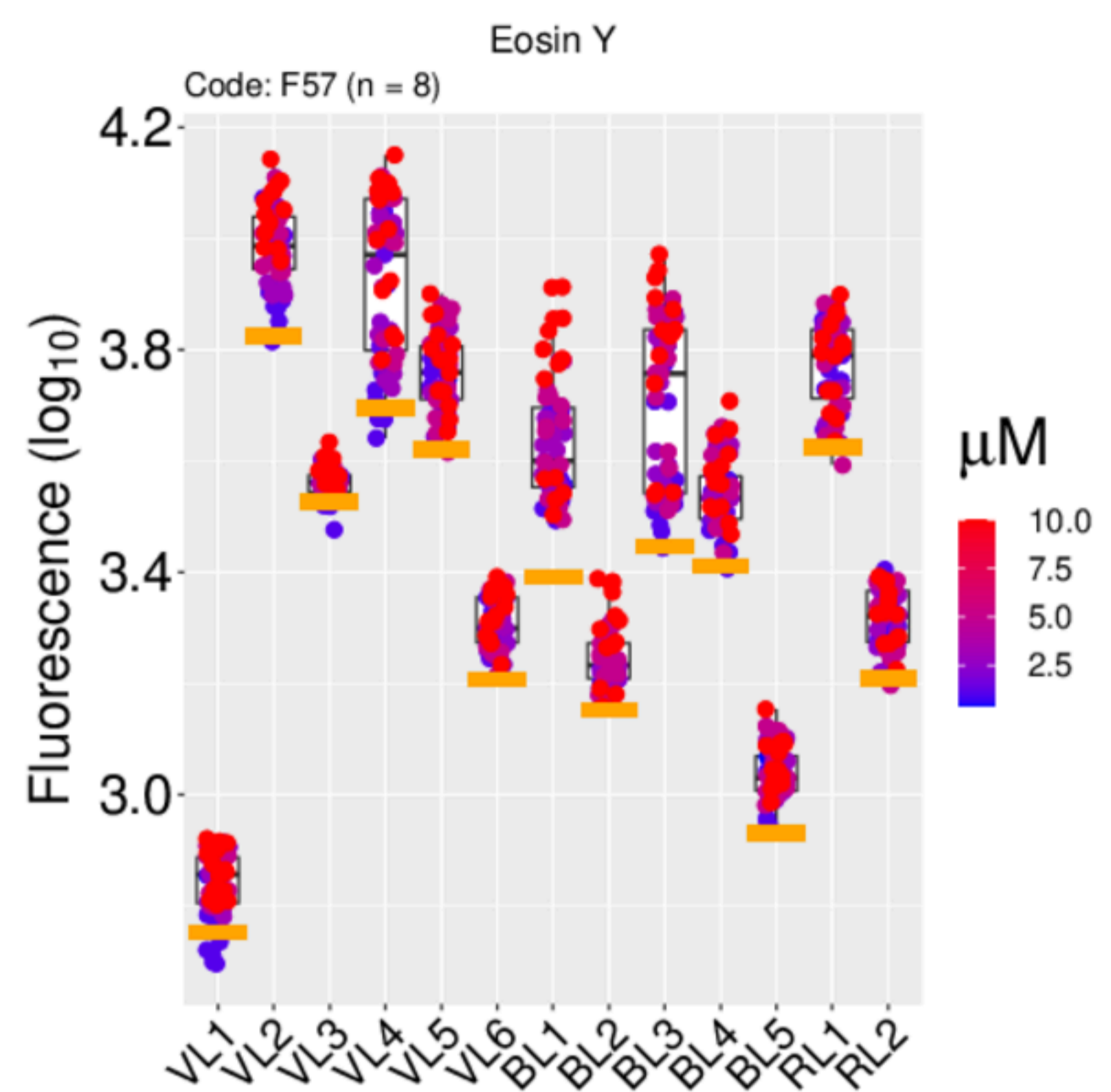
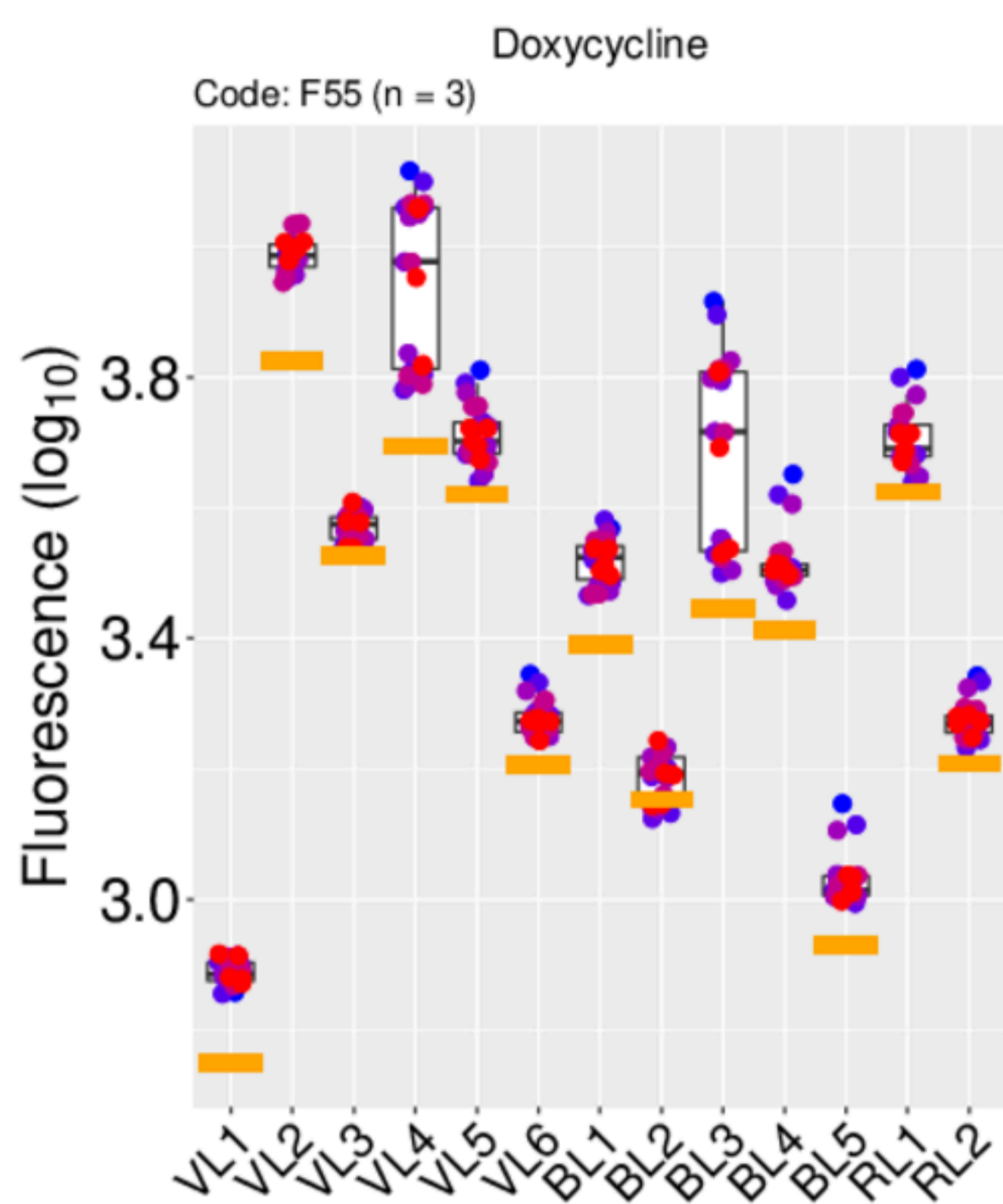
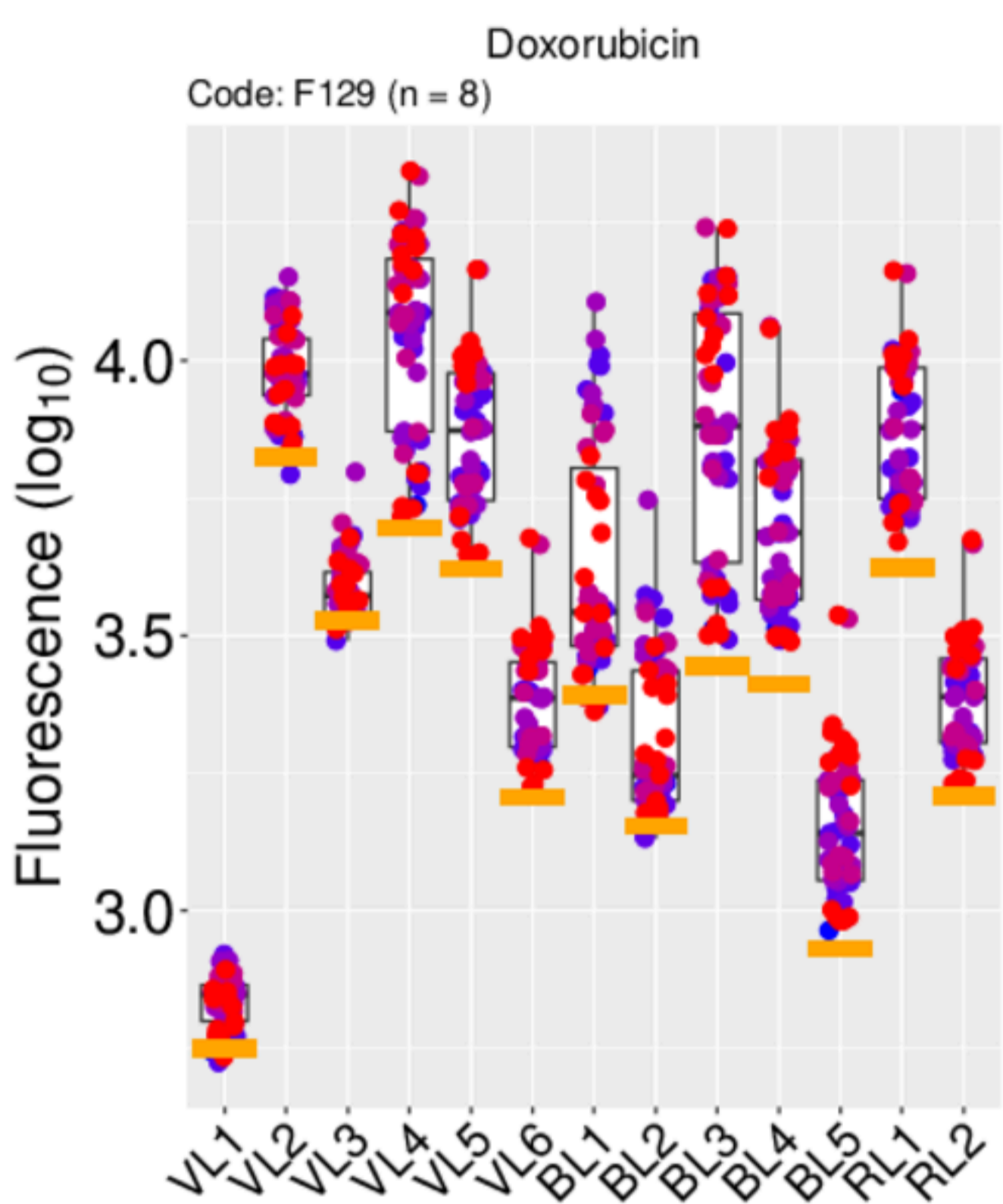
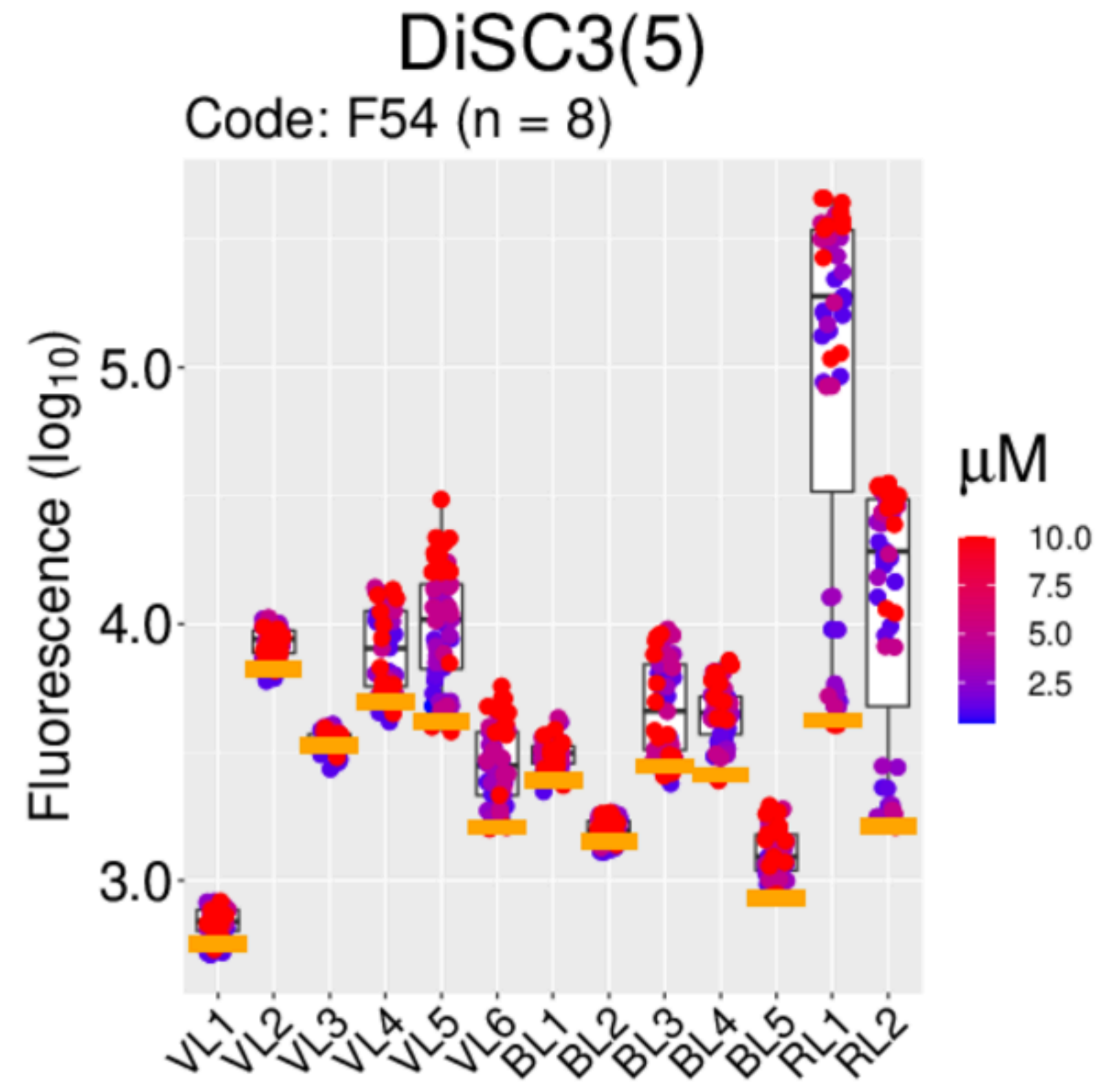
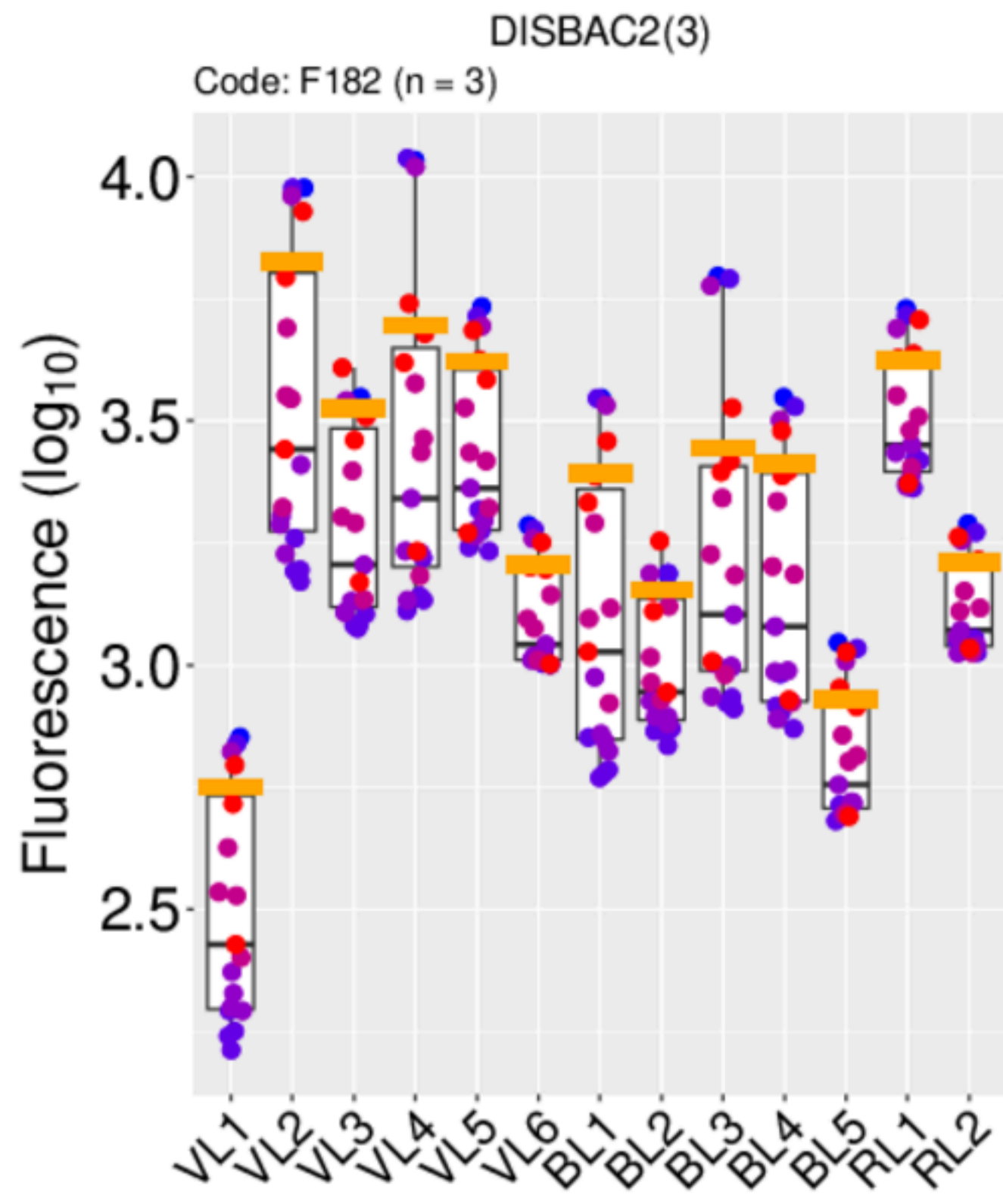
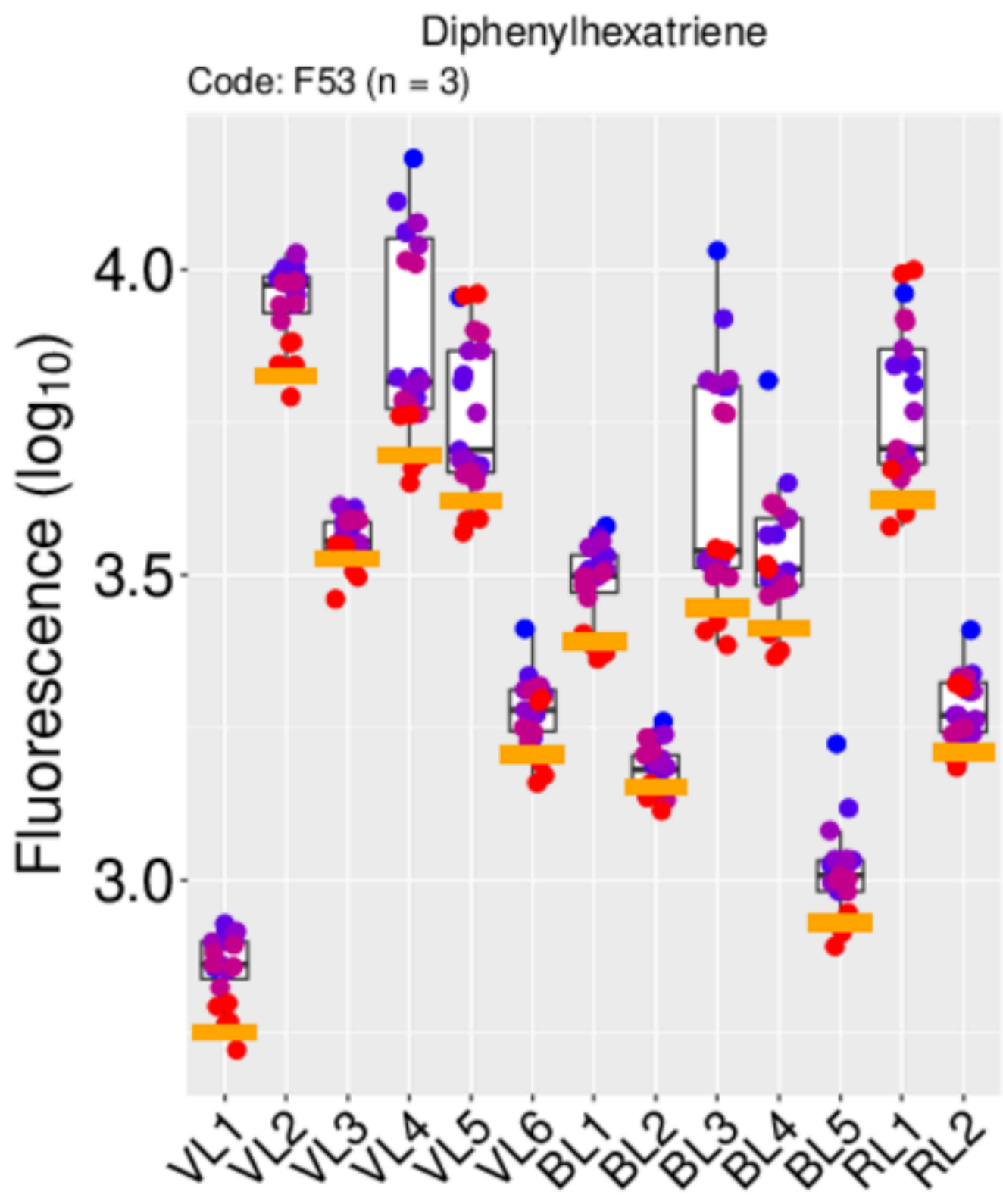
9-aminoacridine

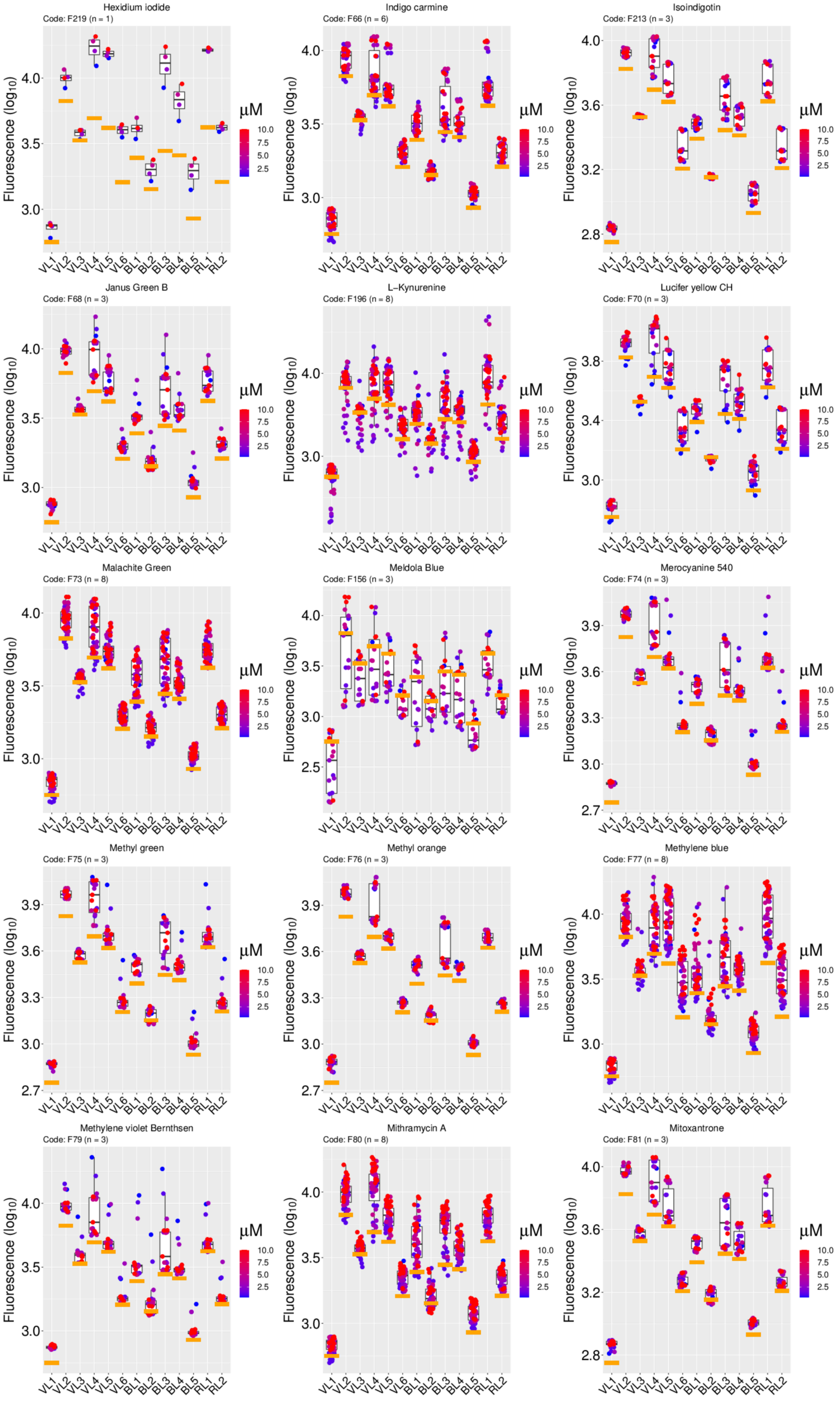




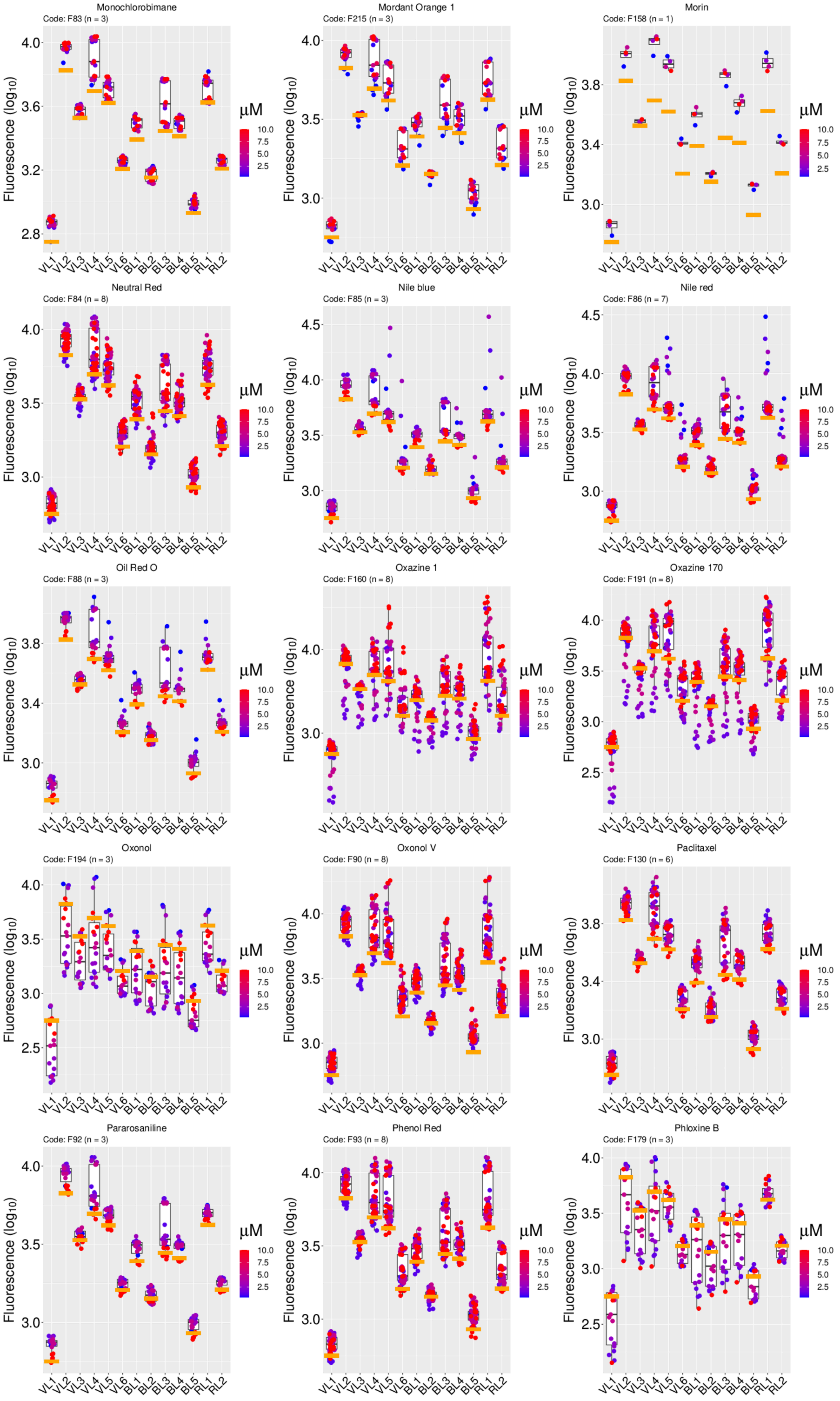


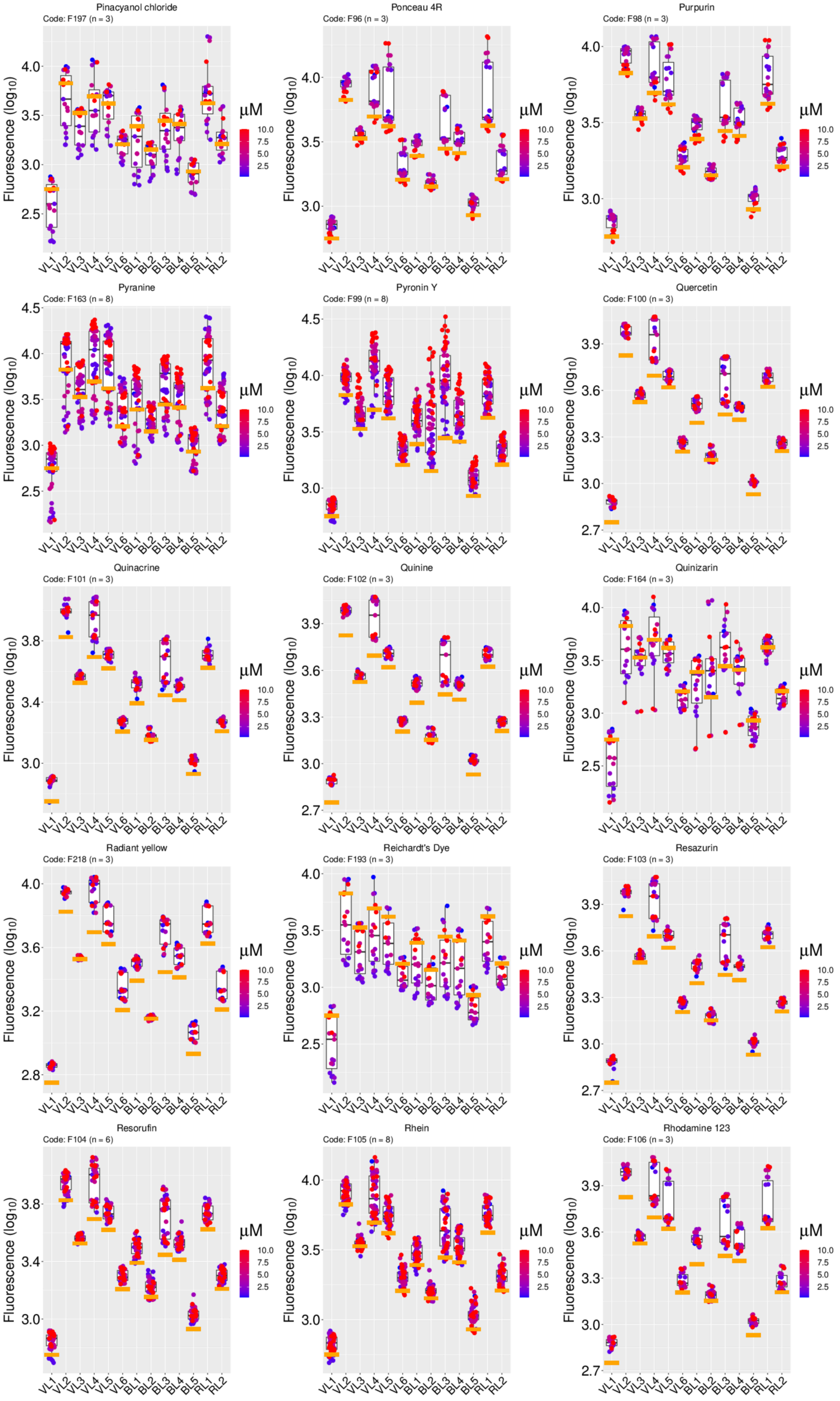




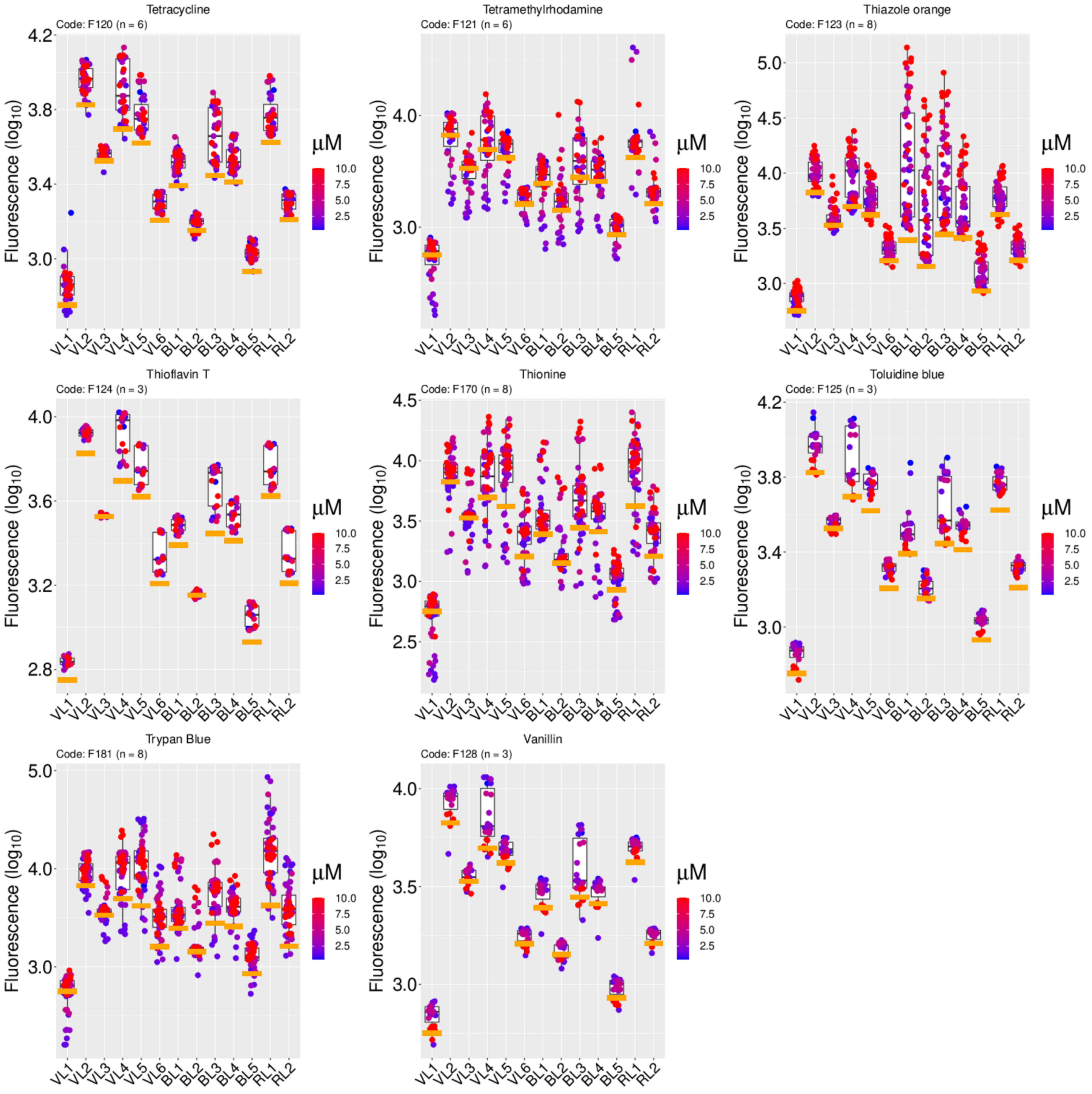




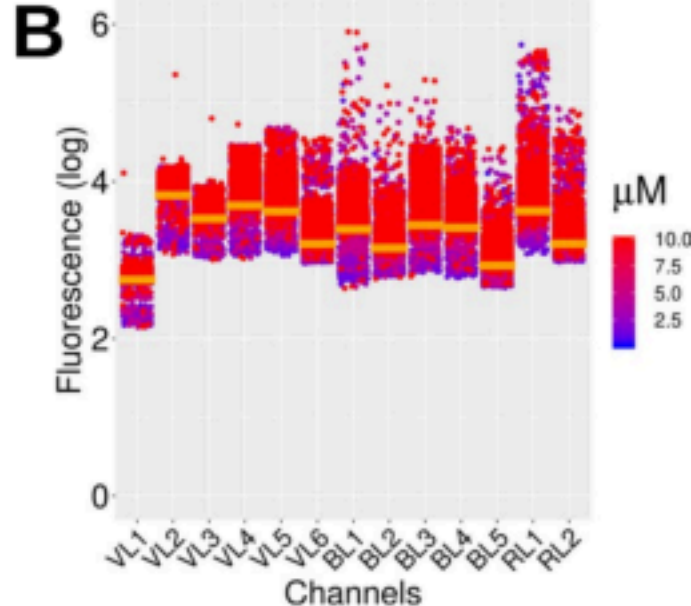
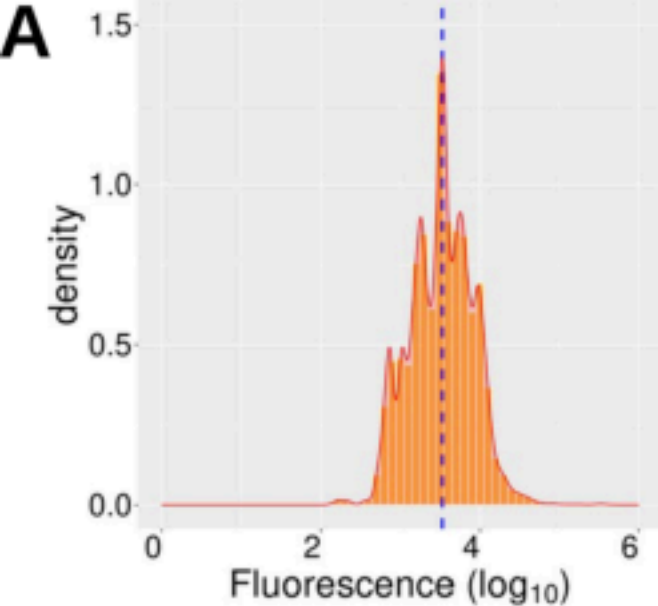




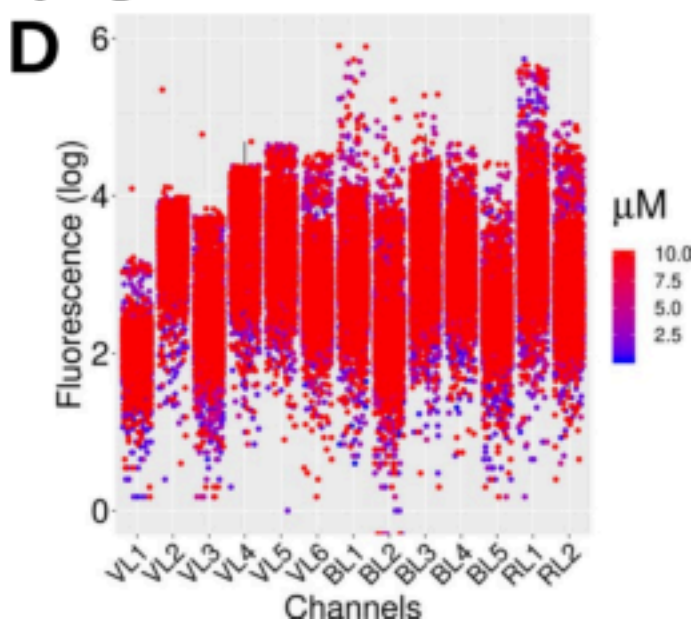
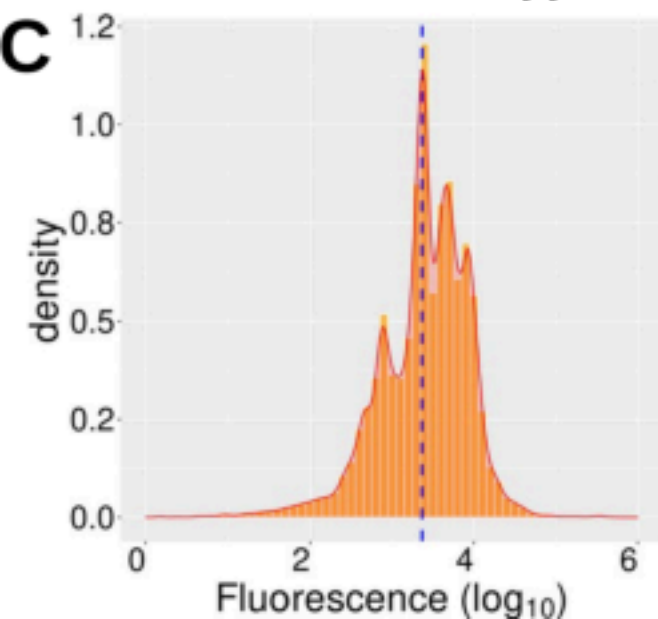


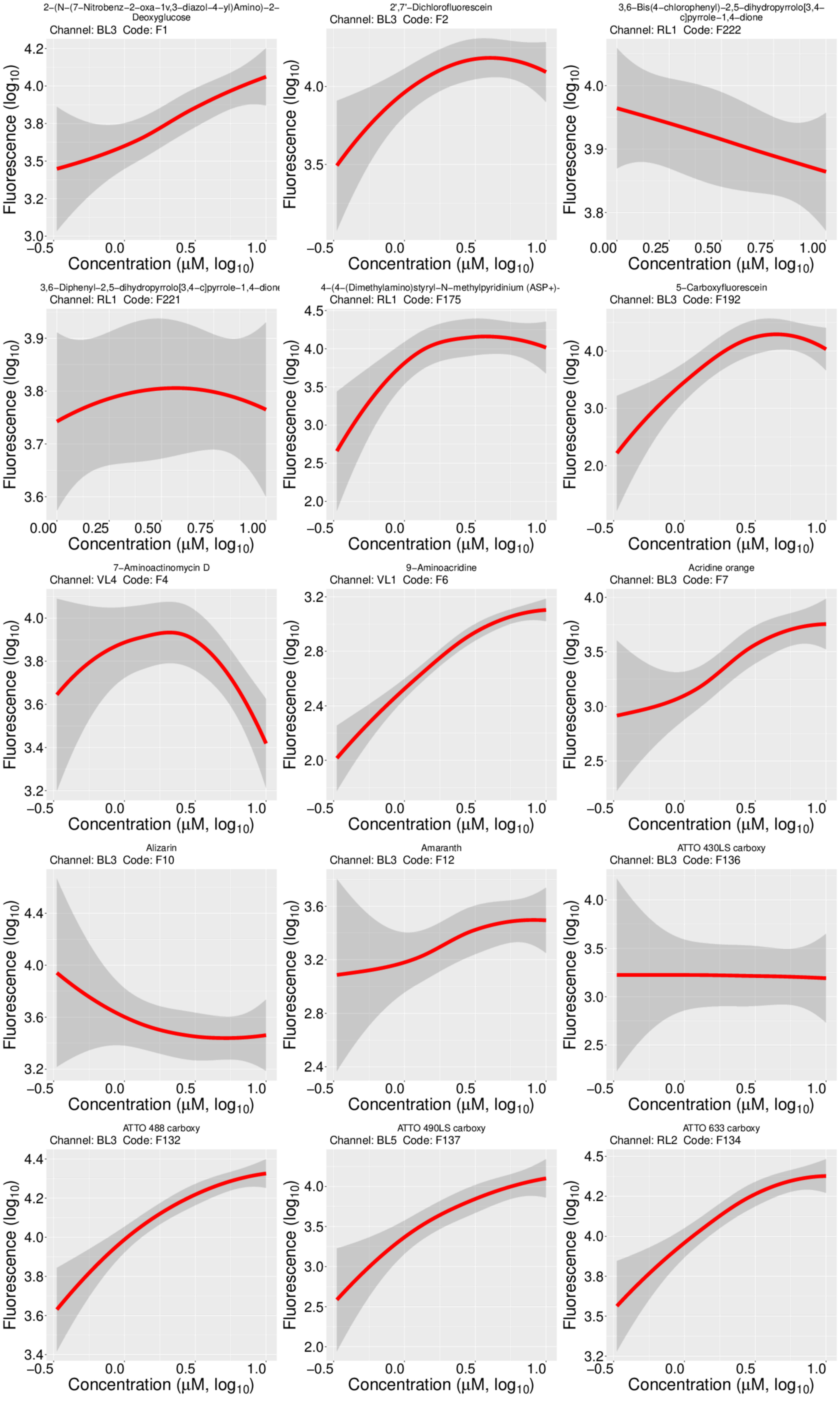


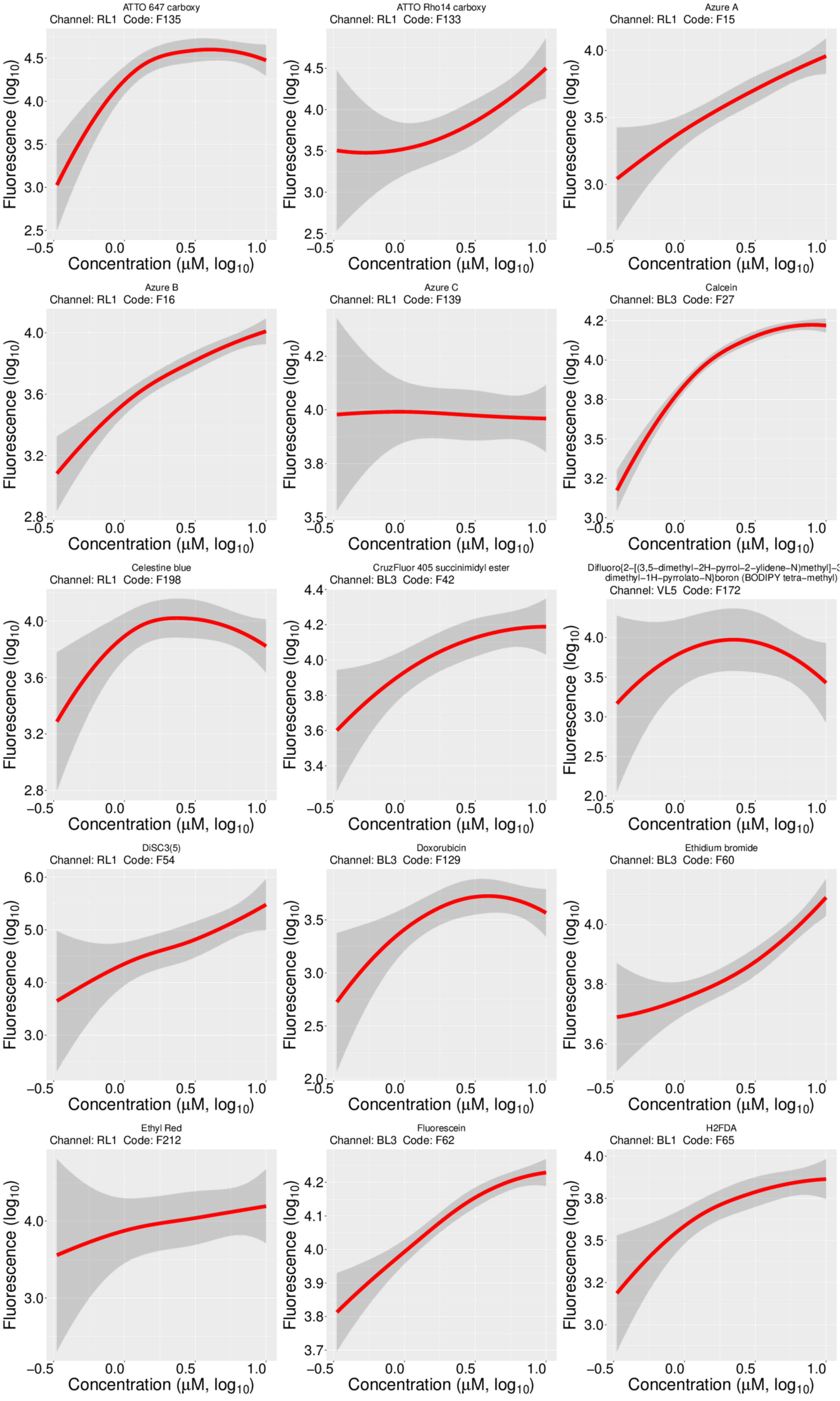
**Supplementary Figure 1**

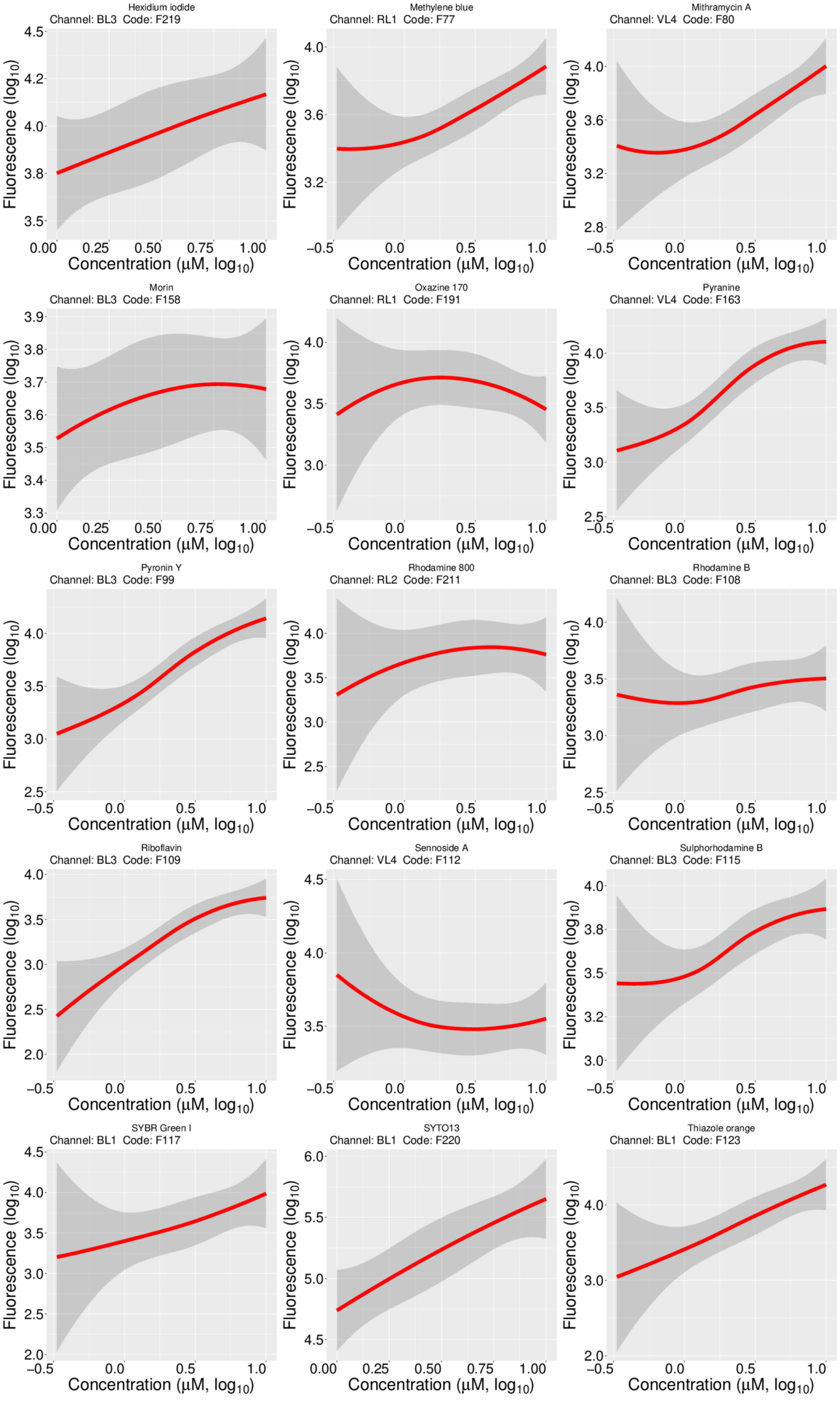


**Supplementary Figure 2**

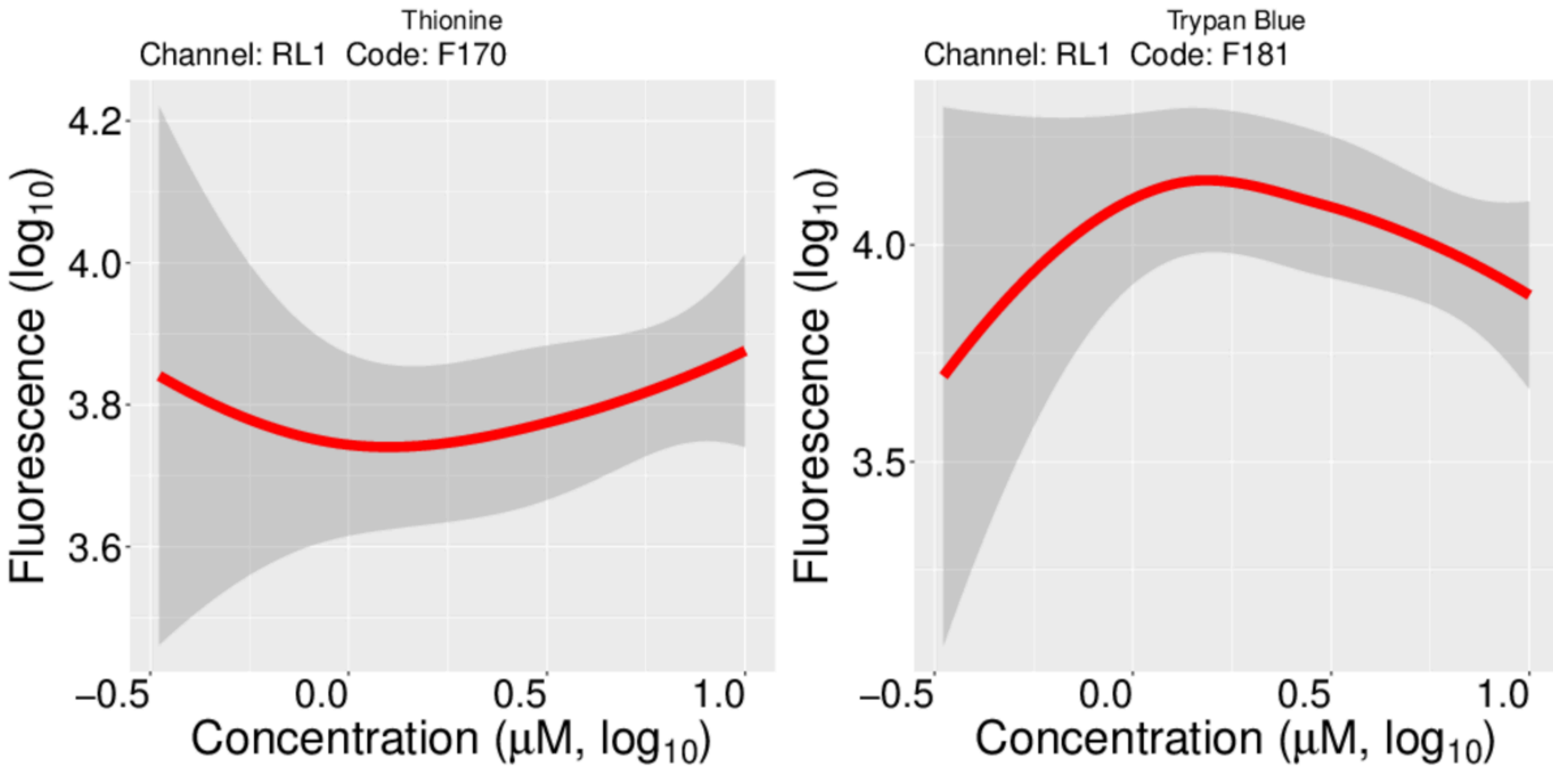




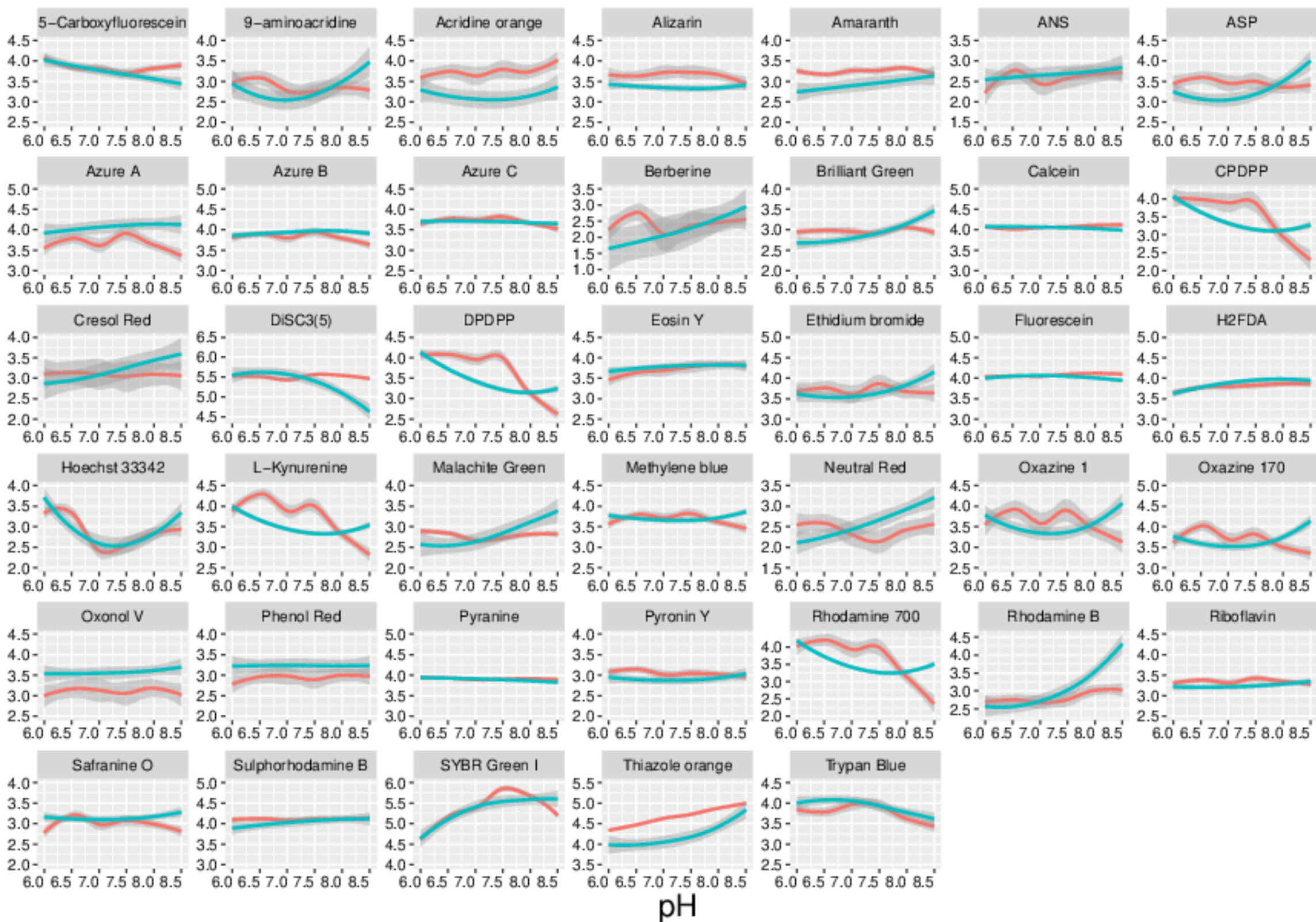








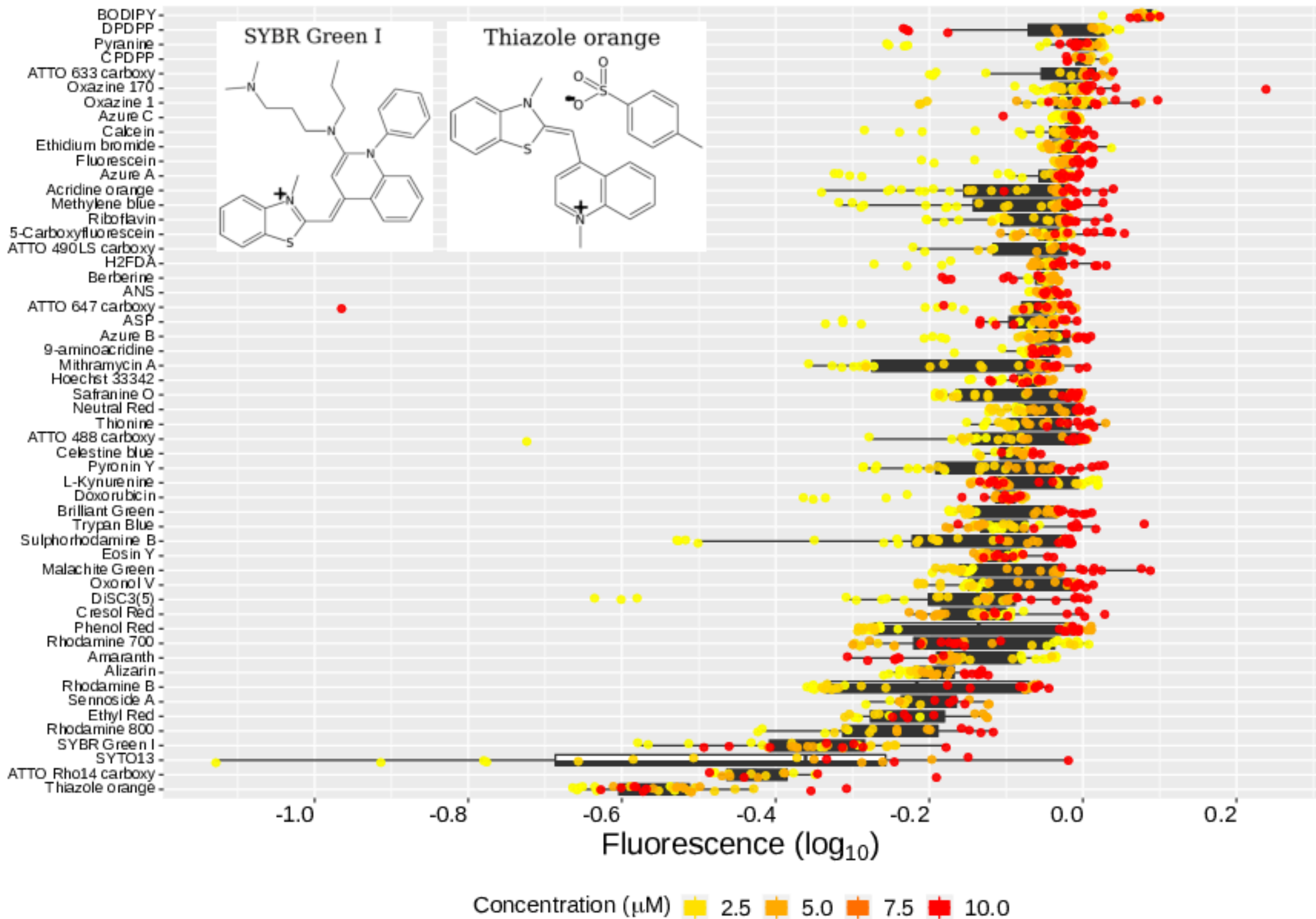
**Supplementary Figure 3**



— BW25113 — BW25113+CPZ

# Supplementary Figure 5

$\Delta yhjV$



# Signal ratio

## Supplementary Figure 6

